

EMBEDDING DIAGRAMS OF $N=2$ VERMA MODULES AND RELAXED $\widehat{sl}(2)$ VERMA MODULES

A. M. Semikhatov and V. A. Sirota

Tamm Theory Division, Lebedev Physics Institute, Russian Academy of Sciences

We classify and explicitly construct the embedding diagrams of Verma modules over the $N=2$ supersymmetric extension of the Virasoro algebra. The essential ingredient of the solution consists in drawing the distinction between two different types of submodules appearing in $N=2$ Verma modules. The problem is simplified by associating to every $N=2$ Verma module a *relaxed Verma* module over the affine algebra $\widehat{sl}(2)$ with an isomorphic embedding diagram. We then make use of the mechanism according to which the structure of the $N=2$ /relaxed- $\widehat{sl}(2)$ embedding diagrams can be found knowing the standard embedding diagrams of $\widehat{sl}(2)$ Verma modules. The resulting classification of the $N=2$ /relaxed- $\widehat{sl}(2)$ embedding diagrams follows the I-II-III pattern extended by an additional indication of the number (0, 1, or 2) and the twists of the standard $\widehat{sl}(2)$ embedding diagrams contained in a given $N=2$ /relaxed- $\widehat{sl}(2)$ embedding diagram.

Contents

1	Introduction	1
2	The $\widehat{sl}(2)$ side: relaxed modules	6
2.1	Twisted Verma modules	6
2.2	Relaxed modules	7
2.3	Submodules and singular vectors in relaxed modules	10
3	Classifying the embedding diagrams	16
3.1	Classifying the degeneration patterns	17
3.2	The diagrams	20
4	The $N=2$ side: Massive and topological Verma modules	34
4.1	The $N=2$ algebra	34
4.2	Massive $N=2$ Verma modules	35
4.3	Topological $N=2$ modules	36
4.4	From $N=2$ to $\widehat{sl}(2)$	37
4.5	Embedding diagrams of the massive $N=2$ Verma modules	42
4.6	$c=3$ singular vectors and embedding diagrams	46
5	Conclusions	50

1 Introduction

In this paper, we solve the long-standing problem of constructing embedding diagrams of Verma modules over the $N=2$ superconformal algebra in two dimensions (the $N=2$ extension of the Virasoro algebra). This algebra appeared originally in the construction of $N=2$ strings [A], however it turned out later on

arXiv:hep-th/9712102v1 9 Dec 1997

that, in addition to its role in the $N=2$ strings ([OV, M], and references therein), the $N=2$ superconformal symmetry in two dimensions is important in the heterotic string compactifications [G], which has led to investigating its relations with Calabi–Yau manifolds and with the Landau–Ginzburg theories and singularity theory [Mar, VW]. This algebra is in fact the symmetry of topological conformal theories [W, EY] (see also [FoF, Get] and [Get2] for the discussion in terms of equivariant cohomology) and is therefore related to topological field theories in two dimensions. Much attention has been given to investigating the space of $N=2$ supersymmetric quantum field theories by perturbing $N=2$ superconformal theories, see, e.g., [CGP, CV]. An important tool in constructing $N=2$ superconformal theories are the Kazama–Suzuki models [KS] (see also [OS] for their free-superfield realizations). The $N=2$ algebra is actually realized on the worldsheet of any non-critical string theory [GRS, BLNW]. Therefore, deriving this algebra via the Hamiltonian reduction of affine Lie superalgebra $\widehat{\mathfrak{sl}}(2|1)$ [BO, IK] can be interpreted as deriving the entire bosonic string via the Hamiltonian reduction; this approach has been extended to other string theories [BLLS, RSS], with the corresponding symmetry algebras containing the $N=2$ algebra as a subalgebra. The $N=2$ algebra realized in the bosonic string actually underlies the construction of the physical states [LZ].

‘Non-affine’ complications. From the representation-theoretic point of view (as well as in several other respects, see, e.g., [EG]), the $N=2$ algebra is essentially different from the $N=1$ super-Virasoro algebra, which is primarily due to the existence of the spectral flow transform [SS, LVW] (see also [KL] for the role of the spectral flow in the (critical) $N=2$ strings). In addition, certain complications arising in the $N=2$ representation theory are due to the fact that this algebra is *not* affine. This affects, in particular, finding all possible sequences of submodules of submodules of \dots , appearing in a given $N=2$ Verma module, that is, the *embedding diagrams*. An important related construction is the appropriate version of the BGG-resolution [BGG]. For the Verma modules over affine Lie algebras, the structure of the embedding diagrams and of the BGG resolution is governed by the affine Weyl group. While the embedding diagrams of the $\widehat{\mathfrak{sl}}(2)$ as well as the Virasoro Verma modules are well-known [FF, RCW, Mal, FFr], the problem of constructing the $N=2$ embedding diagrams, although it has been around for some time [Kir, Do, Mat, D], has not been solved yet¹. No standard construction of an ‘affine’ Weyl group applies here. The problem is focused on the embedding diagrams, since the BGG-resolution can be obtained by finding the embedding diagrams first and then reconstructing the associated exact sequences (which, with the underlying Weyl group representation unknown, appears to be the only way to derive the resolution). The resolution should provide one with a tool for systematically deriving the $N=2$ characters.

Submodules and singular vectors. It should be stressed that the embedding diagrams describe embeddings of *modules*, i.e., the occurrence of submodules in a given Verma modules. Submodules in a Verma module \mathcal{U} are often ‘identified’ with singular vectors, since, whenever one finds a state $|S\rangle \in \mathcal{U}$ annihilated by the same elements of the algebra as the highest-weight vector of \mathcal{U} , then there is a submodule $\mathcal{U}' \subset \mathcal{U}$ generated from $|S\rangle$. For the (affine) Lie algebras of rank ≤ 2 [Mal], *any* submodule is a Verma module (or a sum thereof). This is so, in particular for $\widehat{\mathfrak{sl}}(2)$, where the notions of the submodule and of the singular vector can thus be identified. However, the relation between singular vectors and submodules in Verma modules is much more complicated in general [Di, Chap. 7].

In the literature on representations of the $N=2$ superconformal algebra, such an identification between

¹That the earlier conjectures for the $N=2$ embedding diagrams need being corrected was for the first time noticed in [D], see also the remarks in [EG].

submodules and singular vectors appears to have resulted in replacing the analysis of embeddings of $N=2$ Verma modules by the investigation of certain algebraic constructions—some kind of singular vectors, or, more precisely, singular vector operators. In particular, the conclusions regarding the embeddings of submodules were arrived at according to how these constructions compose. This approach, however, runs into a problem whenever, as it may happen, the composition of two $N=2$ singular vector operators vanishes. What happens to the corresponding *submodules* then? Is there an *embedding*, and how a composition of two embeddings (the mappings with *trivial kernels*) can possibly vanish?

The resolution of these problems requires, first of all, that one analyses the *submodules* rather than singular vectors as such. As realized in [ST2], $N=2$ Verma modules contain submodules of two different types, which we distinguish as the massive and the (twisted) topological Verma modules (for example, the submodules generated from the charged singular vectors [BFK] in a massive Verma module are the twisted topological Verma modules). A given state $|S\rangle \in \mathcal{U}$ satisfying the same annihilation conditions as the highest-weight vector of a massive $N=2$ Verma module \mathcal{U} may give rise to either a massive Verma module or a twisted topological Verma module; in this respect, such singular vectors $|S\rangle$ are not very useful as regards investigating the structure of *submodules*. While the topological Verma modules can appear as submodules of the massive ones, the converse is not true: what seems to be an embedding of a massive Verma module \mathcal{U} into a topological Verma module \mathcal{V} necessarily has a kernel given by a topological Verma submodule in \mathcal{U} :

$$0 \longrightarrow \mathcal{V}_1 \longrightarrow \mathcal{U} \longrightarrow \mathcal{V} \longrightarrow 0, \quad (1.1)$$

hence the apparent vanishing of the ‘embedding’. Moreover, once one wishes to deal with the $N=2$ Verma-like modules of only one, massive, type, one extends this sequence into

$$\dots \longrightarrow \mathcal{U}_2 \longrightarrow \mathcal{U}_1 \longrightarrow \mathcal{U} \longrightarrow \mathcal{V} \longrightarrow 0, \quad (1.2)$$

which is simply a resolution of a topological Verma module in terms of the massive ones; the mappings in this *exact* sequence are by no means embeddings then. If, further, the fact that \mathcal{V} is a topological, not massive, Verma module is not recognized, the interpretation of such a sequence becomes quite obscure.

Thus, in particular, one should clearly distinguish between the embedding diagrams and the resolutions. Although the latter are of a primary importance for constructing the characters, we concentrate in this paper on the *embedding* diagrams, as a prerequisite for constructing the resolutions. The $N=2$ embedding diagrams necessarily involve modules of two types, the massive and the twisted topological Verma modules. A convenient way to differentiate between these modules is to have them generated from the vectors satisfying the highest-weight conditions that are correlated with the type of the corresponding submodule. That this is possible for the $N=2$ algebra is a lucky circumstance. One takes the singular vectors to satisfy either the *twisted* (spectral-flow-transformed) topological highest-weight conditions or the massive highest-weight conditions. These singular vectors, constructed in [ST2, ST3], adequately describe the relations between the corresponding submodules; at the same time, they generate *maximal* submodules, therefore providing the description of all submodules in an $N=2$ Verma module without introducing subsingular vectors [ST3].

Equivalence of categories. The problem of “comparing”, in some sense, the *representations* of the $N=2$ algebra with those of the affine Lie algebra $\widehat{\mathfrak{sl}}(2)$ reappears in various contexts both in conformal field theory and in representation theory. It was solved in [FST], where a new type of $\widehat{\mathfrak{sl}}(2)$ modules was introduced and the *equivalence* was then shown to take place between certain categories constructed out

of the $N=2$ and $\widehat{sl}(2)$ representations (because of the universal property of Verma modules in the \mathcal{O} -type categories [K], one can start with the corresponding Verma modules and then extend to the highest-weight-type representations). Namely, one considers an arbitrary complex level $k \in \mathbb{C} \setminus \{-2\}$ on the $\widehat{sl}(2)$ side; on the $N=2$ side, one considers the ‘standard’ representation category (the one implied in, e.g., [BFK, LVW]), which includes the massive Verma modules and their quotients, the (unitary and non-unitary) irreducible representations, etc., along with their images under the spectral flow (*twists*), with the central charge $c \in \mathbb{C} \setminus \{3\}$. *Modulo the spectral flow transform* (see [FST] for the precise statement), this $N=2$ category is equivalent to the category of *relaxed* highest-weight-type $\widehat{sl}(2)$ representations (and their twists).² On the other hand, the standard highest-weight-type $\widehat{sl}(2)$ representations turn out to be related to a narrower category where the ‘universal’ Verma-like objects are the *twisted topological $N=2$ Verma modules*.

A statement regarding the equivalence of two categories can often be interpreted to the effect that there are two different languages describing the same structure. In this way, any ‘structural’ result about $N=2$ Verma modules can in principle be seen in relaxed $\widehat{sl}(2)$ modules, and vice versa. As it may (and does) happen with equivalence of categories, however, a number of facts that are fairly obvious on one side translate into the statements which are not quite obvious on the other side. Thus, the $\widehat{sl}(2)$ representations that correspond to the massive $N=2$ Verma modules are the relaxed (Verma) modules, which, in general, have infinitely many highest-weight vectors. Although this may seem strange at a first glance, it is a good example of the effects related to the equivalence of categories, since the ‘proliferation’ of the highest-weight vectors is a counterpart of the situation well-known in the massive $N=2$ Verma modules. Further, singular vectors in the relaxed- $\widehat{sl}(2)$ and massive $N=2$ Verma modules are given by similar constructions (see [FST] and [ST3], respectively), yet the $\widehat{sl}(2)$ one is somewhat more straightforward algebraically. On the other hand, proving that these constructions give *all* singular vectors is easier on the $N=2$ side, where the Kač determinant has been known for some time [BFK]. An important consequence of the equivalence is that the embedding diagrams of massive $N=2$ Verma modules are isomorphic to those of the relaxed $\widehat{sl}(2)$ modules³.

$N=2$ and relaxed- $\widehat{sl}(2)$ embedding diagrams. Thus, the $N=2$ embedding diagrams can be arrived at using the results of either [FST] or [ST3]: Degenerations of massive $N=2$ Verma modules were directly analysed in [ST3], where the possible types of submodules were classified and the conditions were given for the different combinations of submodules to appear in a given massive Verma module. Alternatively, the equivalence of categories allows us to translate the $N=2$ problem into the relaxed- $\widehat{sl}(2)$ context and then to apply the results of [FST] on the classification of possible degenerations (reducibility patterns) of the relaxed $\widehat{sl}(2)$ modules. In view of the equivalence of categories, the distinction between two types of submodules applies on the $\widehat{sl}(2)$ side as well. In the $\widehat{sl}(2)$ setting, however, things are considerably simplified due to the absence of arbitrary twists.

In this paper, therefore, rather than directly analysing how the $N=2$ Verma modules can be embedded into one another, we take another root to the $N=2$ embedding diagrams by making use of the fact that these are isomorphic to the relaxed- $\widehat{sl}(2)$ embedding diagrams. The analysis of the latter is easier also because the affine-Lie algebra representation theory is available then and certain subdiagrams in the relaxed embedding diagrams are literally the standard $\widehat{sl}(2)$ embedding diagrams [RCW, Mal]. Moreover,

²In this paper, ‘relaxed module’ \equiv ‘relaxed Verma module’ of [FST].

³The direct and the inverse functors of [FST] establish the equivalence between the *chains* of spectral-flow-transformed modules. However, all degenerations occur simultaneously in every module in the chain and the embedding diagrams are isomorphic for all the spectral-flow-transformed modules.

even though the relaxed $\widehat{s\ell}(2)$ Verma modules are not a ‘classical’ object in the representation theory of affine Lie algebras, the problem of enumerating submodules of relaxed modules can be reduced, to a large extent, to the classical problem of the standard $\widehat{s\ell}(2)$ -embedding diagrams. Thus, for a given relaxed module \mathcal{R} , one can find an “auxiliary” usual-Verma module M whose submodules are in a 1 : 1 (or, in some degenerate cases, essentially in a 2 : 1) correspondence with the relaxed submodules in \mathcal{R} . If, further, \mathcal{R} contains no submodules generated from the *charged singular vectors*, then its embedding diagram is immediately read off from the embedding diagram of the Verma module M . If, on the other hand, there are charged singular vectors in \mathcal{R} , the picture is slightly more complicated because the entire embedding diagram consisting of the usual-Verma modules is attached to the embedding diagram of \mathcal{R} .

We would like to point out once again that all these effects can, of course, be seen directly on the $N=2$ side as well; as we have mentioned, the role of the usual-Verma $\widehat{s\ell}(2)$ modules is played there by the topological Verma modules. Analysing the structure of a given massive $N=2$ Verma module \mathcal{U} , again, is reduced [ST3] to analysing an auxiliary twisted topological Verma module V . In particular, singular vectors (submodules) in V translate, in a certain way, into singular vectors in \mathcal{U} . In addition, it may happen that one or two of the auxiliary topological Verma modules become actual submodules of the massive Verma module, in which case the *charged* singular vectors occur in the latter module. Accordingly, the embedding diagrams of massive Verma modules can be reconstructed, with some work, from those of the topological Verma modules⁴; the latter are isomorphic, in their own turn, to embedding diagrams of the usual $\widehat{s\ell}(2)$ Verma modules. In the end of the day, one arrives at the same embedding diagrams as for the relaxed $\widehat{s\ell}(2)$ modules, read with somewhat different conventions.

In what follows, we first classify the relaxed- $\widehat{s\ell}(2)$ embedding diagrams and then explain the legend that allows one to read the same diagrams in the $N=2$ language. The classification of embedding diagrams that we obtain agrees with the classification of degeneration patterns of $N=2$ Verma modules given in [ST3], more precisely, the present construction is a (considerable) refinement of the previous classification.

The $N=2$ /relaxed- $\widehat{s\ell}(2)$ embedding diagrams which we construct are somewhat more complicated than the Virasoro or the standard $\widehat{s\ell}(2)$ ones; in particular, a significant difference in the classification is that there does not exist a ‘generic’ case such that all the other cases correspond to its degenerations⁵. Yet, the embedding diagrams follow the familiar I-II-III pattern [FF], which has to be extended by an additional indication of how many (0, 1, or 2) charged singular vectors exist in the module.

From our results, one can reproduce the well-known embedding diagrams of the Virasoro Verma modules [FF] by contracting—in the conventions that we discuss in what follows—all the horizontal arrows in the $N=2$ /relaxed- $\widehat{s\ell}(2)$ embedding diagrams. In addition, there are two types of relations between the relaxed- $\widehat{s\ell}(2)$ /massive- $N=2$ and the standard $\widehat{s\ell}(2)$ Verma module embedding diagrams [RCW, Mal]: first, as we have noted, different embedding patterns of the relaxed/ $N=2$ Verma modules are sensitive to the type of the embedding diagram of the auxiliary Verma module. Therefore, when enumerating all degenerations of relaxed modules, one has to use the classification of the standard embedding diagrams of $\widehat{s\ell}(2)$ Verma modules (in fact, one has to be even more detailed than in the standard case!). Second, whenever a charged singular vector appears in a relaxed module \mathcal{R} , the quotient of \mathcal{R} over the corresponding (maximal) submodule is (up to a twist) the usual Verma module, therefore the usual-Verma embedding

⁴This is parallel and, apparently, not unrelated, to the well-known situation with $N=2$ theories, where the *topological* sector allows one to reconstruct a considerable amount of the information about the entire theory.

⁵We thank F. Malikov for stressing this point in relation with the search of a possible analogue of the affine Weyl group.

diagrams are also reproduced by taking the quotients of the relaxed/ $N = 2$ embedding diagrams with respect to the embedding diagrams of Verma submodules.

This paper is organized as follows. We begin in Sec. 2 with recalling the $\widehat{s\ell}(2)$ algebra and representations. In Sec. 2.1, we introduce the *twisted* $\widehat{s\ell}(2)$ Verma modules, the relaxed modules are defined in Sec. 2.2, while in Sec. 2.3 we consider singular vectors in relaxed modules and review the structural results regarding the corresponding submodules. Relaxed- $\widehat{s\ell}(2)$ embedding diagrams are considered in Sec. 3, where we first classify the possible cases (Sec. 3.1, with the summary in the Table on p. 21) and then, in Sec. 3.2, list the corresponding embedding diagrams. The $N = 2$ superconformal algebra is considered in Sec. 4. Here, we introduce the massive (Sec. 4.2) and topological (Sec. 4.3) Verma modules, and also recall, in Sec. 4.4, the construction that allows one to map the $N = 2$ highest-weight-type representations theory onto the relaxed-highest-weight-type representations of the affine $s\ell(2)$. The embedding diagrams of $N = 2$ Verma modules are literally the same as those in Sec. 3.2, however we give several comments in Sec. 4.5 as to the notations that apply in the $N = 2$ case; we also repeat here, in the intrinsic $N = 2$ language, the classification of the embedding diagram patterns, so that these now apply directly to the massive $N = 2$ Verma modules. The case of the $N = 2$ central charge $c = 3$ has to be analysed separately, which is done in Sec. 4.6. Section 5 contains several concluding remarks.

2 The $\widehat{s\ell}(2)$ side: relaxed modules

2.1 Twisted Verma modules

The affine $s\ell(2)$ algebra is defined as

$$\begin{aligned} [J_m^0, J_n^\pm] &= \pm J_{m+n}^\pm, & [J_m^0, J_n^0] &= \frac{K}{2} m \delta_{m+n,0}, \\ [J_m^+, J_n^-] &= K m \delta_{m+n,0} + 2J_{m+n}^0, \end{aligned} \quad (2.1)$$

with K being the central element, whose eigenvalue will be denoted by $t - 2$. In what follows, we assume $t \neq 0$. The spectral flow transform [BH, FST] is the automorphism

$$\mathcal{U}_\theta : J_n^+ \mapsto J_{n+\theta}^+, \quad J_n^- \mapsto J_{n-\theta}^-, \quad J_n^0 \mapsto J_n^0 + \frac{t-2}{2} \theta \delta_{n,0}, \quad \theta \in \mathbb{Z}. \quad (2.2)$$

A twisted Verma module $\mathfrak{M}_{j,t;\theta}$ is freely generated by $J_{\leq \theta-1}^+$, $J_{\leq -\theta}^-$, and $J_{\leq -1}^0$ from a twisted highest-weight vector $|j, t; \theta\rangle$ defined by the conditions

$$\begin{aligned} J_{\geq \theta}^+ |j, t; \theta\rangle &= J_{\geq 1}^0 |j, t; \theta\rangle = J_{\geq -\theta+1}^- |j, t; \theta\rangle = 0, \\ \left(J_0^0 + \frac{t-2}{2} \theta \right) |j, t; \theta\rangle &= j |j, t; \theta\rangle. \end{aligned} \quad (2.3)$$

In what follows, j is referred to as the *spin* of the highest-weight vector $|j, t; \theta\rangle$. We define $|j, t\rangle = |j, t; 0\rangle$. We also denote $\mathcal{M}_{j,t} = \mathfrak{M}_{j,t;0}$. The structure of $\widehat{s\ell}(2)$ Verma modules is conveniently encoded in the *extremal diagram*, which in the ‘untwisted’ case $\theta = 0$ reads as

$$\begin{array}{ccccccccccc} \cdot & \cdot & \cdot & * & \leftarrow^{J_0^-} & * & \leftarrow^{J_0^-} & * & \leftarrow^{J_0^-} & \bullet & \searrow^{J_{-1}^+} & * & \searrow^{J_{-1}^+} & * & \searrow^{J_{-1}^+} & * & \dots & \dots \end{array} \quad (2.4)$$

This expresses the fact that J_{-1}^+ and J_0^- are the highest-level operators that do not yet annihilate the highest-weight state \bullet . The $\widehat{sl}(2)$ modules being graded with respect to the charge⁶ and the level, *extremal vectors* are those with the boundary value of (charge, level). All the other states of the module should be thought of as lying in the interior of the angle in the above diagram. In our conventions, increasing the charge by 1 corresponds to shifting to the neighbouring site on the right, while increasing the level corresponds to moving down. In these conventions, e.g., J_{-1}^0 is represented by a downward vertical arrow.

A singular vector exists in the Verma module $\mathcal{M}_{j,t}$ over the affine $sl(2)$ algebra if and only if either $j = j^+(r, s, t)$ or $j = j^-(r, s, t)$, where

$$\begin{aligned} j^+(r, s, t) &= \frac{r-1}{2} - t\frac{s-1}{2}, \\ j^-(r, s, t) &= -\frac{r+1}{2} + t\frac{s}{2}, \end{aligned} \quad r, s \in \mathbb{N}, \quad t \in \mathbb{C}. \quad (2.5)$$

Singular vectors in the module $\mathcal{M}_{j^\pm(r,s,t),t}$ are given by the explicit constructions [MFF]:

$$\begin{aligned} |\text{MFF}^+(r, s, t)\rangle &= (J_0^-)^{r+(s-1)t} (J_{-1}^+)^{r+(s-2)t} \dots (J_{-1}^+)^{r-(s-2)t} (J_0^-)^{r-(s-1)t} |j^+(r, s, t), t\rangle_{sl(2)}, \\ |\text{MFF}^-(r, s, t)\rangle &= (J_{-1}^+)^{r+(s-1)t} (J_0^-)^{r+(s-2)t} \dots (J_0^-)^{r-(s-2)t} (J_{-1}^+)^{r-(s-1)t} |j^-(r, s, t), t\rangle_{sl(2)}. \end{aligned} \quad (2.6)$$

As is well known, these formulae evaluate as Verma-module elements using the following relations:

$$\begin{aligned} (J_0^-)^\alpha J_m^+ &= -\alpha(\alpha-1)J_m^-(J_0^-)^{\alpha-2} - 2\alpha J_m^0 (J_0^-)^{\alpha-1} + J_m^+ (J_0^-)^\alpha, \\ (J_0^-)^\alpha J_m^0 &= \alpha J_m^-(J_0^-)^{\alpha-1} + J_m^0 (J_0^-)^\alpha, \\ (J_{-1}^+)^\alpha J_m^- &= -\alpha(\alpha-1)J_{m-2}^+(J_{-1}^+)^{\alpha-2} - k\alpha \delta_{m-1,0} (J_{-1}^+)^{\alpha-1} + 2\alpha J_{m-1}^0 (J_{-1}^+)^{\alpha-1} + J_m^- (J_{-1}^+)^\alpha, \\ (J_{-1}^+)^\alpha J_m^0 &= -\alpha J_{m-1}^+(J_{-1}^+)^{\alpha-1} + J_m^0 (J_{-1}^+)^\alpha, \end{aligned} \quad (2.7)$$

which can be derived for α being a positive integer and then continued to an arbitrary complex α .

Equations (2.6) produce a singular vector in $\mathcal{M}_{j,t}$ for any pair of positive integers r and s that solve $j = j^\pm(r, s, t)$. At most two of these singular vectors are *primitive*, i.e., are not in a submodule determined by some other singular vector. By looking for primitive singular vectors in the submodules generated by each of the primitive vector, etc., one obtains all of the singular vectors in the Verma module. For generic rational t , one-half of them are directly obtained from the highest-weight vector as described in (2.6).

2.2 Relaxed modules

Definition 2.1 For an unordered pair of complex numbers $\{\mu_1, \mu_2\}$, the following set of conditions define the relaxed highest-weight state $|\mu_1, \mu_2, t\rangle$:

$$J_{\geq 1}^+ |\mu_1, \mu_2, t\rangle = J_{\geq 1}^0 |\mu_1, \mu_2, t\rangle = J_{\geq 1}^- |\mu_1, \mu_2, t\rangle = 0, \quad (2.8)$$

$$J_0^- J_0^+ |\mu_1, \mu_2, t\rangle = -\mu_1 \mu_2 |\mu_1, \mu_2, t\rangle. \quad (2.9)$$

$$J_0^0 |\mu_1, \mu_2, t\rangle = -\frac{1}{2}(1 + \mu_1 + \mu_2) |\mu_1, \mu_2, t\rangle, \quad (2.10)$$

$$K |\mu_1, \mu_2, t\rangle = (t-2) |\mu_1, \mu_2, t\rangle. \quad (2.11)$$

These equations are called the relaxed highest-weight conditions.

⁶by the *charge*—more precisely, the J_0^0 -charge— we mean the eigenvalue of J_0^0 ; this is different from spin j for the twisted modules, in accordance with (2.3).

Definition 2.2 The relaxed module⁷ $\mathcal{R}_{\mu_1, \mu_2, t}$ is generated from a relaxed highest-weight state $|\mu_1, \mu_2, t\rangle$ by the free action of operators $J_{\leq 0}^+$, $J_{\leq 0}^-$, and $J_{\leq -1}^0$ modulo the constraint (2.9).

Thus, the relaxed module can also be defined as the induced representation from the $sl(2)$ Lie algebra representation without a highest- or a lowest-weight. It is convenient to consider the extremal diagram of the relaxed module:

$$\cdot \cdot \cdot \star \xleftarrow{J_0^-} \star \xleftarrow{J_0^-} \star \xleftarrow{J_0^-} \star \xrightarrow{J_0^+} \star \xrightarrow{J_0^+} \star \xrightarrow{J_0^+} \star \cdot \cdot \cdot \quad (2.12)$$

where \star denotes the state $|\mu_1, \mu_2, t\rangle$. The *extremal states*

$$(J_0^-)^{-i} |\mu_1, \mu_2, t\rangle, \quad i < 0, \quad \text{and} \quad (J_0^+)^i |\mu_1, \mu_2, t\rangle, \quad i > 0, \quad (2.13)$$

constitute precisely the $sl(2)$ -representation, while the other states of the $\widehat{sl}(2)$ module belong to the homogeneous (charge, level) subspaces represented by a rectangular lattice lying *below* the line of extremal states.

Whenever $\mu_\alpha = 0$, the definition of the relaxed module is such that the state $|0, \mu, t|1\rangle \equiv J_0^+ |0, \mu, t\rangle \neq 0$ satisfies the condition $J_0^- |0, \mu, t|1\rangle = 0$. Similarly, $\mu_\alpha = -1$ means that the state $|-1, \mu, t|-1\rangle \equiv J_0^- |-1, \mu, t\rangle \neq 0$ satisfies the condition $J_0^+ |-1, \mu, t|-1\rangle = 0$.

In general, the relaxed module may also be generated from other extremal states than $|\mu_1, \mu_2, t\rangle$ since each of the extremal states (2.13) satisfies the relaxed highest-weight conditions with

$$\mu_\alpha \mapsto \mu_\alpha^{(i)} = \mu_\alpha - i. \quad (2.14)$$

Generically, all of these states generate the same module because each is a descendant of the others:

$$\cdot \cdot \cdot \star \xleftarrow{J_0^-} \star \xleftarrow{J_0^-} \star \xleftarrow{J_0^-} \star \xleftarrow{J_0^-} \star \xleftarrow{J_0^-} \star \xleftarrow{J_0^-} \star \cdot \cdot \cdot \\ \xrightarrow{J_0^+} \star \xrightarrow{J_0^+} \star \xrightarrow{J_0^+} \star \xrightarrow{J_0^+} \star \xrightarrow{J_0^+} \star \xrightarrow{J_0^+} \star \cdot \cdot \cdot \quad (2.15)$$

where the composition of any pair of the outward and the return arrows gives the operator of a multiplication with a number. However, as soon as this number is zero, the equivalence between the extremal states breaks down and some of the states generate only a submodule of the entire module. Those extremal states that do generate the same module can be described as follows.

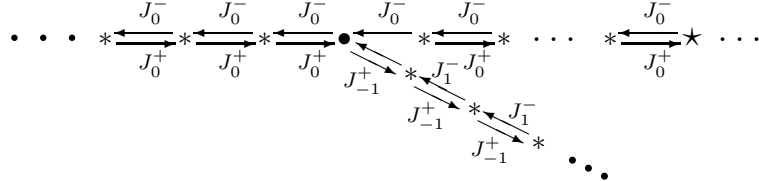
Definition 2.3 By the orbit of an (unordered) pair $\{\mu_1, \mu_2\}$ where $\mu_\alpha \neq 0$ and $\neq -1$, we will mean the maximal set of unordered pairs $(\{\mu_1^{(i)}, \mu_2^{(i)}\})_{i \in [a, b] \subset \mathbb{Z}}$, where $-\infty \leq a \leq -1$ and $1 \leq b \leq +\infty$, such that $\mu_\alpha^{(i)} \neq 0$ for $i \in [a, -1]$ and $\mu_\alpha^{(i)} \neq -1$ for $i \in [1, b]$. If $\mu_1 = -1$, $\mu_2 \neq 0$, the orbit is the maximal set of unordered pairs $(\{\mu_1^{(i)}, \mu_2^{(i)}\})_{i \in [0, b] \subset \mathbb{Z}}$, where $1 \leq b \leq +\infty$, such that $\mu_2^{(i)} \neq -1$ for $i \in [1, b]$; if, further, $\mu_1 = 0$, $\mu_2 \neq -1$, the orbit is the maximal set of unordered pairs $(\{\mu_1^{(i)}, \mu_2^{(i)}\})_{i \in [a, 0] \subset \mathbb{Z}}$, where $-\infty \leq a \leq -1$, such that $\mu_2^{(i)} \neq 0$ for $i \in [a, -1]$; finally, the orbit of $\{\mu_1, \mu_2\} = \{-1, 0\}$ consists of only that point.

⁷We follow [FST], however we have changed the parametrization of relaxed modules to the one that will be more convenient for our present purposes. We also call relaxed Verma modules simply as relaxed modules.

Then, as easy to see, the relaxed module $\mathcal{R}_{\mu_1, \mu_2, t}$ is determined by any point of the orbit of $\{\mu_1, \mu_2\}$. If none of the μ_α are integers, the orbit is infinite in both directions and can be identified with the set of extremal states in (2.12). On the other hand, whenever $\mu_1 = n \in -\mathbb{N}$,⁸ we have

$$J_0^+ \cdot (J_0^-)^{-n} |n, \mu_2, t\rangle = 0, \quad (2.16)$$

in which case diagram (2.15) branches as

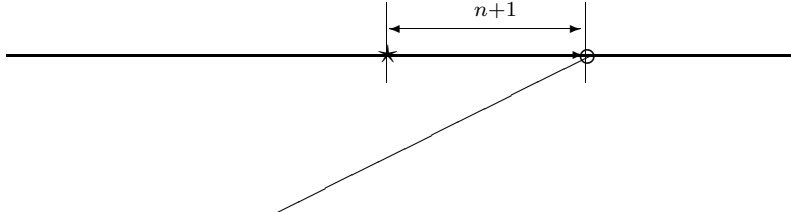


$$(2.17)$$

where we recognize the ordinary Verma module (2.4) as a submodule of the relaxed module. Similarly, whenever $\mu_1 = n \in \mathbb{N}_0$, we have

$$J_0^- \cdot (J_0^+)^{n+1} |n, \mu_2, t\rangle = 0. \quad (2.18)$$

Somewhat more schematically than in (2.17), this can be represented as follows:



$$(2.19)$$

In this case, the submodule is a Verma module twisted by the spectral flow transform with $\theta = 1$; in particular, the state at the branch point satisfies the annihilation conditions from (2.3) with $\theta = 1$.

Whenever μ_α are integers of different signs, the orbit contains a finite number of points (and, thus, can be identified with a finite-dimensional representation of the Lie algebra $sl(2)$). As will be seen in what follows, this case is always special, being considerably different even from the case where μ_1 and μ_2 are integers of the same sign. Let us also note that, obviously, $\mu_1 - \mu_2$ is invariant under the \mathbb{Z} -action (2.14), as is the fact that one or both of the μ_α is an integer. Further, the signs of each of the μ_α are also preserved along the orbit.

In contrast to relaxed modules, by Verma modules over $\widehat{sl}(2)$, we will always mean the standard Verma modules. The twisted Verma modules that we encounter in this paper, are always with the twist parameter $\theta = 1$.

In what follows, we will also need the twisted relaxed modules. For a fixed $\theta \in \mathbb{N}$, the module $\mathfrak{R}_{\mu_1, \mu_2, t; \theta}$ is generated from the state $|\mu_1, \mu_2, t; \theta\rangle$ that satisfies the annihilation conditions

$$J_{\geq 1+\theta}^+ |\mu_1, \mu_2, t; \theta\rangle = J_{\geq 1}^0 |\mu_1, \mu_2, t; \theta\rangle = J_{\geq 1-\theta}^- |\mu_1, \mu_2, t; \theta\rangle = 0 \quad (2.20)$$

⁸Here and henceforth, $\mathbb{N} = 1, 2, \dots$ and $\mathbb{N}_0 = 0, 1, 2, \dots$. We also use notations of the type of $\mathbb{Q}_- = \{x \in \mathbb{Q} \mid x < 0\}$, etc.

by a free action of the operators $J_{\leq -\theta-1}^+$, $J_{\leq -\theta-1}^-$, and $J_{\leq -1}^0$ and by the action of J_{θ}^+ and $J_{-\theta}^-$ subject to the constraint

$$J_{-\theta}^- J_{\theta}^+ |\mu_1, \mu_2, t; \theta\rangle = -\mu_1 \mu_2 |\mu_1, \mu_2, t; \theta\rangle. \quad (2.21)$$

In addition, the highest-weight state $|\mu_1, \mu_2, t; \theta\rangle$ satisfies

$$\left(J_0^0 + \frac{t-2}{2}\theta\right) |\mu_1, \mu_2, t; \theta\rangle = -\frac{1}{2}(1 + \mu_1 + \mu_2) |\mu_1, \mu_2, t; \theta\rangle. \quad (2.22)$$

2.3 Submodules and singular vectors in relaxed modules

The ‘Verma points’ encountered in the top floor of an extremal diagram of the relaxed module can of course be viewed as singular vectors. It is simply a reformulation of the above observations that the states

$$|C(n, \mu, t)\rangle = \begin{cases} (J_0^-)^{-n} |n, \mu, t\rangle, & n \in -\mathbb{N}, \\ (J_0^+)^{n+1} |n, \mu, t\rangle, & n \in \mathbb{N}_0 \end{cases} \quad (2.23)$$

satisfy the Verma highest-weight conditions for $n \leq -1$ and the twisted Verma highest-weight conditions with the twist parameter $\theta = 1$ for $n \geq 0$, hence the corresponding submodule is the Verma module or the twisted Verma module, respectively. The states (2.23) are called the *charged singular vectors*⁹.

The (twisted) Verma submodules may also occur ‘inside’ a given relaxed module \mathcal{R} rather than in its extremal diagram (such would be the submodules in the (twisted) Verma module generated from a charged singular vector; in fact, *every* Verma submodule in \mathcal{R} is necessarily a submodule in some ‘charged’ submodule). Besides the Verma or twisted Verma submodules, a relaxed module \mathcal{R} may also contain *relaxed* submodules. Such submodules are generated from the *relaxed singular vectors*. These states that satisfy the relaxed highest-weight conditions (2.8) (with the eigenvalues of J_0^0 and $J_0^- J_0^+$, obviously, labelled by different parameters than in (2.9)–(2.10)) were defined in [FST] in such a way as to guarantee that they generate the entire ‘floor’ of the extremal states. In what follows, we summarize the general construction for the relaxed singular vectors in the way that is more convenient for our present purposes.

Define the set

$$\mathbb{K}(t) = \left\{ a - bt \mid a, b \in \mathbb{Z}, a \cdot b > 0 \right\}. \quad (2.24)$$

and

$$\overline{\mathbb{K}}(t) = \begin{cases} \mathbb{K}(t) \setminus \{2\tilde{p}\}, & t = -\frac{\tilde{p}}{q}, \tilde{p} \in \mathbb{N}, q \in \mathbb{N}, \\ \mathbb{K}(t) & \text{otherwise.} \end{cases} \quad (2.25)$$

Then,

Theorem 2.4

1. Any submodule in a relaxed module is (a sum of the submodules) of only the following three types: relaxed modules, Verma modules, and the twisted Verma modules with the twist parameter $\theta = 1$.
2. The charged singular vectors in the relaxed module $\mathcal{R}_{\mu_1, \mu_2, t}$ are in the 1 : 1 correspondence with the distinct integers among $\{\mu_1, \mu_2\}$. Whenever $\mu_\alpha = n \in \mathbb{Z}$, the corresponding charged singular vector is given by (2.23). Further,

⁹The reason being that they are in a 1 : 1 correspondence with the $N = 2$ singular vectors that are traditionally called charged [BFK] (although the submodules generated from charged $N = 2$ singular vectors were described correctly only in [ST2]).

- (a) The submodule generated from $|C(n, \mu, t)\rangle$ is a Verma module if $n < 0$ and a twisted Verma module if $n \geq 0$.
 - (b) If both μ_1 and μ_2 are integers and $(\mu_1 + \frac{1}{2})(\mu_2 + \frac{1}{2}) > 0$, then one of the charged singular vectors belongs to the submodule generated from the other charged singular vector.
3. The relaxed module $\mathcal{R}_{\mu_1, \mu_2, t}$ contains at least one relaxed submodule if and only if
- (i) either $(\mu_1 \notin \mathbb{Z} \text{ or } \mu_2 \notin \mathbb{Z})$ and $\mu_1 - \mu_2 \in \mathbb{K}(t)$,
 - (ii) or $(\mu_1 \in \mathbb{Z} \text{ and } \mu_2 \in \mathbb{Z})$ and $\mu_1 - \mu_2 \in \overline{\mathbb{K}}(t)$

In terms of extremal diagrams, the condition in 2b means that the two charged singular vectors are on the same side of the highest-weight vector of the relaxed module. That is, we write $(\mu_1 + \frac{1}{2})(\mu_2 + \frac{1}{2}) > 0$ or < 0 to say that the cases where $(\mu_1 = 0, \mu_2 < 0)$ are considered along with those where $\mu_1\mu_2 < 0$, while $(\mu_1 = 0, \mu_2 > 0)$ is ‘unified’ with $\mu_1\mu_2 > 0$.

Part 1 follows from the analysis of extremal diagrams and the fact that the modules under consideration are the induced representations. Part 2 is obvious from the previous subsection and the explicit formulae (2.23). Apart from the ‘exception’ in 3(ii), ‘if’ statement of Part 3 follows from the explicit construction for singular vectors that we review shortly, while the ‘only if’ part relies on the evaluation of the Kač determinant. This has been done for the $N=2$ Verma modules [BFK], while the equivalence results of [FST] show that the zeros of the determinant are given by $\mu_\alpha \in \mathbb{Z}$ (which we already know to correspond to the charged singular vectors) and by condition $\mu_1 - \mu_2 \in \mathbb{K}(t)$. The exceptional case occurs for negative rational $t = -\frac{\tilde{p}}{q}$ when, in addition, $\mu_1, \mu_2 \in \mathbb{Z}$ are such that $\mu_2 - \mu_1 = 2\tilde{p}$. The determinant formula counts this case along with all the other zeros, however it follows from the analysis of [FST] that the *relaxed* submodule *does not exist* in this case – instead, there is a direct sum of a Verma and a twisted Verma submodule: on a given level, there are precisely as many states satisfying the relaxed highest-weight conditions as there would be if the relaxed submodule existed, however these states do not make up the extremal diagram of a relaxed module.

Further, all the instances where (twisted) Verma modules appear in a relaxed module are described in the following Theorem, which, again, is an immediate consequence of [FST].

Given an embedding of a (twisted) Verma module \mathcal{M} into a highest-weight module \mathcal{P} , let $|\widetilde{e}\rangle$ be the image of the highest-weight vector of \mathcal{M} . For brevity, we will say that \mathcal{M} is embedded onto level l if $|\widetilde{e}\rangle$ is at level l relative to the highest-weight vector of \mathcal{P} . Similarly, we will say that a relaxed module \mathcal{R}' is at level l in another relaxed module \mathcal{R} if the extremal states of \mathcal{R}' are on level l relative to the extremal states of \mathcal{R} . Now,

Theorem 2.5 *Let \mathcal{R} be a relaxed module.*

1. Every Verma or twisted Verma submodule \mathcal{C}' of \mathcal{R} is necessarily a submodule of a submodule $\mathcal{C} \subset \mathcal{R}$ generated from a charged singular vector in \mathcal{R} .
2. If \mathcal{R} contains a relaxed submodule \mathcal{R}' and also a charged singular vector generating a (twisted) Verma module \mathcal{C} , then the intersection $\mathcal{C}' \equiv \mathcal{R}' \cap \mathcal{C}$ is non-empty and is a (twisted) Verma submodule in \mathcal{R} . The highest-weight vector of \mathcal{C}' is a charged singular vector in \mathcal{R}' .

3. Let $|e\rangle$ be the highest-weight vector of a Verma (respectively, a twisted Verma) submodule in \mathcal{R} which is not a charged singular vector in \mathcal{R} . Let j be the charge of $|e\rangle$: $J_0^0|e\rangle = j|e\rangle$. Then one of the following is true:

- (a) there exists a relaxed submodule $\mathcal{R}' \subset \mathcal{R}$ on the same level in \mathcal{R} as the vector $|e\rangle$;
- (b) there exists exactly one twisted Verma (respectively, Verma) submodule in \mathcal{R} on the same level as $|e\rangle$ such that $J_0^0|e'\rangle = j'|e'\rangle$ with $j' = j + 1$ (respectively, $j - 1$). Then there are no relaxed submodules in \mathcal{R} on the same level as $|e\rangle$.

We see from Part 1 that Verma submodules (respectively, twisted Verma submodules) exist in \mathcal{R} if and only if there are charged singular vectors (2.23) with $n < 0$ (respectively, $n \geq 0$). For our present purposes, the significance of this fact is that, whenever a charged singular vector exists in \mathcal{R} , much of the embedding structure of \mathcal{R} can be deduced from the embedding diagram of the Verma module \mathcal{C} generated from the charged singular vector. relaxed submodules in \mathcal{R} correspond to submodules in \mathcal{C} . Since the enumeration of the latter is a classical result [RCW, Mal], we recover the embedding structure of relaxed submodules in \mathcal{R} .

Even more generally, irrespective of whether or not there are charged singular vectors in the relaxed module \mathcal{R} , one can still establish a correspondence between relaxed singular vectors in \mathcal{R} and singular vectors in certain Verma modules.

We will say that condition AD' is satisfied for a Verma submodule $\mathcal{M}' \subset \mathcal{M}_{j,t}$ if

(AD') $\mathcal{M}' \subset \mathcal{M}_{j,t}$, $t = \frac{p}{q} < 0$ is rational and negative, $(2j + 1)/(2p) \in \mathbb{Z}$, and the weight of \mathcal{M}' is antidominant.

Theorem 2.6 *Let $\mathcal{R} \equiv \mathcal{R}_{\mu_1, \mu_2, t}$ be a relaxed module and let $\mathbf{M} = \mathcal{M}_{j,t}$ be the Verma module with spin $j = \frac{1}{2}(\mu_1 - \mu_2 - 1)$.*

1. *If $\mu_1 - \mu_2 \notin \mathbb{Z}$, then relaxed submodules in \mathcal{R} are in a 1 : 1 correspondence with submodules in \mathbf{M} , the corresponding submodules being on the same level in \mathbf{M} and in \mathcal{R} . Moreover, two submodules $\mathcal{M}' \subset \mathbf{M}$ and $\mathcal{M}'' \subset \mathbf{M}$ are related by an embedding, $\mathcal{M}'' \subset \mathcal{M}'$, and only if the respective relaxed submodules in \mathcal{R} are related by the embedding $\mathcal{R}'' \subset \mathcal{R}'$.*
2. *If $\mu_1 - \mu_2 \in \mathbb{Z}$, then each submodule $\mathcal{M}' \subset \mathbf{M}$ that does not satisfy condition AD' corresponds to a relaxed submodule in \mathcal{R} . Two Verma modules $\mathcal{M}' \subset \mathbf{M}$ and $\mathcal{M}'' \subset \mathbf{M}$ correspond in this way to the same submodule in \mathcal{R} if and only if \mathcal{M}' and \mathcal{M}'' are on the same level in \mathbf{M} . Vice versa, to every relaxed submodule $\mathcal{R}' \subset \mathcal{R}$ on level l there corresponds at least one Verma submodule $\mathcal{M}' \subset \mathbf{M}$ on level l .*

We now outline the proof of this Theorem in the case where $\mu_1 \notin \mathbb{Z}$ and $\mu_2 \notin \mathbb{Z}$ (the case where the integers among $\{\mu_1, \mu_2\}$ give rise to one charged singular vector or to two charged singular vectors of the same twist is obtained by minor modifications, while the case with two charged singular vectors of different twists is more complicated and we refer the reader to Theorem 2.8).

Using Eqs. (2.7) (and similar relations involving $(J_0^+)^{\alpha}$), it is easy to check that, even though μ_{α} is complex, the states

$$(J_0^-)^{-\mu_{\alpha}} |\mu_1, \mu_2, t\rangle \quad \text{and} \quad (J_0^+)^{\mu_{\alpha}+1} |\mu_1, \mu_2, t\rangle \quad (2.26)$$

formally satisfy the Verma highest-weight conditions (2.3) with $\theta = 0$ or 1 respectively. The *auxiliary Verma modules* are defined as the Verma modules built on states (2.26). We denote these modules as $M_{1,2}^-$ and $M_{1,2}^+$, where the subscript corresponds to taking $\mu_\alpha = \mu_{1,2}$ and the superscript, to the respective vectors in (2.26). We see that

$$\begin{aligned} M_1^- &\approx \mathcal{M}_{\frac{1}{2}(\mu_1 - \mu_2 - 1), t}, & M_1^+ &\approx \mathfrak{M}_{\frac{1}{2}(t + \mu_1 - \mu_2 - 1), t; 1}, \\ M_2^- &\approx \mathcal{M}_{\frac{1}{2}(\mu_2 - \mu_1 - 1), t}, & M_2^+ &\approx \mathfrak{M}_{\frac{1}{2}(t + \mu_2 - \mu_1 - 1), t; 1}. \end{aligned} \quad (2.27)$$

Now, the condition that there be singular vectors in the auxiliary (twisted) Verma modules reads as follows:

$$\begin{aligned} \frac{1}{2}(\pm(\mu_1 - \mu_2) - 1) = j^+(r, s, t) &\iff \frac{1}{2}(t \mp (\mu_1 - \mu_2) - 1) = j^-(r, s, t), \\ \frac{1}{2}(\pm(\mu_1 - \mu_2) - 1) = j^-(r, s, t) &\iff \frac{1}{2}(t \mp (\mu_1 - \mu_2) - 1) = j^+(r, s, t). \end{aligned} \quad (2.28)$$

We now see that singular vectors exist in (at least one of) the auxiliary Verma modules if and only if $\mu_1 - \mu_2 \in \mathbb{K}(t)$. For example, singular vectors in the auxiliary Verma module M_1^- and in the twisted auxiliary Verma module M_2^+ read as

$$\begin{aligned} \mathcal{MFF}^-(r, s, t) (J_0^-)^{-\mu_1} |\mu_1, \mu_2, t\rangle, & \quad \mathcal{MFF}^+(r', s', t) (J_0^-)^{-\mu_1} |\mu_1, \mu_2, t\rangle, \\ \mathcal{MFF}^{+,1}(r, s, t) (J_0^+)^{\mu_2+1} |\mu_1, \mu_2, t\rangle, & \quad \mathcal{MFF}^{-,1}(r', s', t) (J_0^+)^{\mu_2+1} |\mu_1, \mu_2, t\rangle, \end{aligned} \quad \begin{cases} \mu_1 - \mu_2 = -r + ts, \\ \mu_1 - \mu_2 = r' - t(s' - 1), \\ r, s, r', s' \in \mathbb{N}, \end{cases} \quad (2.29)$$

where $\mathcal{MFF}^-(r, s, t)$ is the singular vector *operator* (read off by dropping the highest-weight state in (2.6)), and $\mathcal{MFF}^{+, \theta}(r, s, t)$ is the spectral flow transform (2.2) of the singular vector operator $\mathcal{MFF}^+(r, s, t)$. Similar expressions for the other two auxiliary vectors are obtained by changing $\mu_1 \leftrightarrow \mu_2$.

Note that, because of equivalence (2.28), the auxiliary Verma module M_1^- and the twisted module M_2^+ have the embedding diagrams that are mirror-symmetric to each other with respect to charge in the charge-level lattice: we see from (2.28) that a singular vector exists in M_1^- at level l if and only if a singular vector exists in M_2^+ at the same level l . If the singular vector in M_1^- is given by one of the expressions in the first line of (2.29), then the vector in M_2^+ is given by the corresponding expression in the second line of (2.29).

The construction of [FST], which we review in a moment, maps singular vectors (2.29) in the auxiliary modules into the states in $\mathcal{R}_{\mu_1, \mu_2, t}$ that satisfy the relaxed highest-weight conditions. Then in all cases except those described in Part 3(ii) of Theorem 2.4, there exists [FST] at least one extremal state that generates a relaxed submodule, therefore condition $\mu_1 - \mu_2 \in \overline{\mathbb{K}}(t)$ is sufficient in order that a relaxed singular vector exist in $\mathcal{R}_{\mu_1, \mu_2, t}$. That the condition $\mu_1 - \mu_2 \in \mathbb{K}(t)$ is necessary follows from the equivalence with the $N=2$ superconformal representation theory that was proved independently in [FST]. On the $N=2$ side, the expression of the Kač determinant is known, with this condition guaranteeing a zero (which is at the same time *not* the one corresponding to a charged singular vector).

To map singular vectors (2.29) back to $\mathcal{R}_{\mu_1, \mu_2, t}$, we use, again, complex powers of J_0^\pm . In order that no non-integral powers of J_0^\pm remain in the final expressions, we act on the respective states in (2.29) with $(J_0^-)^{\mu_1+N}$ and $(J_0^-)^{-\mu_2-1+N}$, where N is an integer, and make use of Eqs. (2.7). Analysing the relative J_0^0 charge and level of singular vectors (2.6), it is not difficult to see that, in order to be left with only *positive* integral powers after the rearrangements, the integer N has to be $\geq r + rs$. We thus define

$$\left| \Sigma_1^-(r, s, \mu_1 + \mu_2, t) \right\rangle = (J_0^-)^{\mu_1+r+rs} \mathcal{MFF}^-(r, s, t) (J_0^-)^{-\mu_1} |\mu_1, \mu_2, t\rangle, \quad \mu_1 - \mu_2 = -r + ts, \quad r, s \in \mathbb{N} \quad (2.30)$$

and

$$\left| \Sigma_2^+(r, s, \mu_1 + \mu_2, t) \right\rangle = (J_0^+)^{-\mu_2 - 1 + r + rs} \mathcal{MFF}^{+,1}(r, s, t) (J_0^+)^{\mu_2 + 1} |\mu_1, \mu_2, t\rangle, \quad \mu_1 - \mu_2 = -r + ts, \quad r, s \in \mathbb{N}, \quad (2.31)$$

and also $|\Sigma_2^-(r, s, \mu_1 + \mu_2, t)\rangle$ and $|\Sigma_1^+(r, s, \mu_1 + \mu_2, t)\rangle$, which are obtained by replacing $\mu_1 \leftrightarrow \mu_2$. Note that we do not discuss the vectors constructed by applying the \mathcal{MFF}^+ operators to $(J_0^-)^{-\mu_\alpha} \cdot |\mu_1, \mu_2, t\rangle$ and the $\mathcal{MFF}^{-,1}$ operators, to $(J_0^+)^{\mu_\alpha + 1} |\mu_1, \mu_2, t\rangle$. The reason is that these differ from the singular vectors in the auxiliary Verma (twisted Verma) module corresponding to the complementary μ by a power of J_0^- (resp., of J_0^+) and hence the construction of the type of (2.30) (resp., (2.31)) produces the same vectors in the relaxed module. Also, there is no need to consider all the four auxiliary Verma modules built on vectors (2.26), since singular vectors in these modules are correlated in accordance with (2.28).

Thus, $M_1^- \ni \mathcal{MFF}^+(r, s, t) (J_0^-)^{-\mu_1} |\mu_1, \mu_2, t\rangle$ with $s \neq 1$ if and only if $M_2^- \ni \mathcal{MFF}^-(r, s - 1, t) \cdot (J_0^-)^{-\mu_2} |\mu_1, \mu_2, t\rangle$; similarly, $M_2^+ \ni \mathcal{MFF}^{-,1}(r, s, t) (J_0^+)^{\mu_2 + 1} |\mu_1, \mu_2, t\rangle$ with $s \neq 1$ if and only if $M_1^+ \ni \mathcal{MFF}^{+,1}(r, s - 1, t) (J_0^+)^{\mu_1 + 1} |\mu_1, \mu_2, t\rangle$ (where $\mu_1 - \mu_2 = -r + t(s - 1)$, $r, s \in \mathbb{N}$).

The basic facts about singular vectors (2.30) and (2.31) are as follows:

Theorem 2.7 ([FST]) *Let $\mathcal{R} = \mathcal{R}_{\mu_1, \mu_2, t}$ be a relaxed module with $\mu_\alpha \notin \mathbb{Z}$.*

1. *Expressions (2.30) and (2.31) evaluate as elements of the relaxed module \mathcal{R} and satisfy the relaxed-highest-weight conditions*

$$\begin{aligned} J_{\geq 1}^+ \left| \Sigma_{1,2}^\pm(r, s, \mu_1 + \mu_2, t) \right\rangle &= J_{\geq 1}^0 \left| \Sigma_{1,2}^\pm(r, s, \mu_1 + \mu_2, t) \right\rangle = J_{\geq 1}^- \left| \Sigma_{1,2}^\pm(r, s, \mu_1 + \mu_2, t) \right\rangle = 0, \\ J_0^- J_0^+ \left| \Sigma_{1,2}^\pm(r, s, \mu_1 + \mu_2, t) \right\rangle &= -\mu_1^\pm \mu_2^\pm \left| \Sigma_{1,2}^\pm(r, s, \mu_1 + \mu_2, t) \right\rangle, \\ J_0^0 \left| \Sigma_{1,2}^\pm(r, s, \mu_1 + \mu_2, t) \right\rangle &= -\frac{1}{2}(\mu_1^\pm + \mu_2^\pm + 1) \left| \Sigma_{1,2}^\pm(r, s, \mu_1 + \mu_2, t) \right\rangle, \end{aligned} \quad (2.32)$$

where $\mu_{1,2} - \mu_{2,1} = -r + ts$ (with the first or the second subscript taken depending on whether $(\Sigma_1^-$ and $\Sigma_2^+)$ or $(\Sigma_2^-$ and $\Sigma_1^+)$ are being considered) and

$$\begin{aligned} \mu_1^\pm &= \pm \frac{r}{2} \pm \frac{t}{2}s \mp rs + \frac{\mu_1 + \mu_2}{2}, \\ \mu_2^\pm &= \mp \frac{r}{2} \mp \frac{t}{2}s \mp rs + \frac{\mu_1 + \mu_2}{2}. \end{aligned} \quad (2.33)$$

2. *Each of the vectors $|\Sigma_{1,2}^\pm(r, s, \mu_1 + \mu_2, t)\rangle$ generates a relaxed submodule. Moreover, the vectors $|\Sigma_1^-(r, s, \mu_1 + \mu_2, t)\rangle$ and $|\Sigma_2^+(r, s, \mu_1 + \mu_2, t)\rangle$ and, on the other hand, $|\Sigma_2^-(r', s', \mu_1 + \mu_2, t)\rangle$ and $|\Sigma_1^+(r', s', \mu_1 + \mu_2, t)\rangle$, are on the same level in \mathcal{R} and, moreover, each vector from the respective pair is a J_0^\pm -descendant of the other:*

$$\begin{aligned} \left| \Sigma_{1,2}^-(r, s, \mu_1 + \mu_2, t) \right\rangle &= c_{1,2}^- (J_0^-)^{2rs} \left| \Sigma_{2,1}^+(r, s, \mu_1 + \mu_2, t) \right\rangle, \\ \left| \Sigma_{1,2}^+(r, s, \mu_1 + \mu_2, t) \right\rangle &= c_{1,2}^+ (J_0^+)^{2rs} \left| \Sigma_{2,1}^-(r, s, \mu_1 + \mu_2, t) \right\rangle, \end{aligned} \quad (2.34)$$

where the numerical coefficients $c_{1,2}^\pm$ depend on $r, s, \mu_1 + \mu_2$, and t .

This construction can be illustrated in the following extremal diagram:

$$\begin{array}{c} \dots * \xleftarrow{J_0^-} * \xleftarrow{J_0^-} * \xleftarrow{J_0^-} * \xrightarrow{J_0^+} * \xrightarrow{J_0^+} * \xrightarrow{J_0^+} * \dots \\ \dots * \xleftarrow{J_0^-} * \xleftarrow{J_0^-} * \xleftarrow{J_0^-} * \xrightarrow{J_0^+} * \xrightarrow{J_0^+} * \xrightarrow{J_0^+} * \dots \\ \dots * \xleftarrow{J_0^-} * \xleftarrow{J_0^-} * \xleftarrow{J_0^-} * \xrightarrow{J_0^+} * \xrightarrow{J_0^+} * \xrightarrow{J_0^+} * \dots \end{array} \quad (2.35)$$

The lower floor is the extremal diagram of the relaxed *submodule*, every point in the lower floor satisfying the relaxed highest-weight conditions (2.8). The auxiliary Verma module (and its submodule) on the right are ‘rotated’ by the spectral flow transform with $\theta = 1$. The submodules arise in the auxiliary Verma modules simultaneously, in accordance with the above statements. The auxiliary Verma modules are to be thought of as disconnected from the extremal diagram of the relaxed module $\mathcal{R}_{\mu_1, \mu_2, t}$, since they do not belong to $\mathcal{R}_{\mu_1, \mu_2, t}$ as long as the mappings shown in dotted lines are given by complex powers of the generators.

To return to Theorem 2.6, we see that (in the case where with the relevant parameters do *not* become integers), the structure of embeddings of the relaxed submodules repeats the Verma-module embedding diagram for each of the auxiliary Verma modules, while all of the latter are identical up to mirror-symmetry. Theorem 2.7 ensures that the respective pairs of singular vectors in M_1^- and in M_2^+ give rise to the same relaxed submodule in $\mathcal{R}_{\mu_1, \mu_2, t}$. This shows Part 1 of Theorem 2.6.

On the other hand, in the case where $s = 1$, which is possible when $\Delta \equiv \mu_2 - \mu_1 \in \mathbb{Z}$, one of the auxiliary Verma modules is embedded into the other, and similarly for the twisted auxiliary modules; if, for definiteness, $\Delta \geq 0$, we have

$$\begin{aligned} (J_0^-)^{-\mu_1} |\mu_1, \mu_2, t\rangle &= (J_0^-)^\Delta \left((J_0^-)^{-\mu_2} |\mu_1, \mu_2, t\rangle \right) = \mathcal{MFF}^-(\Delta, 1, t) (J_0^-)^{-\mu_2} |\mu_1, \mu_2, t\rangle, \\ (J_0^+)^{\mu_2+1} |\mu_1, \mu_2, t\rangle &= (J_0^+)^\Delta \left((J_0^+)^{\mu_1+1} |\mu_1, \mu_2, t\rangle \right) = \mathcal{MFF}^{+,1}(\Delta, 1, t) (J_0^+)^{\mu_1+1} |\mu_1, \mu_2, t\rangle. \end{aligned} \quad (2.36)$$

Now, in the situation where $\Delta \in \mathbb{K}(t)$ —i.e., the auxiliary modules contain submodules—the standard fact about Verma-module embedding diagrams is that submodules in the auxiliary modules occur in pairs, with the highest-weight vectors of the submodules from the same pair embedded onto the same level. Moreover, one of these two highest-weight vectors is a J_0^- -descendant of the other. We thus see that the corresponding Σ^- vectors generate the same relaxed submodule in $\mathcal{R}_{\mu_1, \mu_2, t}$. The same is true for the twisted auxiliary Verma module. We thus arrive at Part 2 of Theorem 2.6 in the case where none of the μ_α are integers.

Let us now discuss briefly the case where exactly one of the μ_α is an integer. Then one of the vectors (2.26) becomes a charged singular vector, and the corresponding (twisted) auxiliary module becomes a Verma submodule of $\mathcal{R}_{\mu_1, \mu_2, t}$, while the relaxed submodules in \mathcal{R} are still generated from the other auxiliary Verma modules in accordance with the above procedure. One of the relations (2.34) may not hold then if the corresponding Σ^\pm vector lies in the Verma submodule \mathcal{C} generated from a charged singular vector in relaxed submodule \mathcal{R}' . Then, obviously, the corresponding vector Σ^+ (or Σ^-) does not generate the entire relaxed module \mathcal{R}' . However, the other vector Σ^- (respectively, Σ^+) does generate the relaxed submodule.

Next, in the case where the relaxed module $\mathcal{R}_{\mu_1, \mu_2, t}$ contains two charged singular vectors of the same twist, the relaxed submodules may be generated by the auxiliary Verma modules with the complementary twist. Then, we have $\mu_1 - \mu_2 \in \mathbb{Z}$, hence each relaxed submodule corresponds to a pair of singular vectors in the auxiliary Verma module and contains two charged singular vectors. A minor additional problem is encountered in the case where μ_1 equals -1 or 0 . Then one may be unable to arrive at highest-weight state of the auxiliary Verma module using formulae (2.26). However, replacing the highest-weight vector with a different point from the orbit (see Definition 2.3), the situation is reduced to the previous one.

Further, in the case where $\mu_1 = \mu_2 \in \mathbb{Z}$, there is only one charged singular vector, however if $0 = \mu_1 - \mu_2 \in \mathbb{K}(t)$ (which may be the case only when $t \in \mathbb{Q}$, $t > 0$), then there are relaxed submodules

in $\mathcal{R}_{\mu_1, \mu_2, t}$, each of which contains two charged singular vectors (obviously, with the same sign of n from (2.23)) and, therefore, each relaxed submodule corresponds to a pair of Verma-module singular vectors.

Finally, the case where $\mu_1 \in -\mathbb{N}$ and $\mu_2 \in \mathbb{N}_0$, is more involved. It will be described in more detail in Sec. 3.2, paragraphs $\mathbf{III}_{\pm}^0(2, -+)$ and $\mathbf{III}_{\pm}^{00}(2, -+)$, while now we only formulate the following general result [FST]:

Theorem 2.8 *Let $\mathcal{R} \equiv \mathcal{R}_{\mu_1, \mu_2, t}$ be a relaxed module, and $\mu_1 \in -\mathbb{N}$ and $\mu_2 \in \mathbb{N}_0$. Let then \mathcal{C}_- , and \mathcal{C}_+ be the corresponding Verma module and the twisted Verma module, respectively, generated from the charged singular vectors. Then*

1. *whenever two Verma modules $\tilde{\mathcal{C}}_-''$ and \mathcal{C}_-'' are embedded onto the same level l in \mathcal{R} , there exist two twisted Verma modules $\tilde{\mathcal{C}}_+''$ and \mathcal{C}_+'' embedded onto the same level, and vice versa. In this case, there is a relaxed submodule \mathcal{R}' whose highest-weight vector is on the same level l . We label the modules so that $\tilde{\mathcal{C}}_-'' \supset \mathcal{C}_-''$ and $\tilde{\mathcal{C}}_+'' \supset \mathcal{C}_+''$. Then we have the embeddings*

$$\begin{array}{ccc}
 & \tilde{\mathcal{C}}_-'' \oplus \tilde{\mathcal{C}}_+'' & \\
 \nearrow & \uparrow & \nwarrow \\
 \mathcal{C}_-'' & \longrightarrow \mathcal{R}' & \longleftarrow \mathcal{C}_+''
 \end{array} \tag{2.37}$$

2. *if there is exactly one Verma submodule \mathcal{C}'_- embedded on a given level l in \mathcal{R} , then there also exists exactly one twisted Verma module \mathcal{C}'_+ on the same level, and vice versa. In this case, one of the following is true:*
 - (a) \mathcal{C}'_- (\mathcal{C}'_+) satisfies condition AD' in \mathcal{C}_- (respectively, \mathcal{C}_+); then there are no relaxed submodules on any level $\geq l$ in \mathcal{R} ;
 - (b) the Verma module \mathcal{C}'_- (hence, also \mathcal{C}'_+) contains proper submodule(s); then there exists a relaxed submodule \mathcal{R}' on level l in \mathcal{R} and, moreover, \mathcal{C}'_- and \mathcal{C}'_+ are generated from the charged singular vectors in \mathcal{R}' . In this case, further, \mathcal{R}' is a maximal submodule in \mathcal{R} in the following sense: for a relaxed module $\tilde{\mathcal{R}}$, we have $\mathcal{R}' \subset \tilde{\mathcal{R}} \subset \mathcal{R} \implies \tilde{\mathcal{R}} = \mathcal{R}'$ or $\tilde{\mathcal{R}} = \mathcal{R}$.

3 Classifying the embedding diagrams

As we have seen, singular vectors in relaxed modules are of two basic types: the charged ones, which occur directly in the extremal diagram, and all the others, i.e., those occurring ‘inside’ the module, which can be either (twisted) Verma modules or the relaxed modules. The crucial point is that, in the general position, the relaxed submodules are determined by the usual singular vectors in the auxiliary Verma modules. Accordingly, the embedding diagrams of relaxed modules can be determined knowing the standard $\widehat{\mathfrak{sl}}(2)$ Verma-module embedding diagrams and analysing the possible existence of charged singular vectors. The appearance of a charged singular vector can be interpreted as the case where the entire embedding diagram of auxiliary Verma module is attached to the ‘relaxed’ embedding diagram. When this happens with two charged singular vectors, the rule according to which the ‘relaxed’ part of the diagram is determined by its Verma parts becomes slightly more complicated, but it is still true that the ‘relaxed’ part can be reconstructed knowing how the Verma modules are embedded into each other. One can also have ‘combined’ degenerations, where charged singular vectors appear simultaneously with further degenerations

occurring in the Verma embedding diagrams. A useful observation is that whenever there is at least one charged singular vector, then, taking the *quotient* (with respect to the maximal submodule if there are two charged singular vectors of the same twist), we are left with the known embedding diagrams of the usual Verma modules. This, in particular, gives another way to recover the standard $\widehat{sl}(2)$ Verma-module embedding diagrams and serves as a good check on the relaxed embedding diagrams given below.

3.1 Classifying the degeneration patterns

We now apply the above Theorems in order to derive the classification of embedding diagrams of relaxed modules. The result consists in the embedding diagrams of the relaxed modules $\mathcal{R}_{\mu_1, \mu_2, t}$ listed below. The different entries of the following list (summarized in the Table on p. 21) are labelled using the familiar I-II-III pattern [FF, FFr], with an additional indication of how many (0, 1, or 2) of the μ_α are integers and what their signs are. Thus, numbers 0, 1, and 2 refer to the existence of submodules generated from charged singular vectors, whereas the Roman numbers I, II, and III indicate the existence of relaxed submodules (0, 1, and ≥ 2 , respectively). Whenever there are submodules generated from charged singular vectors, we also use the signs $-$ or $+$ to indicate whether these correspond to negative or non-negative n in (2.23), respectively. The signs can also be read as the indication of the twists: the modules generated from charged singular vectors with $n \leq -1$ have twist 0, while those generated from charged singular vectors with $n \geq 0$, twist 1. Thus, for example, III(2, $-+$) indicates two submodules generated from charged singular vectors, one of which is untwisted and the other is twisted (always by $\theta = 1$). Note, however, that we use the notation III $_+$ for the *positive* zone $t > 0$, and III $_-$ for the negative zone $t < 0$, which is opposite to the notations used by some other authors. Further, whenever exactly one of μ_1, μ_2 is an integer, we take this to be μ_1 ; when both μ_1 and μ_2 are integers, we choose $\mu_1 \leq \mu_2$. Finally, for a rational t in the negative zone, $t = -\tilde{p}/q$, we will be interested in the total number of submodules in a given relaxed module. Whenever there *is* at least one relaxed submodule, we have $\mu_1 - \mu_2 \in \overline{\mathbb{K}}(t)$ (hence, in particular, $\mu_1 - \mu_2 \in \mathbb{Q}$); in fact, already for $\mu_1 - \mu_2 \in \mathbb{K}(t)$, we can write

$$|\mu_1 - \mu_2| = \tilde{p}\xi + \zeta + \eta \frac{\tilde{p}}{q} \quad (3.1)$$

where, in general, $0 \leq \zeta < \tilde{p}$, $0 \leq \eta < q$, and $\xi \in \mathbb{N}_0$, with $\xi^2 + \zeta^2 \neq 0$, $\xi^2 + \eta^2 \neq 0$, and $\xi^2 + \eta^2 + \zeta^2 \neq 1$. Then ξ is responsible for the number of submodules, as we will see in each of the particular cases.

An important remark is in order regarding how we divide the set of (μ_1, μ_2, t) into different cases. One may classify the different embedding diagram patterns using, among others, the same criterion as in [FF], where the cases were singled out according to the number of integral points on a certain line in the $(\mu_1 - \mu_2, t)$ plane. Instead, we have chosen a more ‘direct’ classification according to the values of μ_1, μ_2 , etc. However, the price to be paid is that we have to explicitly point out that some of the diagrams with negative rational t — namely, those in which there are a ‘minimal’ number of submodules — are identical to the irrational- t diagrams, where the very fact that $t \notin \mathbb{Q}$ implies that only the ‘minimal’ number of submodules be possible. That is, while the generic situation for the rational t is that there exists a chain of embedded submodules, this chain becomes finite in the negative zone and, moreover, may contain at most one submodule of each kind when $\xi = 0, 1, 2, 3$ in Eq. (3.1). We believe that this obvious fact does not confuse the classification of different degeneration patterns, therefore we will characterize the I-II-III cases by the ‘generic’ conditions (e.g., $t \notin \mathbb{Q}$). To be completely explicit, however, we will also point out such ‘small- ξ exceptions’ explicitly.

Now, the classification is as follows.

I: $\mu_1 - \mu_2 \notin \mathbb{K}(t)$. The simple diagrams shown in (3.2) and (3.3) exhaust the possibilities that can occur in this case. Namely, the different cases are as follows:

I(0): $\mu_1 \notin \mathbb{Z}, \mu_2 \notin \mathbb{Z}$. This is the trivial case, the embedding diagram consisting of the lonely relaxed module.

I(1): $\mu_1 \in \mathbb{Z}, \mu_2 \notin \mathbb{Z}$ or $\mu_1 = \mu_2 \in \mathbb{Z}$. In this case we have a single Verma or a twisted Verma submodule:

I(1,-): a Verma module if $\mu_1 \in -\mathbb{N}$, or

I(1,+): a twisted Verma module if $\mu_1 \in \mathbb{N}_0$,

which is embedded via a charged singular vector, Eq. (3.2).

I(2): $\mu_1 \in \mathbb{Z}, \mu_2 \in \mathbb{Z}, \mu_1 \neq \mu_2$. Whenever $\mu_1 \cdot \mu_2 > 0$, we have one of the following two ‘mirror-symmetric’ cases depending on whether μ_1 and μ_2 are negative or positive:

I(2,-,-): $\mu_1, \mu_2 \in -\mathbb{N}$, the first diagram in (3.3).

I(2,+,+): $\mu_1, \mu_2 \in \mathbb{N}_0$, the second diagram in (3.3).

If, on the other hand, μ_1 and μ_2 are of different signs, we have

I(2,-,+): $\mu_1 \in -\mathbb{N}, \mu_2 \in \mathbb{N}_0$, with the third diagram in (3.3).

II: $\mu_1 - \mu_2 \in \mathbb{K}(t), t \notin \mathbb{Q}$. The first condition guarantees that there exists at least one relaxed submodule; on the other hand, $t \notin \mathbb{Q}$ implies that there will be not more than one relaxed submodule.

II(0): $\mu_1 \notin \mathbb{Z}, \mu_2 \notin \mathbb{Z}$. In this case we have the first of the diagrams (3.4). In addition, this diagram can be viewed as a particular case of some of the diagrams of case III (those with rational t), namely with $t = -\frac{\tilde{p}}{q}$ and $|\mu_1 - \mu_2|$ as in (3.5).

II(1): $\mu_1 \in \mathbb{Z}, \mu_2 \notin \mathbb{Z}$. In this case, we have the respective diagrams (3.4), depending on the sign of μ_1 :

II(1,-): $\mu_1 \in -\mathbb{N}$,

II(1,+): $\mu_1 \in \mathbb{N}_0$.

These two diagrams are mirror-symmetric in the obvious sense.

In addition, the same diagram can be viewed as a particular case of some of the embedding diagrams of the rational- t case III, namely those where $t = -\frac{\tilde{p}}{q}$ and $|\mu_1 - \mu_2|$ is as in (10).

III: $\mu_1 - \mu_2 \in \mathbb{K}(t), t \in \mathbb{Q}$. This case comprises all the most interesting embedding diagrams.

III $_{\pm}$: $\mu_1 - \mu_2 \notin \mathbb{Z}, (\mu_1 - \mu_2)/t \notin \mathbb{Z}$. We then have the following cases:

III $_{\pm}$ (0): $\mu_1 \notin \mathbb{Z}, \mu_2 \notin \mathbb{Z}$. This corresponds to the double-chain (3.7) of relaxed modules. The chain is finite or infinite depending on whether t is negative/positive. In either case, the structure of the embedding diagram of the relaxed module repeats [FST] the structure of the embedding diagram of the auxiliary Verma module.

III $_{\pm}$ (1): $\mu_1 \in \mathbb{Z}, \mu_2 \notin \mathbb{Z}$. Depending on the sign of μ_1 , we have one of the following ‘mirror-symmetric’ cases:

III $_{\pm}(1,-)$: $\mu_1 \in -\mathbb{N}$, diagram (3.9). Embeddings via charged singular vectors (the horizontal arrows) repeat for every relaxed module in the diagram. Again, the Verma dots are placed on the left of the boxes representing relaxed modules, in accordance with how the Verma modules are embedded via charged singular vectors into the relaxed module, see (2.17).

III $_{\pm}(1,+)$: $\mu_1 \in \mathbb{N}_0$. We have diagram (3.10) with the open dots representing twisted Verma modules. In view of how the twisted Verma submodules appear in relaxed modules, see (2.19), the twisted-Verma modules are drawn on the right of the relaxed ones.

III $_{\pm}^0$: *Either* $(\mu_1 - \mu_2 \in \mathbb{Z}, (\mu_1 - \mu_2)/t \notin \mathbb{Z})$ *or* $(\mu_1 - \mu_2 \notin \mathbb{Z}, (\mu_1 - \mu_2)/t \in \mathbb{Z})$.

III $_{\pm}^0(0)$: $\mu_1 \notin \mathbb{Z}, \mu_2 \notin \mathbb{Z}$, with the embedding diagram (3.11). One of the following two things happens in the auxiliary Verma module, with the same effect on the embedding diagram of relaxed modules: (a) the auxiliary Verma-module embedding diagram degenerates into a single-chain (whenever $(\mu_1 - \mu_2)/t \in \mathbb{Z}$); (b) it acquires embeddings via $\text{MFF}^+(r, 1, t)$ singular vectors (whenever $\mu_1 - \mu_2 \in \mathbb{Z}$, see Part 2 of Theorem 2.6). In either case, the ‘relaxed’ double-chain (3.7) collapses to a single chain (3.11).

III $_{\pm}^0(1)$: $\mu_1 \in \mathbb{Z}, \mu_2 \notin \mathbb{Z}$. This means that $\mu_1 - \mu_2 \notin \mathbb{Z}$, hence we should have $(\mu_1 - \mu_2)/t \in \mathbb{Z}$. Then there are two possibilities:

III $_{\pm}^0(1,-)$: $\mu_1 \in -\mathbb{N}$, diagram (3.12);

III $_{\pm}^0(1,+)$: $\mu_1 \in \mathbb{N}_0$, the embedding diagram being the vertical mirror of (3.12), with the replacement $\bullet \rightsquigarrow \circ$.

As can be seen, the single-chain of relaxed modules is in this case due to the fact that the Verma embedding diagram is also a single chain (because of $(\mu_1 - \mu_2)/t \in \mathbb{Z}$); as usual, $\mu_1 \in \mathbb{Z}$ implies that the Verma and the ‘relaxed’ diagrams are attached to each other by embeddings via charged singular vectors.

III $_{\pm}^0(2)$: $\mu_1 \in \mathbb{Z}, \mu_2 \in \mathbb{Z}$. Since $\mu_1 - \mu_2 \in \mathbb{Z}$, we should have $(\mu_1 - \mu_2)/t \notin \mathbb{Z}$. Then, there are the following cases depending on the signs of μ_1 and μ_2 :

III $_{\pm}^0(2,-)$: $\mu_1 \in -\mathbb{N}, \mu_2 \in -\mathbb{N}$, with the diagram (3.13), in which each pair of Verma modules on the same level (i.e., with one embedded into the other by an $\text{MFF}^+(r, 1, t)$ singular vector) correspond to one relaxed module.

III $_{\pm}^0(2,++)$: $\mu_1 \in \mathbb{N}_0, \mu_2 \in \mathbb{N}_0$. We have a vertical mirror of (3.13), with the Verma modules replaced by spectral-flow-transformed Verma modules with $\theta = 1$.

III $_{\pm}^0(2,-+)$: $\mu_1 \in -\mathbb{N}, \mu_2 \in \mathbb{N}_0$, diagram (3.32). This case is considerably different from the previous ones, since two charged singular vectors in the relaxed module appear on different sides of the highest-weight vector. Thus, both Verma and twisted-Verma submodules are present simultaneously.

III $_{\pm}^{00}$: $\mu_1 - \mu_2 \in \mathbb{Z}, (\mu_1 - \mu_2)/t \in \mathbb{Z}$. Setting $t = \frac{p}{q}$, we have $(\mu_1 - \mu_2)/t \in \mathbb{Z}$ if and only if $(\mu_1 - \mu_2)/p \in \mathbb{Z}$.

III $_{\pm}^{00}(0)$: $\mu_1 \notin \mathbb{Z}, \mu_2 \notin \mathbb{Z}$. The embedding diagram is a single-chain as in (3.11). However, *in the negative zone*, the diagram is half that long as (3.11), which is in accordance with

the ‘double’ degeneration taking place in the auxiliary Verma module, where one has a single-chain of Verma modules, with *two* modules embedded on each level.

$\text{III}_{\pm}^{00}(2)$: $\mu_1 \in \mathbb{Z}, \mu_2 \in \mathbb{Z}$. Whenever $\mu_1 \cdot \mu_2 > 0$, we have one of the following two possibilities:

$\text{III}_{\pm}^{00}(2,--)$: $\mu_1 \in -\mathbb{N}, \mu_2 \in -\mathbb{N}$, diagram (3.35), where the Verma dots make up the ‘doubly-degenerate’ embedding diagram as the one mentioned in $\text{III}_{\pm}^{00}(0)$. *In the negative zone* ($t < 0$), where the embedding diagram is finite, we can further distinguish the following two cases depending on how the modules arrange near the bottom of the embedding diagram:

- i) $(\mu_1 - \mu_2)/p$ is odd, in which case the embeddings terminate as in the first diagram in (3.37).
- ii) $(\mu_1 - \mu_2)/p$ is even, in which case the embeddings terminate as in the second diagram in (3.37).

In the case where $\mu_1 = \mu_2$ (which is possible only when $t > 0$), a special subcase is described by diagram (3.36).

$\text{III}_{\pm}^{00}(2,++)$: $\mu_1 \in \mathbb{N}_0, \mu_2 \in \mathbb{N}_0$. The embedding diagram is the mirror of (3.35), with Verma modules replaced by twisted Verma modules. *In the negative zone*, in complete similarity with $\text{III}_{\pm}^{00}(2,--)$, we can distinguish two cases,

- i) $(\mu_1 - \mu_2)/p$ odd,
- ii) $(\mu_1 - \mu_2)/p$ even,

which, again, are the mirror of (3.37), and similarly with the special case where $\mu_1 = \mu_2$.

If, on the other hand, $\mu_1 \cdot \mu_2 < 0$, we have the following case:

$\text{III}_{\pm}^{00}(2,-+)$: $\mu_1 \in -\mathbb{N}, \mu_2 \in \mathbb{N}_0$. We have the embedding diagram (3.40), where the pairs of Verma modules are at the same level as the corresponding pair of twisted Verma modules. *In the negative zone*, the diagram is finite and we have two possibilities of its structure near the bottom, shown in (3.41):

- i) $(\mu_1 - \mu_2)/p$ is odd,
- ii) $(\mu_1 - \mu_2)/p$ is even. Then the Verma modules with the antidominant weights are not embedded by charged singular vectors into any relaxed module—*there is no relaxed module* at the bottom level in the diagram. In the particular case where, in addition to the requirements specified above, $\mu_2 - \mu_1 = 2\tilde{p}$, with $t = -\frac{\tilde{q}}{q}$ for $\tilde{p}, q \in \mathbb{N}$, we have the ‘exceptional’ diagram (3.42) with no relaxed submodules.

The above cases are summarized in the Table, where we include references to the corresponding diagrams. We now list the corresponding embedding diagrams and comment on their structure.

3.2 The diagrams

Notations. *The arrows are always drawn in the direction from the parent module to the child (embedded) module.* The filled dots \bullet denote the usual Verma modules, the open dots \circ are the twisted Verma modules

	$\mu_1, \mu_2 \notin \mathbb{Z}$	$\mu_1 \in \mathbb{Z}, \mu_2 \notin \mathbb{Z}$	$\mu_1, \mu_2 \in \mathbb{Z}$	
			$\mu_1 \cdot \mu_2 > 0$	$\mu_1 \cdot \mu_2 < 0$
$\mu_1 - \mu_2 \notin \mathbb{K}(t),$	I(0), Eq. (3.2)	I(1), Eq. (3.2)	I(2, --) and I(2, ++), Eq. (3.3)	I(2, -+), Eq. (3.3)
$\mu_1 - \mu_2 \in \mathbb{K}(t),$ $t \notin \mathbb{Q}$	II(0), Eq. (3.4)	II(1), Eq. (3.4)	—	—
$\mu_1 - \mu_2 \in \mathbb{K}(t),$ $t \in \mathbb{Q},$ $\mu_1 - \mu_2 \notin \mathbb{Z},$ $(\mu_1 - \mu_2)/t \notin \mathbb{Z}$	III $_{\pm}$ (0), Eq. (3.7)	III $_{\pm}$ (1), Eq. (3.9) and (3.10)	—	—
$\mu_1 - \mu_2 \in \mathbb{K}(t),$ $t \in \mathbb{Q},$ $\mu_1 - \mu_2 \in \mathbb{Z},$ $(\mu_1 - \mu_2)/t \notin \mathbb{Z}$	III $_{\pm}^0$ (0), Eq. (3.11)	—	III $_{\pm}^0$ (2, --), Eq. (3.13), and III $_{\pm}^0$ (2, ++)	III $_{\pm}^0$ (2, -+), Eq. (3.32)
$\mu_1 - \mu_2 \in \mathbb{K}(t),$ $t \in \mathbb{Q},$ $\mu_1 - \mu_2 \notin \mathbb{Z},$ $(\mu_1 - \mu_2)/t \in \mathbb{Z}$	—	III $_{\pm}^0$ (1), Eq. (3.12)	—	—
$\mu_1 - \mu_2 \in \mathbb{K}(t),$ $t \in \mathbb{Q},$ $\mu_1 - \mu_2 \in \mathbb{Z},$ $(\mu_1 - \mu_2)/t \in \mathbb{Z}$	III $_{\pm}^{00}$ (0)	—	III $_{\pm}^{00}$ (2, --), Eq. (3.35), and III $_{\pm}^{00}$ (2, ++)	III $_{\pm}^{00}$ (2, -+), Eq. (3.40)

Table 1: *Classification of the embedding diagram patterns.* For brevity, the notation $\mu_1\mu_2 < 0$ is used for the column that also includes the cases where $\mu_1 = 0$ and $\mu_2 < 0$, and similarly with $\mu_1\mu_2 > 0$, where it may be the case that $\mu_1 = 0$ and $\mu_2 > 0$.

with the twist parameter $\theta = 1$, and \blacksquare are the relaxed modules. Embeddings of Verma modules and of twisted Verma modules into relaxed modules associated with charged singular vectors are shown with horizontal arrows, because the highest-weight vector of the Verma submodule (see (2.17)) and that of the twisted Verma submodule (see (2.19)) are on the same level as the relaxed highest-weight vector. Then, we also have to use horizontal arrows to represent the embeddings of Verma modules into each other performed by the $\text{MFF}^+(r, 1, t)$ singular vectors and, similarly, for the embeddings of twisted Verma modules performed by the $\text{MFF}^-(r, 1, t)$ singular vectors. Moreover, in accordance with how the Verma- and twisted Verma submodules appear in relaxed modules (see (2.17) and (2.19)), we place the Verma modules on the left, and the twisted Verma modules, on the right of the symbol designating the relaxed module into which they are embedded via a charged singular vector. Then the x -coordinate in the embedding diagrams can qualitatively be associated with the J_0^0 -charge of highest-weight vectors¹⁰.

¹⁰Although we do not indicate them explicitly, the (charge, level) coordinates are not difficult to specify for each module in every embedding diagram, for instance by taking the relevant parameters from the standard *Verma* embedding diagrams and then applying the above Theorems in order to translate these into the μ_1 and μ_2 parameters of each of the relaxed modules.

I. $\mu_1 - \mu_2 \notin \mathbb{K}(t)$. In the cases where $(\mu_1 \notin \mathbb{Z}, \mu_2 \notin \mathbb{Z})$, $(\mu_1 \in -\mathbb{N}, \mu_2 \notin \mathbb{Z})$, and $(\mu_1 \in \mathbb{N}_0, \mu_2 \notin \mathbb{Z})$, we have the following simple diagrams, respectively:

$$\begin{array}{ccc}
 \blacksquare & \bullet \longleftarrow \blacksquare & \blacksquare \longrightarrow \circ \\
 \text{I}(0) & \text{I}(1,-) & \text{I}(1,+)
 \end{array} \tag{3.2}$$

The second and the third diagram also describe the case of $\mu_1 = \mu_2 \in \mathbb{Z}$. Note that, in the $\text{I}(1, \pm)$ cases, taking the quotient with respect to the Verma submodule embedded via the charged singular vector, we are left with an irreducible (twisted) Verma module, in accordance with the fact that the Verma-module spin j is such that $2j + 1 = \mu_1 - \mu_2 \notin \mathbb{K}(t)$.

Whenever both μ_1 and μ_2 are (distinct) integers, the diagrams are as follows:

$$\begin{array}{ccc}
 \bullet \longleftarrow \bullet \longleftarrow \blacksquare & \blacksquare \longrightarrow \circ \longrightarrow \circ & \bullet \longleftarrow \blacksquare \longrightarrow \circ \\
 \text{I}(2,--) & \text{I}(2,++) & \text{I}(2,-+)
 \end{array} \tag{3.3}$$

for $(\mu_1, \mu_2 \in -\mathbb{N})$, $(\mu_1, \mu_2 \in \mathbb{N}_0)$, and $(\mu_1 \in -\mathbb{N}, \mu_2 \in \mathbb{N}_0)$, respectively.

As regards the cases shown in (3.3), it may be useful to explicitly solve the conditions $(\mu_1 - \mu_2 \notin \mathbb{K}(t), \mu_1 - \mu_2 \in \mathbb{Z})$. We thus find that either $t \notin \mathbb{Q}$ or $t \in \mathbb{Q}_-$, $t = -\frac{\tilde{p}}{q}$, $|\mu_1 - \mu_2| \leq \tilde{p}$.

II. $\mu_1 - \mu_2 \in \mathbb{K}(t)$, $t \notin \mathbb{Q}$. When none or precisely one of μ_1 and μ_2 is an integer, we have the diagrams (in the cases where $(\mu_1 \notin \mathbb{Z}, \mu_2 \notin \mathbb{Z})$, $(\mu_1 \in -\mathbb{N}, \mu_2 \notin \mathbb{Z})$, and $(\mu_1 \in \mathbb{N}_0, \mu_2 \notin \mathbb{Z})$, respectively):

$$\begin{array}{ccc}
 \blacksquare & \begin{array}{ccc} \bullet & \longleftarrow & \blacksquare \\ \downarrow & & \downarrow \\ \bullet & \longleftarrow & \blacksquare \end{array} & \begin{array}{ccc} \blacksquare & \longrightarrow & \circ \\ \downarrow & & \downarrow \\ \blacksquare & \longrightarrow & \circ \end{array} \\
 \text{II}(0) & \text{II}(1,-) & \text{II}(1,+)
 \end{array} \tag{3.4}$$

Diagrams $\text{II}(1,-)$ and $\text{II}(1,+)$ are mirror-symmetric in the obvious sense, which is in fact the general relation between the $(1,-)$ and $(1,+)$ embedding diagrams. In the diagrams, we place the submodules embedded via charged singular vectors with $\mu_1 \in -\mathbb{N}$ on the left of the relaxed module in accordance with how such a charged singular vector actually appears in the relaxed module, Eq (2.17). Similarly (see (2.19)), the twisted Verma submodules embedded via charged singular vectors with $\mu_1 \in \mathbb{N}_0$ are shown on the right of the relaxed module.

The same extremal diagrams occur for the rational negative $t = -\frac{\tilde{p}}{q}$ and for $\mu_\alpha \notin \mathbb{Z}$ such that

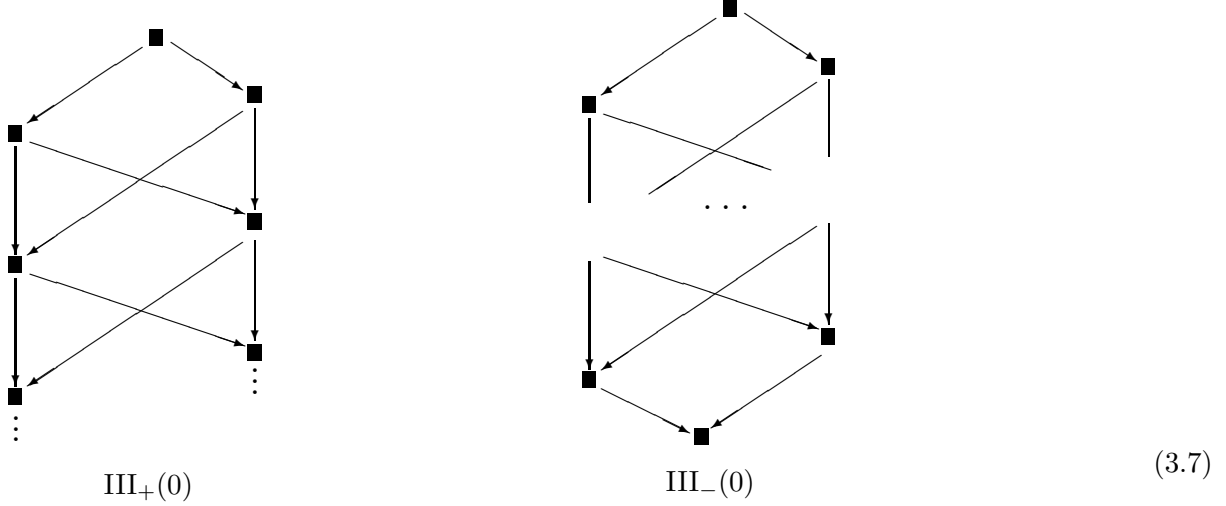
$$\pm(\mu_1 - \mu_2) = \begin{cases} \tilde{p} + \zeta, & 0 < \zeta < \tilde{p}, \\ \omega + \eta \frac{\tilde{p}}{q}, & 0 < \omega \leq \tilde{p}, 0 < \eta < q, \\ 2\tilde{p}, \\ 3\tilde{p} \end{cases} \implies \text{diagram II}(0) \tag{3.5}$$

and for $\mu_1 \in \mathbb{Z}$, $\mu_2 \notin \mathbb{Z}$ such that

$$|\mu_1 - \mu_2| = \omega + \eta \frac{\tilde{p}}{q}, \quad 0 < \omega \leq \tilde{p}, \quad 0 < \eta < q, \quad \implies \text{diagrams II}(1). \tag{3.6}$$

Again, taking the quotient of, e.g., the $\text{II}(1,+)$ diagram with respect to the charged singular vector, we are left with a Verma module $\mathcal{M}_{-\frac{1}{2}(\mu_2 - \mu_1 + 1), t}$, which has precisely one singular vector.

III_±(0). $\mu_1 - \mu_2 \in \mathbb{K}(t)$, $t \in \mathbb{Q}$, $\mu_1 - \mu_2 \notin \mathbb{Z}$, $(\mu_1 - \mu_2)/t \notin \mathbb{Z}$, $\mu_1 \notin \mathbb{Z}$, $\mu_2 \notin \mathbb{Z}$. In accordance with Part 1 of Theorem 2.6, we have the double-chain of relaxed modules



which, therefore, looks identical to the standard embedding diagrams of the ordinary Verma modules.

In the negative zone $t \in \mathbb{Q}_-$, the chain is finite. Since we have required $\mu_1 - \mu_2 \notin \mathbb{Z}$ and $(\mu_1 - \mu_2)/t \notin \mathbb{Z}$, we have

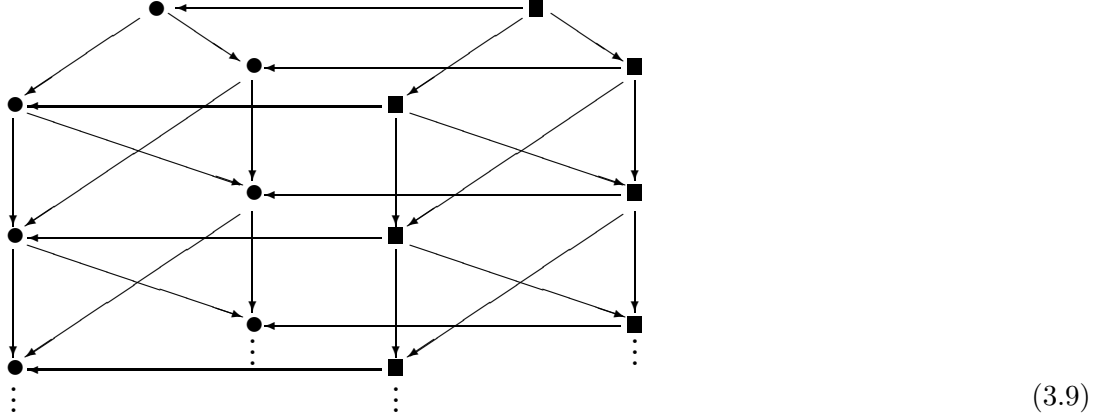
$$0 < \zeta < \tilde{p}, \quad 0 < \eta < q, \quad \xi \in \mathbb{N}_0 \quad (3.8)$$

in (3.1). Then the total number of *embedded* submodules in the III₋(0) case is $2\xi + 1$ (ξ submodules in each branch, plus the bottom one). Thus, the case where $\xi = 0$ may be placed into II(0), since the embedding diagrams are then identical to those in (3.4). We leave it to the reader's choice to either place the set of the corresponding parameters $(\mu_1, \mu_2, t = -\frac{\tilde{p}}{q})$ with $|\mu_1 - \mu_2| = \zeta + \eta\frac{\tilde{p}}{q}$, $0 < \zeta < \tilde{p}$, $0 < \eta < q$, into case II(0), at the same time excluding it from the III₋(0) case, or to be content with the understanding that, as the number of relaxed submodules diminishes to 1, the embedding diagram becomes identical to the one for irrational t (where 1 is the largest possible number of relaxed submodules).

Further degenerations can occur along two lines. First, whenever charged singular vectors appear in the relaxed module, the entire *Verma*-module embedding diagram joins the above diagram (3.7), the embeddings being given by charged singular vectors. In the case where the integer μ_1 is positive, as we have seen, the Verma module and hence all of the modules embedded into it are twisted by the spectral flow transform with $\theta = 1$. Second, the Verma-module embedding diagram may acquire a special form, which would also affect the 'relaxed' embedding diagram, making it into a single chain. In addition, these possibilities may occur simultaneously.

III_±(1, -). $t \in \mathbb{Q}$, $(\mu_1 - \mu_2)/t \notin \mathbb{Z}$, $\mu_1 \in -\mathbb{N}$, $\mu_2 \notin \mathbb{Z}$. Then the correspondence between relaxed submodules in $\mathcal{R}_{\mu_1, \mu_2, t}$ and the Verma submodules in the module generated from the charged singular

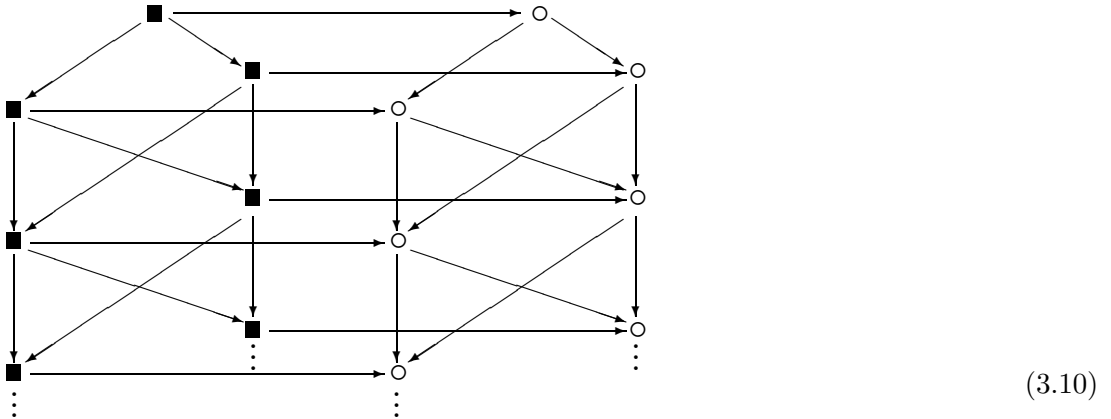
vector is described in Parts 2 and 3a of Theorem 2.5. We have the following embedding diagram:



which is finite or infinite depending on whether $t < 0$ (III_-) or $t > 0$ (III_+), respectively. The top Verma module is the submodule in the relaxed module associated with a charged singular vector. Each of the subsequent Verma modules is embedded via a charged singular vector into the corresponding relaxed module. In the negative zone, the relaxed-module part of the diagram ends in the same way as in the corresponding case in (3.7), and similarly with the Verma-module part of the diagram, the Verma module with the antidominant weight is then embedded into the bottom relaxed module via a charged singular vector.

As in the above, in the special case where $\xi = 0$ in (3.1), the $\text{III}_-(1, -)$ diagram becomes that of case $\text{II}(1, -)$, Eq. (3.4). Thus, one could explicitly exclude from case $\text{III}_-(1)$ the parameters $(\mu_1 \in \mathbb{Z}, \mu_2 \notin \mathbb{Z}, t = -\frac{\tilde{p}}{q})$ with $|\mu_1 - \mu_2| = \zeta + \eta\frac{\tilde{p}}{q}$, $0 < \zeta < \tilde{p}$, $0 < \eta < q$, placing these in the $\text{II}(1)$ case.

$\text{III}_\pm(1, +)$. $\mu_1 - \mu_2 \in \mathbb{K}(t)$, $t \in \mathbb{Q}$, $(\mu_1 - \mu_2)/t \notin \mathbb{Z}$, $\mu_1 \in \mathbb{N}_0$, $\mu_2 \notin \mathbb{Z}$. This case, too, is described by Parts 2 and 3a of Theorem 2.5. We have a diagram similar to the above, with Verma modules \bullet replaced by twisted-Verma modules \circ (with the spectral parameter $\theta = 1$).



This diagram, too, is finite in the $\text{III}_-(1, +)$ case, and infinite, in the $\text{III}_+(1, +)$ case (i.e., for $t < 0$ and $t > 0$ respectively). Obviously, the case of $\xi = 0$ in (3.1) leaves us with the diagram $\text{II}(1, +)$, Eq. (3.4).

As before, taking the quotient of $\mathcal{R}_{\mu_1, \mu_2, t}$ with respect to the charged singular vector amounts to removing the \circ dots and replacing $\blacksquare \rightarrow \bullet$. In this way, the remaining part of the embedding diagram becomes that of the Verma module $\mathcal{M}_{-\frac{1}{2}(\mu_2 - \mu_1 + 1), t}$, which, of course, reproduces the standard result.

III_±⁰(0). $\mu_1 - \mu_2 \in \mathbb{K}(t)$, $t \in \mathbb{Q}$, $\mu_1 \notin \mathbb{Z}$, $\mu_2 \notin \mathbb{Z}$, and, in addition, one *but not both* of the following conditions satisfied: either $\mu_1 - \mu_2 \in \mathbb{Z}$ or $(\mu_1 - \mu_2)/t \in \mathbb{Z}$. We then have a single-chain of relaxed modules,

$$\begin{array}{ccc}
 \begin{array}{c} \blacksquare \\ \downarrow \\ \blacksquare \\ \downarrow \\ \blacksquare \\ \downarrow \\ \vdots \end{array} & \begin{array}{c} \blacksquare \\ \downarrow \\ \blacksquare \\ \vdots \\ \blacksquare \\ \downarrow \\ \blacksquare \\ \downarrow \\ \vdots \end{array} & \\
 \text{III}_+^0(0) & \text{III}_-^0(0) & (3.11)
 \end{array}$$

That the single chain takes the place of the double chain can be explained in terms of the auxiliary Verma module M . There, either the Verma-module embedding diagram becomes a single chain (in the case where $(\mu_1 - \mu_2)/t \in \mathbb{Z}$), in which case we still have the correspondence described in Part 1 of Theorem 2.6, or the embedding diagram of the auxiliary Verma module contains pairs of Verma modules embedded onto the same level; every such pair corresponds to one relaxed module, as described in Part 2 of Theorem 2.6.

In the negative zone, we use (3.1), where now $\eta = 0$, $0 < \zeta < \tilde{p}$ in the case where $\mu_1 - \mu_2 \in \mathbb{Z}$, and $\zeta = 0$, $0 < \eta < q$ in the case where $(\mu_1 - \mu_2)/t \in \mathbb{Z}$. In either case, we have $\xi = \left\lfloor \frac{|\mu_1 - \mu_2|}{p} \right\rfloor \in \mathbb{N}$ *embedded* relaxed submodules. In the case where $\xi = 1$, the diagram ‘degenerates’ to that of $\text{II}(0)$, Eq. (3.4), therefore one may wish to explicitly exclude from $\text{III}_-^0(0)$ the parameters $(\mu_1, \mu_2, t = -\frac{\tilde{p}}{q})$ such that either $|\mu_1 - \mu_2| = \tilde{p} + \zeta$, $0 < \zeta < \tilde{p}$, or $|\mu_1 - \mu_2| = \tilde{p} + \eta \frac{\tilde{p}}{q}$, $0 < \eta < q$ (and with $\mu_\alpha \notin \mathbb{Z}$ in both cases, obviously).

III_±⁰(1, -). $\mu_1 - \mu_2 \in \mathbb{K}(t)$, $t \in \mathbb{Q}$, $\mu_1 \in -\mathbb{N}$, $\mu_2 \notin \mathbb{Z}$, $(\mu_1 - \mu_2)/t \in \mathbb{Z}$. This is a particular case described in Part 1 of Theorem 2.6. The embedding diagram can be written in one of the following ways:

$$\begin{array}{ccc}
 \begin{array}{c} \bullet \leftarrow \blacksquare \\ \bullet \leftarrow \blacksquare \\ \bullet \leftarrow \blacksquare \\ \bullet \leftarrow \blacksquare \\ \bullet \leftarrow \blacksquare \\ \downarrow \end{array} & \begin{array}{c} \bullet \leftarrow \blacksquare \\ \bullet \leftarrow \blacksquare \\ \bullet \leftarrow \blacksquare \\ \bullet \leftarrow \blacksquare \\ \bullet \leftarrow \blacksquare \\ \downarrow \end{array} & \\
 \mu_1 - \mu_2 < 0 & \mu_1 - \mu_2 > 0 & (3.12)
 \end{array}$$

These diagrams are of course isomorphic as embedding diagrams, however it may be helpful to associate the x -coordinate in the *Verma*-part with the J_0^0 -eigenvalue of the highest-weight vector in the corresponding

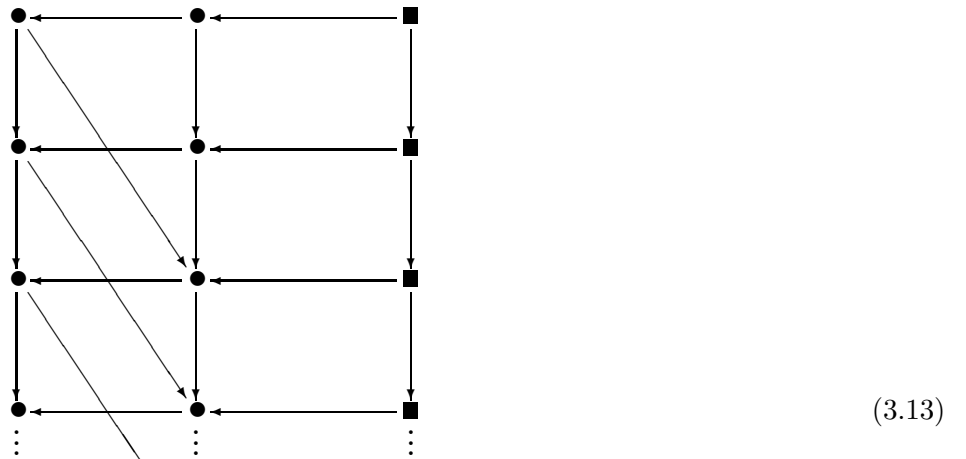
modules; then, depending on whether $\mu_1 - \mu_2$ is positive or negative, the first Verma-module embedding is performed by an $\text{MFF}^-(r, s, t)$ or an $\text{MFF}^+(r, s, t)$ vector, we have the first or the second of the above diagrams, respectively. In fact, specifying precise $x \equiv$ charge coordinates for the highest-weight vector of every module requires drawing the \bullet -part of the diagrams as growing either wider or narrower as one moves down, according to whether $t > 0$ or $t < 0$, respectively (which we do not do here).

The diagrams are finite in the negative zone ($\text{III}_-^0(1, -)$) and infinite, in the positive zone ($\text{III}_+^0(1, -)$). The structure of the $\text{III}_-^0(1, -)$ -diagram at the bottom is obvious. As in the corresponding case in $\text{III}_\pm^0(0)$, we have only one embedded relaxed submodule whenever $\xi = 1$ in the negative zone and, thus, the diagram becomes that of $\text{II}(1, -)$, Eq. (3.4). Again, whenever $|\mu_1 - \mu_2| = \tilde{p} + \eta \frac{\tilde{q}}{q}$ with $0 < \eta < q$, the parameters $(\mu_1 \in \mathbb{Z}, \mu_2 \notin \mathbb{Z}, t = -\frac{\tilde{q}}{q})$ may be removed from case $\text{III}_-^0(1)$.

After taking the quotient over the charged singular vector and replacing $\blacksquare \rightarrow \circ$ and then ‘untwisting’, we obtain the embedding diagram of the quotient module $\mathcal{M}_{-\frac{1}{2}(\mu_2 - \mu_1 + 1), t}$ which is a single-chain in accordance with the fact that $(\mu_1 - \mu_2)/t \in \mathbb{Z}$.

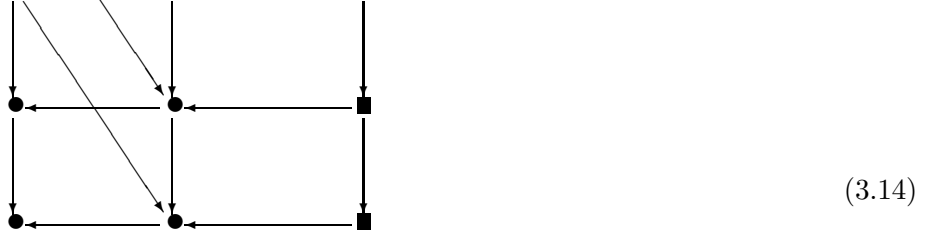
$\text{III}_\pm^0(1, +)$. $\mu_1 - \mu_2 \in \mathbb{K}(t)$, $t \in \mathbb{Q}$, $\mu_1 \in \mathbb{N}_0$, $\mu_2 \notin \mathbb{Z}$, $(\mu_1 - \mu_2)/t \in \mathbb{Z}$. In complete similarity with the previous case, this one is also described in Part 1 of Theorem 2.6. The embedding diagram is a mirror of the above with the Verma modules \bullet replaced by twisted-Verma modules \circ . The diagrams are finite in the negative zone ($\text{III}_-^0(1, +)$) and infinite, in the positive zone ($\text{III}_+^0(1, +)$). Clearly, $\xi = 1$ leaves with the diagram $\text{II}(1, +)$.

$\text{III}_\pm^0(2, --)$. $\mu_1 - \mu_2 \in \mathbb{K}(t)$, $t \in \mathbb{Q}$, $(\mu_1 - \mu_2)/t \notin \mathbb{Z}$, $\mu_1 \in -\mathbb{N}$, $\mu_2 \in -\mathbb{N}$. This is described in Part 2 of Theorem 2.6. With μ_1 and μ_2 being integers of the same sign, there are two charged singular vectors in the relaxed module on one side of the highest-weight vector. In the present case, with μ_1 and μ_2 both negative, the embedding diagram takes the following form, where the Verma part is nothing but the standard double-chain embedding diagram with a part of the arrows drawn horizontal:



As usual, the diagram is finite or infinite depending on whether $t < 0$ ($\text{III}_-^0(2, --)$) or $t > 0$ ($\text{III}_+^0(2, --)$)

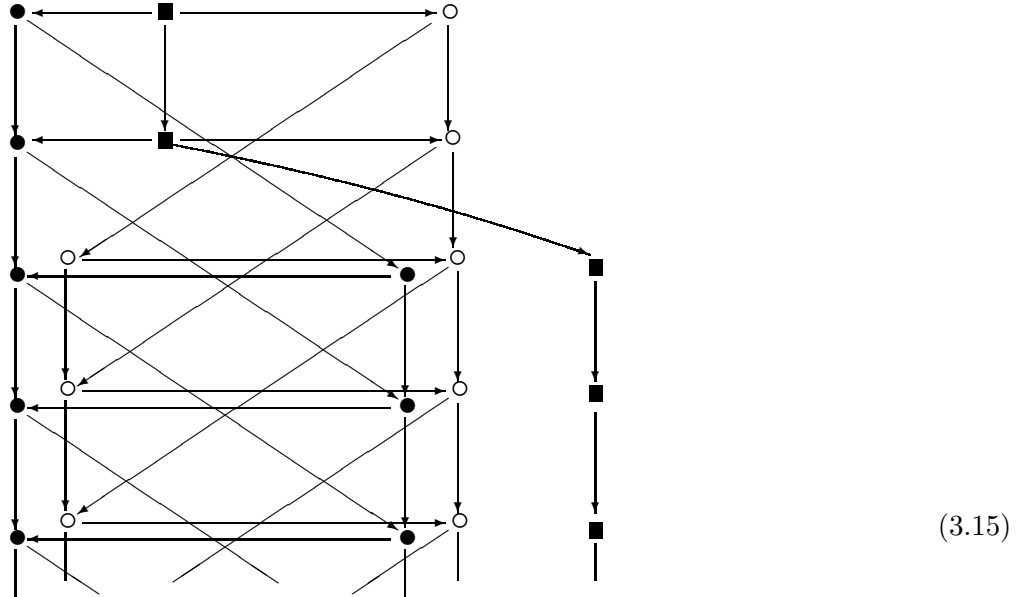
respectively. In the negative zone, the structure of the embedding diagram near the bottom is as follows:



$\mathbf{III}_{\pm}^0(2, ++)$. $\mu_1 - \mu_2 \in \mathbb{K}(t)$, $t \in \mathbb{Q}$, $(\mu_1 - \mu_2)/t \notin \mathbb{Z}$, $\mu_1 \in \mathbb{N}_0$, $\mu_2 \in \mathbb{N}_0$. This time, μ_1 and μ_2 are both positive, and the embedding diagram is obtained from (3.13)–(3.14) by replacing the Verma modules \bullet with twisted-Verma modules \circ and placing them on the right of the relaxed modules (cf. (3.10)). Thus, the diagram is a vertical mirror of (3.13) with $\bullet \rightsquigarrow \circ$.

$\mathbf{III}_{\pm}^0(2, -+)$. $\mu_1 - \mu_2 \in \mathbb{K}(t)$, $t \in \mathbb{Q}$, $(\mu_1 - \mu_2)/t \notin \mathbb{Z}$, $\mu_1 \in -\mathbb{N}$, $\mu_2 \in \mathbb{N}$. With μ_1 and μ_2 being of different signs, there are charged singular vectors on different sides of the highest-weight vector of the relaxed module. One of the charged singular vectors comes with the embedding diagram of Verma modules, while the other contributes a similar (in fact, mirror-symmetric with respect to charge in the (charge, level) coordinates) diagram of twisted-Verma modules. Superposition of these diagrams has a nontrivial effect which we describe in two steps: We first draw a diagram showing all the relevant modules, but *not* all of the embeddings. Then we describe the subtleties related to the embeddings as those in (2.37), after which we draw the final embedding diagram (Eq. (3.32)), which may indeed look rather complicated.

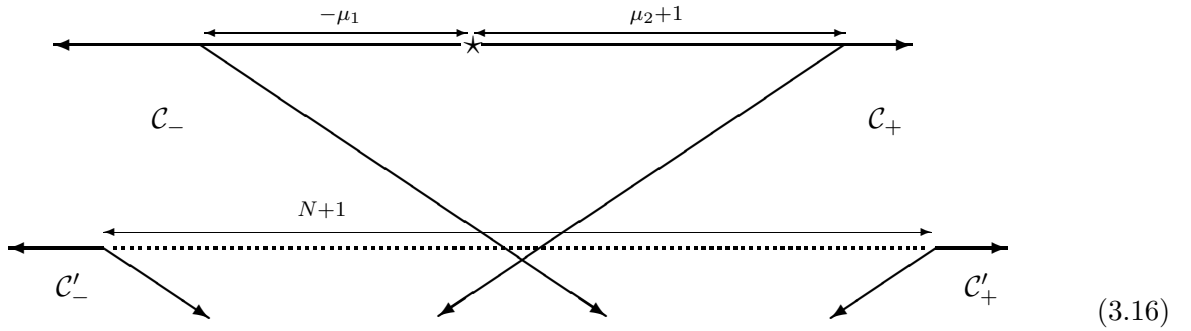
The superposition of the Verma and twisted-Verma embedding diagrams looks as follows:



where *not all of the embeddings are yet shown*. The three modules at the second level (assuming the top level to be the first) are described by Part 2b of Theorem 2.8. We denote by \mathcal{C}'_- , \mathcal{R}' , and \mathcal{C}'_+ the Verma module, the relaxed module, and the twisted Verma module at that level, respectively. Further down, there are two Verma and two twisted-Verma modules embedded onto the same level (in the diagram, these are

shown slightly displaced so as not to confuse the different arrows¹¹). We introduce the notations $\tilde{\mathcal{C}}_-''$ and \mathcal{C}_-'' for two Verma modules related by the embedding $\mathcal{C}_-'' \subset \tilde{\mathcal{C}}_-''$, and also $\tilde{\mathcal{C}}_+'' \supset \mathcal{C}_+''$ for the twisted Verma modules at a given level. Let also \mathcal{R}'' be the relaxed module at that level. If the J_0^0 -charge of the highest-weight vector of \mathcal{C}_-'' is j , then the charge of the highest-weight vector of $\tilde{\mathcal{C}}_+''$ is $j + 1$. Further, the J_0^0 -charge of the ‘parent’ Verma module $\tilde{\mathcal{C}}_-''$ is $j' > j$ and that of the ‘child’ *twisted* Verma module \mathcal{C}_+'' is $j' + 1$.

Let us first describe the embedding of \mathcal{C}'_- , \mathcal{R}' , and \mathcal{C}'_+ into $\mathcal{R} \equiv \mathcal{R}_{\mu_1, \mu_2, t}$. The following analysis is a direct consequence of [FST].¹² In the positive zone $t = \frac{p}{q} > 0$, the module \mathcal{C}'_- is embedded into \mathcal{C}_- by singular vector $|\text{MFF}^+(r, s, t)\rangle$ with $r < p$; in the negative zone, this is $|\text{MFF}^-(r, s, t)\rangle$ with $r < |p|$; then \mathcal{C}'_+ is embedded into \mathcal{C}_+ by $|\text{MFF}^{-,1}(r, s, t)\rangle$ (in the negative zone, by $|\text{MFF}^{+,1}(r, s, t)\rangle$). The modules \mathcal{C}'_- and \mathcal{C}'_+ are embedded into \mathcal{R}' via charged singular vectors in accordance with Theorem 2.5 (Parts 3a and 2). We, thus, have the extremal diagram



Here, the relaxed module \mathcal{R}' can be generated from any of $N = \mu_2 - \mu_1 + 2r$ (or, in the negative zone, $N = \mu_2 - \mu_1 - 2r$) extremal states

$$|g'(i)\rangle, \quad i = 1, \dots, N. \quad (3.17)$$

between the two charged singular vectors. We can choose $|g'(i+1)\rangle = J_0^+ |g'(i)\rangle$ for $1 \leq i \leq N$. Let also $|g'(0)\rangle$ be the highest-weight state of the \mathcal{C}'_- submodule, and $|g'(N+1)\rangle$, the highest-weight state of \mathcal{C}'_+ . We know from [FST] that relation

$$J_0^- |g'(1)\rangle = |g'(0)\rangle \quad (3.18)$$

can be inverted as

$$|g'(1)\rangle = (J_0^-)^{-1} |g'(0)\rangle, \quad (3.19)$$

where the action of $(J_0^-)^{-1}$ is defined in the spirit of (2.7) and $|g'(1)\rangle$ satisfies relaxed highest-weight conditions. Such a $|g'(1)\rangle$ is unique. A similar construction starting with the highest-weight vector of \mathcal{C}'_+ allows us to define the extremal states

$$|g'_+(N)\rangle = (J_0^+)^{-1} |g'_+(N+1)\rangle, \quad |g'_+(i)\rangle = (J_0^-)^{N-i} |g'_+(N)\rangle. \quad (3.20)$$

Then it follows from the results of [FST] that

$$|g'(i)\rangle = a'(i) |g'_+(i)\rangle, \quad 1 \leq i \leq N, \quad a'(i) \neq 0, \quad (3.21)$$

¹¹and, for the same reason, the relaxed modules are drawn outside the Verma/twisted-Verma part of the diagram.

¹²The difference of our present approach from that of [FST] is that we are now interested in describing *all* submodules in a given relaxed module and in finding the sequence in which submodules are embedded into one another, whereas the (simpler) problem addressed in [FST] was to give the configuration of submodules that occur ‘*somewhere*’ inside the relaxed module as soon as the parameters (in our present conventions) μ_1 , μ_2 , and t admit a certain representation involving several integers.

where $a'(i)$ depends also on t , μ_1 , μ_2 , and r .

Let now \mathcal{R}'' be the relaxed module that is the third from the top in (3.15). The embedding $\iota'' : \mathcal{R}'' \hookrightarrow \mathcal{R}'$ is described precisely as the embedding $\iota' : \mathcal{R}' \hookrightarrow \mathcal{R}$, the only difference being that μ_1 , μ_2 , and r have to be replaced with μ'_1 , μ'_2 , and r' such that $\mu'_2 - \mu'_1 = N$, $r' = |p| - r$, and $N' = N + 2r'$ (or $N' = N - 2r'$ in the negative zone), where $t = \frac{p}{q}$. Among four (twisted) Verma modules $\mathcal{C}''_- \subset \tilde{\mathcal{C}}''_-$ and $\tilde{\mathcal{C}}''_+ \supset \mathcal{C}''_+$ that are embedded onto the same level as \mathcal{R}'' , \mathcal{C}''_- and \mathcal{C}''_+ are embedded into \mathcal{R}'' via charged singular vectors. Thus, we simply rewrite the above extremal diagram in the modified notations:

$$(3.22)$$

We now have, in complete similarity with the above,

$$|g''(1)\rangle = (J_0^-)^{-1}|g''(0)\rangle, \quad |g''(i)\rangle = (J_0^+)^{i-1}|g''(1)\rangle, \quad (3.23)$$

$$|g''_+(N')\rangle = (J_0^+)^{-1}|g''_+(N'+1)\rangle, \quad |g''_+(i)\rangle = (J_0^-)^{N'-i}|g''_+(N')\rangle, \quad (3.24)$$

$$|g''(i)\rangle = a''(i)|g''_+(i)\rangle. \quad (3.25)$$

Let now $|G(i)\rangle = \iota|g''(i)\rangle$ be the image of $|g''(i)\rangle$ under the embedding $\iota = \iota' \circ \iota'' : \mathcal{R}'' \hookrightarrow \mathcal{R}$; in particular, $|G(0)\rangle$ and $|G(N'+1)\rangle$ are the highest-weight vectors of the embedding of \mathcal{C}''_- and \mathcal{C}''_+ , respectively.

From the embedding diagrams of the Verma module \mathcal{C}_- (respectively, \mathcal{C}_+) we see that there actually exists the submodule $\tilde{\mathcal{C}}''_-$ (resp., $\tilde{\mathcal{C}}''_+$) at the same level as \mathcal{C}''_- (resp., \mathcal{C}''_+) such that $\mathcal{C}''_- \subset \tilde{\mathcal{C}}''_-$ (resp., $\mathcal{C}''_+ \subset \tilde{\mathcal{C}}''_+$). Moreover, these are embedded into \mathcal{R} as follows (with the highest-weight vector of each module shown, for convenience, by the same symbol as the corresponding *module* in the *embedding diagram*)

$$(3.26)$$

where distance 1 is in the units of the J_0^0 -charge. This has the following drastic effect on the solutions to the analogue of Eq. (3.18), $J_0^-|X\rangle = |G(0)\rangle$ (where $|X\rangle$ is to satisfy relaxed highest-weight conditions).

The solution is not unique, since one can add a vector proportional to the highest-weight vector of $\tilde{\mathcal{C}}_+''$; conversely, any two solutions (satisfying, in addition, the relaxed highest-weight conditions) differ by a vector proportional to the highest-weight state of $\tilde{\mathcal{C}}_+''$. The appearance of submodule $\tilde{\mathcal{C}}_-''$ has a similar effect on representing $|G(N'+1)\rangle$ (which is the highest-weight vector of \mathcal{C}_+'') as J_0^+ acting on another vector satisfying relaxed highest-weight conditions.

We can *define* $(J_0^-)^{-1}|G(0)\rangle$ to be a vector inside the $\tilde{\mathcal{C}}_-''$ Verma module, and similarly for the vector $|G(N')\rangle$:

$$|G_-(1)\rangle = (J_0^-)^{-1}|G_-(0)\rangle \in \tilde{\mathcal{C}}_-'', \quad |G_+(N')\rangle = (J_0^+)^{-1}|G_+(N'+1)\rangle \in \tilde{\mathcal{C}}_+'' \quad (3.27)$$

Setting now

$$|G_-(i)\rangle = (J_0^+)^{i-1}|G_-(1)\rangle \in \tilde{\mathcal{C}}_-'', \quad |G_+(i)\rangle = (J_0^-)^{N'-i}|G_+(N')\rangle \in \tilde{\mathcal{C}}_+'', \quad (3.28)$$

we have

$$\iota|g''(i)\rangle \equiv |G(i)\rangle = |G_-(i)\rangle + a''(i)|G_+(i)\rangle, \quad i = 1, \dots, N', \quad (3.29)$$

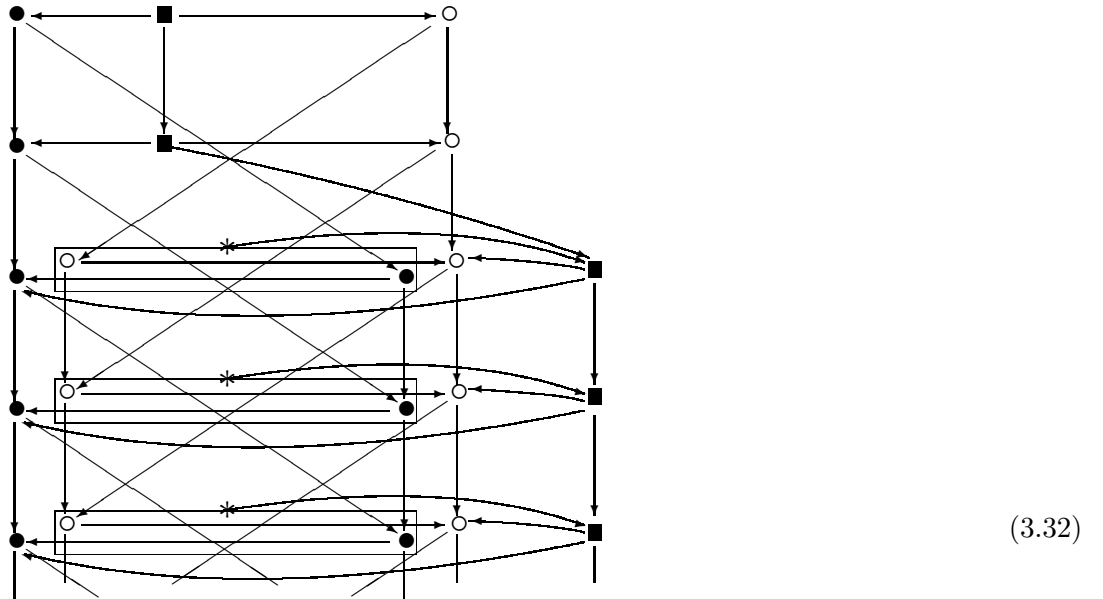
where $a''(i)$ are as in (3.25). This defines the embedding

$$\mathcal{R}'' \hookrightarrow \tilde{\mathcal{C}}_-'' \oplus \tilde{\mathcal{C}}_+'' \quad (3.30)$$

on the extremal states and, hence, on any vector from \mathcal{R}'' . At the same time,

$$\mathcal{R}'' \cap \tilde{\mathcal{C}}_-'' = \mathcal{C}_-'', \quad \mathcal{R}'' \cap \tilde{\mathcal{C}}_+'' = \mathcal{C}_+''. \quad (3.31)$$

This situation repeats at every subsequent level in (3.15). Thus, in addition to the embeddings of \mathcal{C}_-'' and \mathcal{C}_+'' into \mathcal{R}'' performed by charged singular vectors, there is embedding (3.30) of \mathcal{R}'' into the direct sum. Taking all this into account, we finally complete (3.15) to the following embedding diagram:



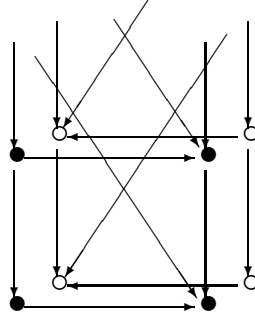
Here, the frame around the respective Verma and twisted-Verma modules represents the direct sum of these modules. Accordingly, an arrow drawn from that frame (symbolized by a $*$) to the corresponding relaxed module indicates that the relaxed module is embedded into the direct sum. On the other hand,

the relaxed module has two submodules associated with charged singular vectors, as shown by the arrows drawn *from* the relaxed module.

The diagram is finite for $\text{III}_-^0(2, -+)$ and infinite, for $\text{III}_+^0(2, -+)$. In the negative zone, where $t = -\tilde{p}/q$ with $\tilde{p}, q \in \mathbb{N}$, Eq. (3.1) now takes the form

$$\mu_2 - \mu_1 = \xi \tilde{p} + \zeta, \quad \xi \in \mathbb{N}, \quad 1 \leq \zeta < \tilde{p}. \quad (3.33)$$

As in all of the III_-^0 cases, the number of the embedding levels (\equiv the number of relaxed modules except the top one) is $\xi = \left\lceil \frac{|\mu_1 - \mu_2|}{\tilde{p}} \right\rceil$. In the negative zone, further, the structure of the *Verma* and *twisted-Verma* parts of the embedding diagram near the bottom is as follows:

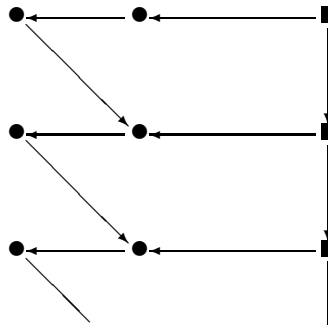


(3.34)

In the units of the J_0^0 -charge, the distance between the two bottom \bullet -modules in (3.34) is ζ for ξ even and $(\tilde{p} - \zeta)$ for ξ odd; the distance between the adjacent \bullet and \circ modules is always 1. Every quadruple of (twisted) Verma modules is related to the relaxed module at the same level as explained above.

$\text{III}_{\pm}^{00}(\mathbf{0})$. $\mu_1 - \mu_2 \in \mathbb{K}(t)$, $t \in \mathbb{Q}$, $\mu_1 - \mu_2 \in \mathbb{Z}$, $\mu_1 \notin \mathbb{Z}$, $(\mu_1 - \mu_2)/t \in \mathbb{Z}$. This case is covered by Part 2 of Theorem 2.6. We have the diagram of the same form as in (3.11). However, in the negative zone, where the diagrams are finite, the $\text{III}_{\pm}^{00}(\mathbf{0})$ -diagram is half that long as the $\text{III}_{\pm}^0(\mathbf{0})$ -diagram. In terms of Eq. (3.1), we now have $\zeta = \eta = 0$, therefore $|\mu_1 - \mu_2| = \tilde{p}\xi$, $\xi \geq 2$, the number of *embedded* modules being $\left\lceil \frac{\xi}{2} \right\rceil$. This time, we have small- ξ ‘exceptions’ at $\xi = 2$ and $\xi = 3$. Thus, the triples $(\mu_1 \notin \mathbb{Z}, \mu_2 \notin \mathbb{Z}, t = -\frac{\tilde{p}}{q})$ with $|\mu_1 - \mu_2|$ equal to either $2\tilde{p}$ or $3\tilde{p}$ may be excluded from the $\text{III}_-^0(\mathbf{0})$ case and placed into $\text{II}_-(\mathbf{0})$.

$\text{III}_{\pm}^{00}(2, --)$. $t \in \mathbb{Q}$, $\mu_1 \in -\mathbb{N}$, $\mu_2 \in -\mathbb{N}$, $(\mu_1 - \mu_2)/t \in \mathbb{Z}$. We are again in the situation described by part 2 of Theorem 2.6. In this case, we have the embedding diagram



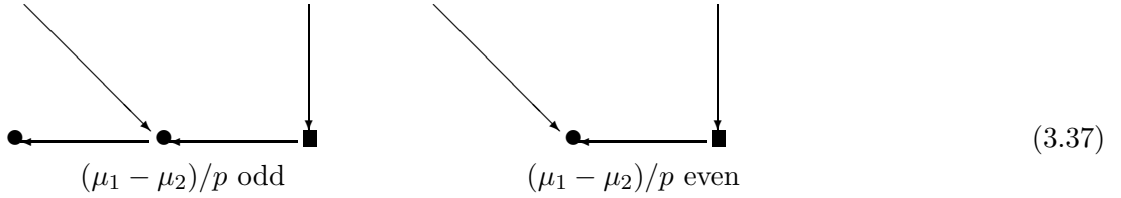
(3.35)

which can be viewed as a degeneration of diagrams (3.13) and/or (3.12). It is finite or infinite depending on whether t is negative or positive respectively. In the case where $\mu_1 = \mu_2$, $t > 0$, the upper floor is somewhat changed:



(3.36)

In the negative zone, the structure of diagram (3.35) near the bottom depends on whether $\xi \equiv (\mu_1 - \mu_2)/\tilde{p}$ is odd or even:

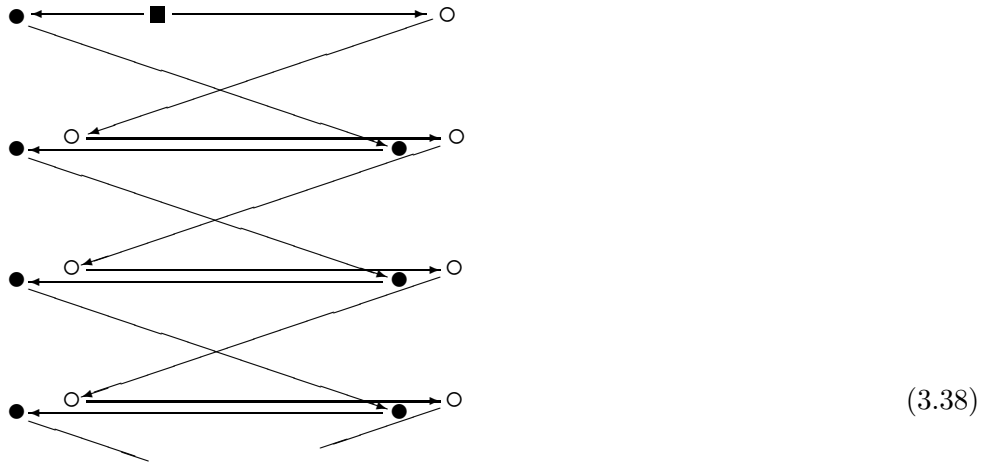


(3.37)

The distance (in the units of the J_0^0 -charge) between two \bullet -modules related by the charged singular vectors in the bottom floor of the first of these diagrams is \tilde{p} .

$\mathbf{III}_{\pm}^{00}(2, ++)$. $t \in \mathbb{Q}$, $\mu_1 \in \mathbb{N}_0$, $\mu_2 \in \mathbb{N}_0$, $(\mu_1 - \mu_2)/t \in \mathbb{Z}$. In this case, the embedding diagrams are the mirror-transform of the $\mathbf{III}_{\pm}^{00}(2, --)$ ones, with the Verma modules replaced by twisted-Verma modules.

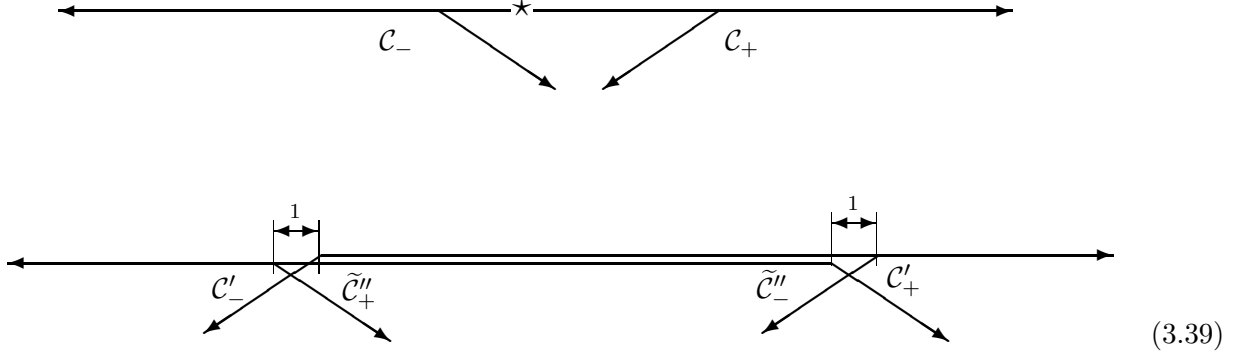
$\mathbf{III}_{\pm}^{00}(2, -+)$. $t \in \mathbb{Q}$, $\mu_1 \in -\mathbb{N}$, $\mu_2 \in \mathbb{N}_0$, $(\mu_1 - \mu_2)/t \in \mathbb{Z}$. This case can be considered as a further degeneration of diagram (3.32). First, the charged singular vectors give rise to the Verma and twisted-Verma embedding diagrams which superpose as follows:



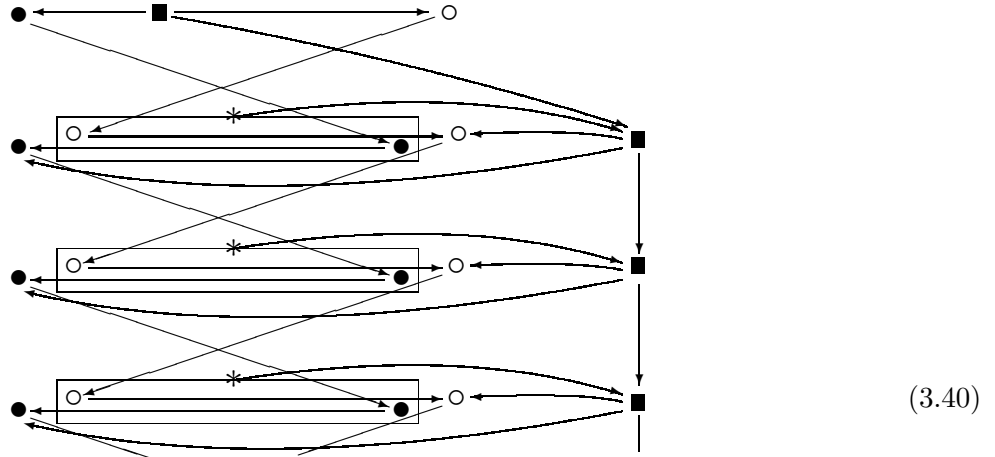
(3.38)

which does not show the relaxed modules and some of the embeddings yet! As in case $\mathbf{III}_{\pm}^{00}(2, -+)$, there are two Verma and two twisted-Verma modules *all at the same level*, which are shown somewhat displaced vertically in order to distinguish between the different arrows. The highest-weight vectors of the corresponding pairs of Verma and twisted Verma modules are separated by the distance of J_0^0 -charge 1. In what follows, we denote by \mathcal{C}_- and \mathcal{C}_+ the Verma and the twisted Verma module, respectively, generated from the corresponding charged singular vector.

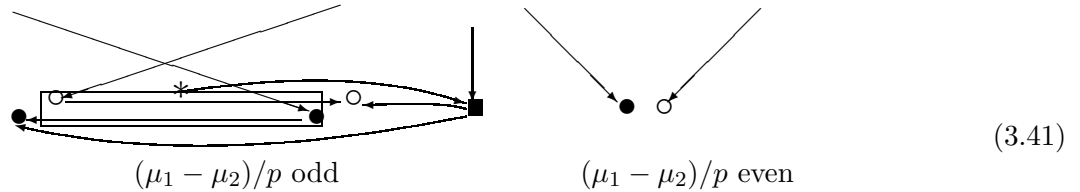
Now, let us describe the relaxed modules that are not yet shown in the above diagram. Since $\mu_2 - \mu_1$ is now a multiple of p (where $t = \frac{p}{q}$), we see from the standard Verma embedding diagram that the first two submodules in Verma module \mathcal{C}_- are $\tilde{\mathcal{C}}''_-$ and \mathcal{C}'_- such that they are related by $\mathcal{C}'_- \subset \tilde{\mathcal{C}}''_-$ and are embedded on the same level in \mathcal{C}_- (hence, by Theorem 2.5, on the same level in \mathcal{R}). We have the extremal diagram



This picture—the grouping of (twisted) Verma submodules into quadruples—is reproduced for every level except, possibly, the bottom one in the negative zone (see below). As in case $\text{III}_\pm^0(2, -+)$, the relaxed module \mathcal{R}'' at every level is embedded into the direct sum of the corresponding $\tilde{\mathcal{C}}''_-$ and $\tilde{\mathcal{C}}''_+$, with $\mathcal{R}'' \cap \tilde{\mathcal{C}}''_- = \mathcal{C}'_-$ and $\mathcal{R}'' \cap \tilde{\mathcal{C}}''_+ = \mathcal{C}'_+$. Thus, the embedding diagram reads as



This is finite or infinite depending on whether t is negative or positive respectively. In the negative zone where $t = -\frac{\tilde{p}}{q}$, the diagram terminates differently depending on whether $(\mu_1 - \mu_2)/\tilde{p}$ is odd or even:



In the second case, *there is no relaxed module in the bottom floor*, as described in Part 3b of Theorem 2.5. The distance between the two Verma modules (as well as between two twisted Verma modules) in the first of these diagrams is \tilde{p} , while the distance between the adjacent Verma and twisted Verma modules is

always 1. When $\xi = 2$ in (3.1), we now have $\mu_2 - \mu_1 = 2\tilde{p}$ and the embeddings terminate already at the second level. The embedding diagram then takes the following exceptional form:

(3.42)

The structure of the module is easily understood in terms of the *extremal* diagram

(3.43)

Thus, there are no states that would generate a relaxed submodule, instead the lower floor consists of a direct sum of the Verma and the twisted Verma modules. However, this configuration corresponds to a zero of the Kač determinant [BFK]; in fact, there are as many states on that level satisfying the relaxed highest-weight conditions as in a relaxed module.

4 The $N=2$ side: Massive and topological Verma modules

In this section, we introduce Verma-like modules over the $N=2$ superconformal algebra—the massive and topological Verma modules. We then explain how the embedding diagrams constructed in the previous section can be read in the $N=2$ terms, as the embedding diagrams of massive $N=2$ Verma modules (while the topological Verma-module embedding diagrams are isomorphic to the standard embedding diagrams of $\widehat{sl}(2)$ Verma modules). This does not cover the embedding diagrams of $N=2$ modules with the central charge $c = 3$, which are considered separately in Sec. 4.6.

4.1 The $N=2$ algebra

The $N=2$ superconformal algebra contains two fermionic currents, \mathcal{Q} and \mathcal{G} , in addition to the Virasoro generators \mathcal{L} and the $U(1)$ current \mathcal{H} . The commutation relations can be chosen as

$$\begin{aligned}
 [\mathcal{L}_m, \mathcal{L}_n] &= (m-n)\mathcal{L}_{m+n}, & [\mathcal{H}_m, \mathcal{H}_n] &= \frac{c}{3}m\delta_{m+n,0}, \\
 [\mathcal{L}_m, \mathcal{G}_n] &= (m-n)\mathcal{G}_{m+n}, & [\mathcal{H}_m, \mathcal{G}_n] &= \mathcal{G}_{m+n}, \\
 [\mathcal{L}_m, \mathcal{Q}_n] &= -n\mathcal{Q}_{m+n}, & [\mathcal{H}_m, \mathcal{Q}_n] &= -\mathcal{Q}_{m+n}, & m, n \in \mathbb{Z}. & (4.1) \\
 [\mathcal{L}_m, \mathcal{H}_n] &= -n\mathcal{H}_{m+n} + \frac{c}{6}(m^2 + m)\delta_{m+n,0}, \\
 \{\mathcal{G}_m, \mathcal{Q}_n\} &= 2\mathcal{L}_{m+n} - 2n\mathcal{H}_{m+n} + \frac{c}{3}(m^2 + m)\delta_{m+n,0},
 \end{aligned}$$

The element C is central; in representations, we will not distinguish between C and its eigenvalue $c \in \mathbb{C}$, which it will be convenient to parametrize as $c = 3 \frac{t-2}{t}$ with $t \in \mathbb{C} \setminus \{0\}$. Then, however, the special point $c = 3$ requires an additional investigation. The central charge appears as the anomaly of the \mathcal{H} current rather than in the Virasoro commutation relations, which is simply a matter of choosing the basis in the algebra.

The spectral flow transform [SS, LVW], which acts as

$$\mathcal{U}_\theta : \begin{array}{ll} \mathcal{L}_n & \mapsto \mathcal{L}_n + \theta \mathcal{H}_n + \frac{\epsilon}{6}(\theta^2 + \theta)\delta_{n,0}, & \mathcal{H}_n & \mapsto \mathcal{H}_n + \frac{\epsilon}{3}\theta\delta_{n,0}, \\ \mathcal{Q}_n & \mapsto \mathcal{Q}_{n-\theta}, & \mathcal{G}_n & \mapsto \mathcal{G}_{n+\theta}, \end{array} \quad (4.2)$$

produces isomorphic images of the above algebra. The family of algebras thus obtained includes the Neveu-Schwarz and Ramond $N=2$ algebras, as well as the algebras in which the fermion modes range over $\pm\theta + \mathbb{Z}$, $\theta \in \mathbb{C}$. Any ‘invariant’ assertion regarding representations of the algebra (4.1) is therefore valid for any of the spectral-flow-transformed algebras as well. The spectral flow transform is an automorphism for $\theta \in \mathbb{Z}$.

4.2 Massive $N=2$ Verma modules

A massive Verma module $\mathcal{U}_{h,\ell,t}$ is freely generated by the generators \mathcal{L}_{-m} , \mathcal{H}_{-m} , \mathcal{G}_{-m} , $m \in \mathbb{N}$, and \mathcal{Q}_{-m} , $m \in \mathbb{N}_0$ from a *massive highest-weight vector* $|h, \ell, t\rangle$ satisfying the following set of highest-weight conditions:

$$\begin{aligned} \mathcal{Q}_{\geq 1} |h, \ell, t\rangle &= \mathcal{G}_{\geq 0} |h, \ell, t\rangle = \mathcal{L}_{\geq 1} |h, \ell, t\rangle = \mathcal{H}_{\geq 1} |h, \ell, t\rangle = 0, \\ \mathcal{H}_0 |h, \ell, t\rangle &= h |h, \ell, t\rangle, \quad \mathcal{L}_0 |h, \ell, t\rangle = \ell |h, \ell, t\rangle. \end{aligned} \quad (4.3)$$

Using the bigrading implied by (charge, level), or more precisely, by the eigenvalues of $(-\mathcal{H}_0, \mathcal{L}_0)$, the extremal diagram of the massive Verma module reads as

$$\begin{array}{ccc} & |h, \ell, t\rangle * & \xrightarrow{\mathcal{Q}_0} * \\ \mathcal{G}_{-1} \swarrow & & \searrow \mathcal{Q}_{-1} \\ * & & * \\ \mathcal{G}_{-2} \swarrow & & \searrow \mathcal{Q}_{-2} \\ * & & * \\ \vdots & & \vdots \end{array} \quad (4.4)$$

It has the shape of a parabola for the simple reason that, once one has acted on the highest-weight vector with, say, \mathcal{Q}_0 , applying the same operator once again would give identical zero, and ‘the best one can do’ to construct a state with the extremal bigrading is to act with the \mathcal{Q}_{-1} mode, etc.

An important fact is that all of the states on the extremal diagram satisfy the annihilation conditions

$$\mathcal{Q}_{-\theta+m+1} \approx \mathcal{G}_{\theta+m} \approx \mathcal{L}_{m+1} \approx \mathcal{H}_{m+1} \approx 0, \quad m \in \mathbb{N}_0 \quad (4.5)$$

for θ ranging over the integers, from $-\infty$ in the left end to $+\infty$ in the right end of the parabola¹³. Further,

¹³Anticipating the discussion in Sec. 4.4, it is instructive to compare (4.4) with relaxed- $\widehat{sl}(2)$ extremal diagram (2.12). There, all of the extremal states satisfy *the same* annihilation conditions. This difference between the behaviour of $\widehat{sl}(2)$ and $N=2$ extremal diagrams is the source of several complications arising on the $N=2$ side, even though, as we will see in Sec. 4.4, the two representation theories are essentially isomorphic.

there can be *two* different types of Verma submodules in $\mathcal{U}_{h,\ell,t}$, which can conveniently be represented as

$$(4.6)$$

In the first case, we have a massive Verma *submodule*, all of the states on its extremal diagram satisfying annihilation conditions (4.5), while in the other case there is a distinguished state, namely the one that satisfies twisted topological highest-weight conditions, which we consider in the next subsection.

4.3 Topological $N=2$ modules

The *twisted topological highest-weight vector* $|h, t; \theta\rangle_{\text{top}}$ satisfies the annihilation conditions

$$\mathcal{Q}_{-\theta+m}|h, t; \theta\rangle_{\text{top}} = \mathcal{G}_{\theta+m}|h, t; \theta\rangle_{\text{top}} = \mathcal{L}_{m+1}|h, t; \theta\rangle_{\text{top}} = \mathcal{H}_{m+1}|h, t; \theta\rangle_{\text{top}} = 0, \quad m \in \mathbb{N}_0 \quad (4.7)$$

for some $\theta \in \mathbb{Z}$, with the following eigenvalues of the Cartan generators:

$$\begin{aligned} (\mathcal{H}_0 + \frac{\epsilon}{3}\theta) |h, t; \theta\rangle_{\text{top}} &= h |h, t; \theta\rangle_{\text{top}}, \\ (\mathcal{L}_0 + \theta\mathcal{H}_0 + \frac{\epsilon}{6}(\theta^2 + \theta)) |h, t; \theta\rangle_{\text{top}} &= 0 \end{aligned} \quad (4.8)$$

(the second equation in (4.8) follows from the annihilation conditions). The state $|h, t; \theta\rangle_{\text{top}}$ is defined in accordance with the action of the automorphism (4.2): $|h, t; \theta\rangle_{\text{top}} = \mathcal{U}_\theta |h, t; 0\rangle_{\text{top}}$. Then $\mathcal{U}_{\theta'} |h, t; \theta\rangle_{\text{top}} = |h, t; \theta + \theta'\rangle_{\text{top}}$. We will also write $|h, t\rangle_{\text{top}} \equiv |h, t; 0\rangle_{\text{top}}$ for the ‘untwisted’ case of $\theta = 0$; then, in particular

$$\mathcal{Q}_0 |h, t\rangle_{\text{top}} = 0, \quad \mathcal{G}_0 |h, t\rangle_{\text{top}} = 0, \quad \mathcal{L}_0 |h, t\rangle_{\text{top}} = 0. \quad (4.9)$$

The *twisted topological Verma module* $\mathfrak{V}_{h,t;\theta}$ is freely generated from $|h, t; \theta\rangle_{\text{top}}$ by $\mathcal{Q}_{\leq -1-\theta}$, $\mathcal{G}_{\leq -1+\theta}$, $\mathcal{L}_{\leq -1}$, and $\mathcal{H}_{\leq -1}$. We also denote by $\mathcal{V}_{h,t} \equiv \mathfrak{V}_{h,t;0}$ the untwisted module. The extremal diagram of a topological Verma module reads (in the ‘untwisted’ case of $\theta = 0$ for simplicity)

$$(4.10)$$

As before, the extremal states satisfy annihilation conditions (4.5). A characteristic feature of the topological extremal diagram, however, is the existence of a ‘cusp’, i.e. the (twisted) topological highest-weight state, which satisfies stronger annihilation conditions than the other extremal states. As a result, the

extremal diagram is narrower than that of a massive Verma module. This can be formalized as the following *criterion of terminating fermionic chains* [FST], which singles out all the modules of the topological highest-weight-type: Given a vector $|X\rangle$ in the module and any $n \in \mathbb{Z}$, by the ‘massive’ parabola $\mathcal{P}(n, X)$ running through $|X\rangle$ we understand the set of states

$$\mathcal{Q}_{n-N} \dots \mathcal{Q}_{n-1} \mathcal{Q}_n |X\rangle, \quad \mathcal{G}_{-n-M} \dots \mathcal{G}_{-n-2} \mathcal{G}_{-n-1} |X\rangle \quad N, M \in \mathbb{N}. \quad (4.11)$$

Then, a module is of the topological highest-weight-type if and only if *any ‘massive’ parabola intersects the boundary (the extremal diagram of the module) on at least one end*, which means that the states (4.11) become zero in at least one branch, either for $N \gg 1$ or for $M \gg 1$. That the massive $N = 2$ Verma modules do not satisfy this criterion is a formal way to express the fact that the extremal diagrams of massive Verma modules are wider than those of the topological Verma modules.

Another way to understand the difference between the massive and the topological $N = 2$ Verma modules is to recall that, in general, Verma-like modules can be defined in terms of induced representations. In the case of the $N = 2$ algebra, one uses representations of Lie superalgebra $gl(1|1)$, all of whose irreducible representations are $(1, 1)$ -dimensional. A proper Verma module is then the one induced from the trivial representation, which leaves us with precisely one extremal state at the top of the extremal diagram and, thus, singles out the *topological* Verma modules. On the other hand, $(1, 1)$ -dimensional representations of $gl(1|1)$ correspond, in an obvious way, to the massive ‘Verma’ modules¹⁴. Thus, although only the topological Verma modules are the ‘true’ *Verma* modules from this point of view, we still use the name of Verma modules also for the massive ones, since this has become traditional in the literature.

4.4 From $N = 2$ to $\widehat{sl}(2)$

We now recall an operator construction [FST] that allows one to build the $\widehat{sl}(2)$ currents out of the $N = 2$ generators and a free ‘Liouville’ scalar with the operator product $\phi(z)\phi(w) = -\ln(z - w)$. As a necessary preparation, we ‘pack’ the modes of the $N = 2$ generators into the corresponding fields, $\mathcal{T}(z) = \sum_{n \in \mathbb{Z}} \mathcal{L}_n z^{-n-2}$, $\mathcal{G}(z) = \sum_{n \in \mathbb{Z}} \mathcal{G}_n z^{-n-2}$, $\mathcal{Q}(z) = \sum_{n \in \mathbb{Z}} \mathcal{Q}_n z^{-n-1}$, and $\mathcal{H}(z) = \sum_{n \in \mathbb{Z}} \mathcal{H}_n z^{-n-1}$, and similarly with the $\widehat{sl}(2)$ currents. We also define vertex operators $\psi = e^\phi$ and $\psi^* = e^{-\phi}$. Then, given the generators of the $N = 2$ algebra with central charge $c \neq 3$, the currents

$$J^+ = \mathcal{Q}\psi, \quad J^- = \frac{3}{3-c} \mathcal{G}\psi^*, \quad J^0 = -\frac{3}{3-c} \mathcal{H} + \frac{c}{3-c} \partial\phi \quad (4.12)$$

satisfy the $\widehat{sl}(2)$ algebra of level $k = \frac{2c}{3-c}$ (or, in terms of $t = k + 2$, we have the familiar relation $c = 3(t - 2)/t$). We also obtain a free scalar, with signature -1 , whose modes commute with the $\widehat{sl}(2)$ generators (4.12):

$$I^- = \sqrt{\frac{t}{2}} (\mathcal{H} - \partial\phi). \quad (4.13)$$

The modes I_n^- introduced as $I^-(z) = \sum_{n=-\infty}^{\infty} I_n^- z^{-n-1}$ generate a Heisenberg algebra $[I_n^-, I_m^-] = -n\delta_{m+n, 0}$. Let \mathcal{F}_q^- be the Fock module over this Heisenberg algebra with the highest-weight vector defined by

$$I_n^- |q\rangle^- = 0, \quad n \geq 1, \quad I_0^- |q\rangle^- = q |q\rangle^-. \quad (4.14)$$

¹⁴We thank I. Shchepochkina for this observation.

The behaviour of *representations* under operator mappings used in conformal field theory can be quite complicated¹⁵. In our case, we take a topological Verma module $\mathcal{V}_{h,t}$ and tensor it with the module Ξ of the ‘Liouville’ scalar. This is defined as $\Xi = \bigoplus_{n \in \mathbb{Z}} \mathcal{F}_n$, where \mathcal{F}_n is a Verma module with the highest-weight vector $|n\rangle_\phi$ such that

$$\phi_m |n\rangle_\phi = 0, \quad m \geq 1, \quad \psi_m |n\rangle_\phi = 0, \quad m \geq n + 1, \quad \psi_m^* |n\rangle_\phi = 0, \quad m \geq -n + 2, \quad (4.15)$$

and $\phi_0 |n\rangle_\phi = -n |n\rangle_\phi$. We then have the following Theorem:

Theorem 4.1 ([FST])

1. *There is an isomorphism of $\widehat{\mathfrak{sl}}(2)$ representations*

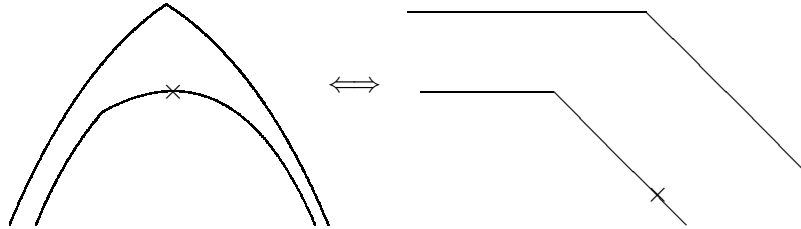
$$\mathcal{V}_{h,t} \otimes \Xi \approx \bigoplus_{\theta \in \mathbb{Z}} \mathfrak{M}_{-\frac{t}{2}h, t; \theta} \otimes \mathcal{F}_{\sqrt{\frac{t}{2}}(h+\theta)}^- \quad (4.16)$$

where on the left-hand side, the $\widehat{\mathfrak{sl}}(2)$ algebra acts by generators (4.12), while on the right-hand side it acts naturally on the twisted Verma module $\mathfrak{M}_{-\frac{t}{2}h, t; \theta}$.

2. *A singular vector exists in the topological Verma module $\mathcal{V}_{h,t}$ if and only if a singular vector exists in one (hence, in all) of the twisted $\widehat{\mathfrak{sl}}(2)$ Verma modules $\mathfrak{M}_{-\frac{t}{2}h, t; \theta}$, $\theta \in \mathbb{Z}$. Whenever this is the case, moreover, the respective submodules associated with the singular vectors, in their own turn, satisfy an equation of the same type as (4.16).*

The Theorem means that, as regards the existence and the embedding structure of submodules, the topological $N=2$ modules are *equivalent* to $\widehat{\mathfrak{sl}}(2)$ Verma modules¹⁶. The statement about the singular vectors appeared, in a rudimentary form, in [S].

While the submodules appear in a twisted topological Verma modules simultaneously with submodules in the corresponding $\widehat{\mathfrak{sl}}(2)$ Verma module, yet the submodules in a topological Verma module are necessarily *twisted* by some $\theta \neq 0$ ¹⁷:



More precisely, to the MFF singular vector $|\text{MFF}(r, s, t)\rangle^\pm$, $r, s \in \mathbb{N}$ (see (2.6)), there corresponds the *topological singular vector* [ST, ST2] $|E(r, s, t)\rangle^\pm$ that satisfies the $\theta = \mp r$ -twisted topological highest-weight conditions

$$\mathcal{Q}_{\geq \pm r} |E(r, s, t)\rangle^\pm = \mathcal{G}_{\geq \mp r} |E(r, s, t)\rangle^\pm = \mathcal{L}_{\geq 1} |E(r, s, t)\rangle^\pm = \mathcal{H}_{\geq 1} |E(r, s, t)\rangle^\pm = 0. \quad (4.17)$$

¹⁵Recall, for instance, how the $\widehat{\mathfrak{sl}}(2)$ Verma modules are rearranged under the Wakimoto bosonization [FFr] — the Wakimoto modules more or less ‘interpolate’ between the Verma and contragredient Verma modules.

¹⁶In particular, the Ξ and \mathcal{F}_- modules in (4.16) are really ‘auxiliary’, since nothing interesting can happen with these modules that would violate the balance between the topological $N=2$ and the Verma $\widehat{\mathfrak{sl}}(2)$ modules.

¹⁷A common feature of the $\widehat{\mathfrak{sl}}(2)$ Verma modules and the topological $N=2$ Verma modules is that all of them are *freely* generated from a state that satisfies stronger annihilation conditions than the other states in the extremal diagram; *when there is no additional degeneration*, one can generate the same submodule from the state marked with a \times , but there are hardly any reasons to do so in the $\widehat{\mathfrak{sl}}(2)$ case. The point of [ST3] is that doing so in the $N=2$ case is equally inconvenient.

As we see from the twist, the submodule generated from $|E^\pm(r, s, t)\rangle^\theta \in \mathfrak{V}_{h,t;\theta}$ is the twisted topological Verma module $\mathfrak{V}_{h \pm r \frac{2}{t}, t; \theta \mp r}$. Equivalently, one may choose to describe the positions of $|E^\pm(r, s, t)\rangle^\theta \in \mathfrak{V}_{h,t;\theta}$ in the (charge, level) lattice by using the *eigenvalues* of \mathcal{H}_0 and \mathcal{L}_0 :

$$\mathcal{H}_0 |E^\pm(r, s, t)\rangle^\theta = h_0^\pm |E^\pm(r, s, t)\rangle^\theta, \quad \mathcal{L}_0 |E^\pm(r, s, t)\rangle^\theta = \ell_0^\pm |E^\pm(r, s, t)\rangle^\theta, \quad (4.18)$$

then

$$h_0^\pm = h_0 \pm r, \quad \ell_0^\pm = \ell_0 + \frac{1}{2}r(r \mp 2\theta + 2s - 1) \quad (4.19)$$

where h_0 and ℓ_0 are the *eigenvalues* of \mathcal{H}_0 and \mathcal{L}_0 , respectively, on the highest-weight vector of the twisted topological Verma module $\mathfrak{V}_{h,t;\theta}$: according to (4.8), we have $h_0 = h - \frac{\epsilon}{3}\theta$ and $\ell_0 = -\theta h + \frac{\epsilon}{6}(\theta^2 - \theta)$. An important consequence of these observations is

Lemma 4.2 *All singular vectors in the twisted topological Verma module $\mathfrak{V}_{h,t;\theta}$ have the same value of $h_0^\pm + \theta^\pm$, which equals $h_0 + \theta$ for the highest-weight state of $\mathfrak{V}_{h,t;\theta}$.*

The topological singular vectors occur in the (twisted) topological Verma module $\mathfrak{V}_{h,t;\theta}$ whenever there exist $r, s \in \mathbb{N}$ such that the h parameter can be represented as $h = \mathfrak{h}^-(r, s, t)$ or $h = \mathfrak{h}^+(r, s, t)$, where

$$\mathfrak{h}^-(r, s, t) = \frac{r+1}{t} - s, \quad \mathfrak{h}^+(r, s, t) = -\frac{r-1}{t} + s - 1. \quad (4.20)$$

The explicit construction for these singular vectors can be outlined as follows [ST, ST2]. As an analogue of the complex powers of generators used in the $\widehat{\mathfrak{sl}}(2)$ case, one now performs the continuation in terms of ‘dense’ products of modes of the fermionic generators \mathcal{G} and \mathcal{Q} : one introduces operators $g(a, b)$ and $q(a, b)$ that can be thought of as a continuation of $\mathcal{G}_{b-N} \mathcal{G}_{b-N+1} \dots \mathcal{G}_b$ and $\mathcal{Q}_{b-N} \mathcal{Q}_{b-N+1} \dots \mathcal{Q}_b$, respectively, to a complex number of factors. In particular, whenever the *length* $b - a + 1$ of $g(a, b)$ or $q(a, b)$ is a non-negative integer, the corresponding operator becomes, by definition, the product of the corresponding modes:

$$g(a, b) = \prod_{i=0}^{L-1} \mathcal{G}_{a+i}, \quad q(a, b) = \prod_{i=0}^{L-1} \mathcal{Q}_{a+i}, \quad \text{iff } L \equiv b - a + 1 = 0, 1, 2, \dots \quad (4.21)$$

It is possible to postulate a number of algebraic properties of the new operators in such a way that these properties become identities whenever the operators reduce to elements of the universal enveloping algebra. This is directly analogous to the rules (2.7) used to operate with complex powers, however some of the algebraic rules that are not even formulated explicitly for the complex powers (e.g., $(J_n^+)^{\alpha} (J_n^+)^{\beta} = (J_n^+)^{\alpha+\beta}$) become less trivial in the $N = 2$ case, see [ST2, ST3]. Then the topological singular vectors in the twisted topological Verma modules read as

$$\begin{aligned} |E^+(r, s, t)\rangle^\theta &= g(-\beta_s^+, \alpha_s^+ - 1) \dots g(-\beta_2^+, \alpha_2^+ - 1) q(-\alpha_2^+, \beta_1^+ - 1) g(-\beta_1^+, \alpha_1^+ - 1) |\mathfrak{h}^+(r, s, t), t; \theta\rangle_{\text{top}}, \\ |E^-(r, s, t)\rangle^\theta &= q(-\beta_s^-, \alpha_s^- - 1) \dots q(-\beta_2^-, \alpha_2^- - 1) g(-\alpha_2^-, \beta_1^- - 1) q(-\beta_1^-, \alpha_1^- - 1) |\mathfrak{h}^-(r, s, t), t; \theta\rangle_{\text{top}} \end{aligned} \quad (4.22)$$

where

$$\alpha_i^\pm = (i - 1)t \pm \theta, \quad \beta_i^\pm = r - (s - i)t \mp \theta. \quad (4.23)$$

Using the algebraic rules satisfied by the g and q operators, one checks that these vectors do indeed satisfy the twisted topological highest-weight conditions with the twist parameter $\theta^\pm = \theta \mp r$ (which

become (4.17) in the $\theta = 0$ case). Singular vectors (4.22) evaluate as the elements of the topological Verma module $\mathfrak{V}_{\mathfrak{h}^\pm(r,s,t);t;\theta}$, with no continued operators left after the algebraic rearrangements.

The idea regarding the correspondence between submodules in $\widehat{\mathfrak{sl}}(2)$ and $N=2$ modules can be developed in the direction of category theory [FST]. Taking the objects to be all the twisted topological $N=2$ Verma modules, the morphisms would have to be the *embeddings*. We have just seen that the embeddings — i.e., the occurrence of *submodules* — are ‘synchronized’ between the topological Verma modules over $N=2$ and the $\widehat{\mathfrak{sl}}(2)$ Verma modules. The corresponding representation categories can be compared after one effectively takes the factor over the spectral flows on the $N=2$ as well as the $\widehat{\mathfrak{sl}}(2)$ sides, see [FST] for a rigorous statement. One eventually concludes that the category of *chains* of twisted topological $N=2$ Verma modules is equivalent to the category of chains of twisted $\widehat{\mathfrak{sl}}(2)$ Verma modules. An immediate consequence of this equivalence is that *embedding diagrams of topological $N=2$ Verma modules are isomorphic to the embedding diagrams of $\widehat{\mathfrak{sl}}(2)$ Verma modules*. The only additional information that may be interesting in the $N=2$ case is that regarding the twists of the modules making up an embedding diagram; however, we saw in (4.17) that the relative twist of a submodule generated from the topological singular vector $|E(r, s, t)\rangle^\pm$ is $\mp r$, therefore the twists are easy to reconstruct from the standard $\widehat{\mathfrak{sl}}(2)$ embedding diagrams.

Now, what is more important for our present purposes of describing embedding diagrams of the *massive* $N=2$ Verma modules, is that Theorem 4.1 can be extended to a similar statement involving massive $N=2$ Verma modules and (twisted) relaxed $\widehat{\mathfrak{sl}}(2)$ modules.

Theorem 4.3 ([FST])

1. *There is an isomorphism of $\widehat{\mathfrak{sl}}(2)$ representations*

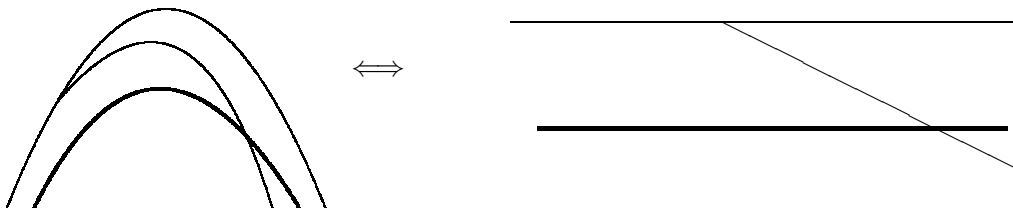
$$\mathcal{U}_{h,\ell,t} \otimes \Xi \approx \bigoplus_{\theta \in \mathbb{Z}} \mathfrak{R}_{\mu_1, \mu_2, t; \theta} \otimes \mathcal{F}^{-\sqrt{\frac{\ell}{2}}(h+\theta)}, \quad \begin{cases} \mu_1 \cdot \mu_2 = -t\ell, \\ \mu_1 + \mu_2 = ht - 1. \end{cases} \quad (4.24)$$

where on the left-hand side the $\widehat{\mathfrak{sl}}(2)$ algebra acts by generators (4.12), while on the right-hand side it acts naturally on twisted relaxed Verma module $\mathfrak{R}_{\mu_1, \mu_2, t; \theta}$.

2. *A singular vector exists in the massive Verma module $\mathcal{U}_{h,\ell,t}$ if and only if a singular vector exists in one (hence, in all) of the relaxed modules $\mathfrak{R}_{\mu_1, \mu_2, t; \theta}$, $\theta \in \mathbb{Z}$. Whenever this is the case, moreover, the respective submodules associated with the singular vectors, in their own turn, satisfy an equation of the same type as (4.24) if these are massive/relaxed submodules, and (the twist of) Eq. (4.16) if these are twisted topological/usual-Verma submodules.*

As a consequence, *the embedding diagram of any massive $N=2$ Verma module $\mathcal{U}_{h,\ell,t}$ is isomorphic to the embedding diagram of the relaxed module $\mathcal{R}_{\mu_1, \mu_2, t}$, where the parameters are related as in (4.24).*

The appearance of the massive/relaxed and topological/usual-Verma submodules can be illustrated in the following extremal diagrams:



Accordingly, the $N=2$ counterparts of singular vectors in the relaxed $\widehat{s\ell}(2)$ Verma modules are as follows.

First, charged singular vectors (2.23) translate into the $N=2$ singular vectors that exist in $\mathcal{U}_{h,\ell,t}$ if and only if $\ell = l_{\text{ch}}(n, h, t)$, where

$$l_{\text{ch}}(n, h, t) = -n\left(h - \frac{n+1}{t}\right), \quad n \in \mathbb{Z}, \quad (4.25)$$

which reproduces a series of zeros of the Kač determinant [BFK]. Just as the charged $\widehat{s\ell}(2)$ singular vectors, the charged $N=2$ singular vectors are given by the simple construction [ST2]

$$|E(n, h, t)\rangle_{\text{ch}} = \begin{cases} \mathcal{Q}_{-n} \dots \mathcal{Q}_0 |h, l_{\text{ch}}(n, h, t), t\rangle & n \geq 0, \\ \mathcal{G}_n \dots \mathcal{G}_{-1} |h, l_{\text{ch}}(n, h, t), t\rangle, & n \leq -1. \end{cases} \quad (4.26)$$

It is elementary to verify in intrinsic $N=2$ terms that every such vector satisfies twisted topological highest-weight conditions (4.17) with $\theta = n$. Thus, in accordance with the Theorem, the submodule generated from this vector is a twisted topological Verma module.

Describing the positions of singular vectors in the (charge, level) lattice, let h'_0 be the *eigenvalue* of \mathcal{H}_0 on the charged singular vector satisfying the twisted topological highest-weight conditions with the twist parameter θ' . It is easy to see that for the charged singular vectors labelled by $n \leq -1$, the value of $h'_0 + \theta'$ (where $\theta' = n$) is equal to the eigenvalue h_0 of \mathcal{H}_0 on the (untwisted) massive highest-weight vector of the massive Verma module. On the other hand, for the charged singular vectors labelled by $n \geq 0$, the value of $h'_0 + \theta'$ equals $h_0 - 1$. In combination with Lemma 4.2 and Theorem 2.4 (translated into the $N=2$ language in accordance with Theorems 4.1 and 4.3), this shows that all of the twisted topological Verma modules that can appear in a massive Verma module are divided into those for which

the highest-weight vector $|e'\rangle$ of the submodule satisfies twisted topological highest-weight conditions with the twist parameter θ' and $\mathcal{H}_0|e'\rangle = (h_0 - \theta')|e'\rangle$, with h_0 being the eigenvalue of \mathcal{H}_0 on the highest-weight vector of the massive Verma module, (4.27)

and those for which

the highest-weight vector $|e'\rangle$ of the submodule satisfies twisted topological highest-weight conditions with the twist parameter θ' and $\mathcal{H}_0|e'\rangle = (h_0 - \theta' - 1)|e'\rangle$, with h_0 being the eigenvalue of \mathcal{H}_0 on the highest-weight vector of the massive Verma module. (4.28)

As regards those singular vectors that generate relaxed submodules in relaxed $\widehat{s\ell}(2)$ modules, they translate into the *massive* singular vectors in $N=2$ Verma modules. The massive singular vectors are in the same relation to topological singular vectors in certain *auxiliary topological Verma* modules as the relaxed- $\widehat{s\ell}(2)$ singular vectors to the auxiliary Verma-module singular vectors. The method applied in Sec. 2.3, Eqs (2.26)–(2.31), now works for the $N=2$ algebra as follows [ST2, ST3]. One constructs singular vectors in the ‘auxiliary’ *topological* Verma modules, the mappings between the given massive $N=2$ Verma module and the auxiliary topological ones being performed with the help of continued operators $g(a, b)$ and $q(a, b)$. When applied to a massive highest-weight state $|h, \ell, t\rangle$, the continued operators g and q map it into a state that, generically, is a twisted massive highest-weight state. However, whenever

$$\ell = -\theta h + \frac{1}{t}(\theta^2 + \theta), \quad (4.29)$$

then

$$g(\theta, -1)|h, \ell, t\rangle \sim \left| h - \frac{2}{t}\theta, t; \theta \right\rangle_{\text{top}}, \quad (4.30)$$

and

$$q(-\theta, 0)|h, \ell, t\rangle \sim \left| h - \frac{2}{t}\theta - 1, t; \theta \right\rangle_{\text{top}}. \quad (4.31)$$

Further, once the twisted topological highest-weight conditions are thus insured, one demands that the corresponding twisted topological highest-weight state admit a topological singular vector $|E^\pm(r, s, t)\rangle$. Thus, requiring that $h - \frac{2}{t}\theta = \mathfrak{h}^-(r, s, t)$, we see that $\ell = \mathfrak{l}(r, s, h, t)$. where

$$\mathfrak{l}(r, s, h, t) = -\frac{t}{4}(h - \mathfrak{h}^-(r, s, t))(h - \mathfrak{h}^+(r, s + 1, t)). \quad (4.32)$$

The same expression for ℓ is arrived at in the case where a $|E(r, s, t)\rangle^+$ singular vector exists in the auxiliary topological Verma module. Finally, one maps the singular vectors in the auxiliary Verma module back to the original massive Verma module. In this way, massive singular vectors are of the following structure:

$$g(-rs, r + \theta' - 1) \cdot \mathcal{E}(r, s, t)^{\pm, \theta'} \cdot g(\theta', -1) |h, \ell, t\rangle, \quad (4.33)$$

or

$$q(1 - rs, r - \theta'' - 1) \mathcal{E}(r, s, t)^{\pm, \theta''} q(-\theta'', 0) |h, \ell, t\rangle, \quad (4.34)$$

where $\mathcal{E}(r, s, t)^{\pm, \theta}$ is the spectral flow transform of the topological singular vector operator $\mathcal{E}(r, s, t)^\pm$ whenever ℓ equals $\mathfrak{l}(r, s, h, t)$ from (4.32). Here, θ' and θ'' are the roots of (4.29), where we substitute $\ell = \mathfrak{l}(r, s, h, t)$.

We, thus, conclude that a massive singular vector occurs in the module $\mathcal{U}_{h, \ell, t}$ whenever $\ell = \mathfrak{l}(r, s, h, t)$. Together with the condition $\ell = \mathfrak{l}_{\text{ch}}(n, h, t)$, this reproduces the zeros of the Kač determinant [BFK]. The representatives of the massive singular vector read as

$$|S(r, s, h, t)\rangle^- = g(-rs, r + \theta^-(r, s, h, t) - 1) \mathcal{E}^{-, \theta^-(r, s, h, t)}(r, s, t) g(\theta^-(r, s, h, t), -1) |h, \mathfrak{l}(r, s, h, t), t\rangle, \quad (4.35)$$

$$|S(r, s, h, t)\rangle^+ = q(1 - rs, r - \theta^+(r, s, h, t) - 1) \mathcal{E}^{+, \theta^+(r, s, h, t)}(r, s, t) q(-\theta^+(r, s, h, t), 0) |h, \mathfrak{l}(r, s, h, t), t\rangle, \quad (4.36)$$

It is now straightforward to check that

$$\begin{aligned} \mathcal{Q}_{\geq 1 \mp rs} |S(r, s, h, t)\rangle^\pm &= \mathcal{H}_{\geq 1} |S(r, s, h, t)\rangle^\pm = \mathcal{L}_{\geq 1} |S(r, s, h, t)\rangle^\pm = \mathcal{G}_{\geq \pm rs} |S(r, s, h, t)\rangle^\pm = 0, \\ \mathcal{L}_0 |S(r, s, h, t)\rangle^\pm &= \mathfrak{l}^\pm(r, s, h, t) |S(r, s, h, t)\rangle^\pm, \\ \mathcal{H}_0 |S(r, s, h, t)\rangle^\pm &= (h \mp rs) |S(r, s, h, t)\rangle^\pm \end{aligned} \quad (4.37)$$

with

$$\mathfrak{l}^\pm(r, s, h, t) = \mathfrak{l}(r, s, h, t) + \frac{1}{2}rs(rs + 2 \mp 1). \quad (4.38)$$

In the general position (for generic (r, s, h, t) , see [ST3]), the vectors $|S(r, s, h, t)\rangle^-$ and $|S(r, s, h, t)\rangle^+$ generate the same submodule. It may be useful to note that the top of the extremal diagram containing $|S(r, s, h, t)\rangle^-$ and $|S(r, s, h, t)\rangle^+$ is the state $|S(r, s, h, t)\rangle^0$ that satisfies massive highest-weight conditions (4.3) and such that $\mathcal{H}_0 |S(r, s, h, t)\rangle^0 = h |S(r, s, h, t)\rangle^0$ and $\mathcal{L}_0 |S(r, s, h, t)\rangle^0 = (\mathfrak{l}(r, s, h, t) + rs) \cdot |S(r, s, h, t)\rangle^0$.

4.5 Embedding diagrams of the massive $N=2$ Verma modules

For $c \neq 3$, the problem of classifying and constructing the $N=2$ embedding diagrams is solved by virtue of the above results on the relaxed- $\widehat{\mathfrak{sl}}(2)$ embedding diagrams. One can parametrize massive $N=2$

Verma modules by μ_1 , μ_2 , and t from (4.24), which is always possible for $c \neq 3$. Then, depending on the values of (μ_1, μ_2, t) , we have for each massive Verma module exactly the same embedding diagram as for the respective relaxed module $\mathcal{R}_{\mu_1, \mu_2, t}$.

In the embedding diagrams of Sec 3.2, \blacksquare now denote the massive $N=2$ Verma modules, while \bullet are the twisted topological Verma modules satisfying condition (4.27) and \circ are the twisted topological Verma modules satisfying condition (4.28). The distances in the units of J_0^0 -charge map into distances in the units of the \mathcal{H}_0 -charge. However, as we have seen, the level of states along $N=2$ extremal diagrams is never constant — which, as a matter of fact, is the main reason making the $N=2$ description more complicated than the relaxed- $\widehat{s\ell}(2)$ description of the same structures. Therefore, a horizontal arrow connecting two modules does *not* mean in the $N=2$ case that the highest-weight vectors of the modules are on the same level. However, the horizontal arrows do have a meaning in the intrinsic $N=2$ terms: a horizontal arrow leads from an $N=2$ module \mathcal{W} (either twisted topological or massive) to a \bullet -module \mathcal{V}_\bullet (see (4.27)) if the embedding of the highest-weight vector $|X\rangle \in \mathcal{V}_\bullet$ reads as

$$|X\rangle = \mathcal{G}_{\theta-N} \dots \mathcal{G}_{\theta-1} |Y\rangle, \quad N \in \mathbb{N}, \quad (4.39)$$

where $|Y\rangle$ is the highest-weight state of \mathcal{W} that satisfies the θ -twisted massive highest-weight conditions. Similarly, a horizontal arrow leads from an $N=2$ module \mathcal{W} to a \circ -module \mathcal{V}_\circ (see (4.28)) if the embedding of the highest-weight vector $|X\rangle \in \mathcal{V}_\circ$ reads as

$$|X\rangle = \mathcal{Q}_{-\theta-M} \dots \mathcal{Q}_{-\theta} |Y\rangle, \quad M \in \mathbb{N}_0, \quad (4.40)$$

where $|Y\rangle$ is the highest-weight state of \mathcal{W} that satisfies the θ -twisted massive highest-weight conditions, or

$$|X\rangle = \mathcal{Q}_{-\theta-M} \dots \mathcal{Q}_{-\theta-1} |Y\rangle, \quad M \in \mathbb{N}_0, \quad (4.41)$$

if $|Y\rangle$ satisfies the θ -twisted topological highest-weight conditions.

We now reproduce the list from Sec. 3.1 in the form directly applicable to the classification of the $N=2$ embedding diagrams in terms of the parameters h and ℓ of the massive Verma module $\mathcal{U}_{h, \ell, t}$. Equations (4.32) and (4.25) exhaust the zeros of the Kač determinant [BFK]. The condition that $\ell = l^\pm(r, s, h, t)$ for some $r, s \in \mathbb{N}$ is, obviously, the analogue of the $\widehat{s\ell}(2)$ condition that $\mu_1 - \mu_2 \in \mathbb{K}(t)$. Accordingly, whenever we write $\ell \neq l(r, s, h, t)$, we mean that there do not exist $r, s \in \mathbb{N}$ such that this would become an equality for a given triple (h, ℓ, t) , and similarly with the condition $\ell \neq l_{\text{ch}}(n, h, t)$, $n \in \mathbb{Z}$. The comments to diagrams (3.2)–(3.41) on pp. 22–33 apply in the $N=2$ case with the following replacements:

Verma module	→	twisted topological Verma module satisfying Eq. (4.27)
twisted Verma module with $\theta = 1$	→	twisted topological Verma module satisfying Eq. (4.28)
charged singular vector (2.23)	→	charged singular vector (4.26)
relaxed (sub)module	→	massive Verma (sub)module
embedding onto the same level	→	embedding via (4.39) or (4.40), (4.41)
$ \text{MFF}^\pm(r, s, t)\rangle$	→	$ E(r, s, t)\rangle^\pm$
relative J_0^0 -charge	→	minus the relative \mathcal{H}_0 -charge

Note also that the positive (negative) zone can now be described as $c < 3$ (respectively, $c > 3$).

We, thus, have the following patterns of embedding diagrams, where we refer to the diagrams from Sec. 3.2 that are to be read using the $N=2$ conventions discussed above.

I: $\ell \neq l(r, s, h, t)$ with $r \in \mathbb{N}$, $s \in \mathbb{N}$. The embedding diagrams shown in (3.2) correspond to the following subcases:

I(0): $\ell \neq l_{\text{ch}}(n, h, t)$ with $n \in \mathbb{Z}$, i.e., $\frac{1}{2} \left(ht - 1 \pm \sqrt{4\ell t + (ht - 1)^2} \right) \notin \mathbb{Z}$. This is the trivial case.

I(1): $\ell = l_{\text{ch}}(n, h, t)$ for some $n \in \mathbb{Z}$, $ht \notin \mathbb{Z}$. We then have

I(1,-): a twisted topological Verma module satisfying Eq. (4.27) if $n \in -\mathbb{N}$, or

I(1,+): a twisted topological Verma module satisfying Eq. (4.28) if $n \in \mathbb{N}_0$,

embedded via a charged singular vector, the corresponding diagrams being given Eq. (3.2).

I(2): $h = \frac{1+n+m}{t}$ and $\ell = -\frac{nm}{t}$ for some $m, n \in \mathbb{Z}$.

I(2,-): $n, m \in -\mathbb{N}$, the first diagram in (3.3).

I(2,+): $n, m \in \mathbb{N}_0$, the second diagram in (3.3).

I(2,-+): $n \in -\mathbb{N}$, $m \in \mathbb{N}_0$, the third diagram in (3.3).

II: $\ell = l(r, s, h, t)$ for some $r, s \in \mathbb{N}$ and $t \notin \mathbb{Q}$. All of the following items in case II refer to the chosen r and s .

II(0): $ht - 1 + st - r \notin 2\mathbb{Z}$ and $ht - 1 - (st - r) \notin 2\mathbb{Z}$. We have the first of the diagrams (3.4).

II(1): $h = \frac{1+2n+r-st}{t}$ or $h = \frac{1+2n-(r-st)}{t}$ for some $n \in \mathbb{Z}$ (then $\ell = -\frac{n(n\pm(r-st))}{t}$, respectively). We have the respective diagrams (3.4), depending on the sign of n :

II(1,-): $n \in -\mathbb{N}$,

II(1,+): $n \in \mathbb{N}_0$.

As before, these cases differ by which of the relations (4.27) or (4.28) is satisfied for the twisted topological Verma submodule.

III: $\ell = l(r, s, h, t)$ for some $r, s \in \mathbb{N}$, $t = \frac{p}{q} \in \mathbb{Q}$. In the following items in case III, we use the chosen r and s .

III $_{\pm}$: $\frac{r}{t} \notin \mathbb{Z}$, $st \notin \mathbb{Z}$. This means that $r \neq \alpha p$, $s \neq \beta q$ for $\alpha, \beta \in \mathbb{Z}$.

III $_{\pm}$ (0): $ht - 1 + st - r \notin 2\mathbb{Z}$ and $ht - 1 - (st - r) \notin 2\mathbb{Z}$. We have the double-chains of massive Verma modules shown in diagram (3.7). These look identical to the familiar embedding diagrams of the topological Verma modules. Indeed, the structure of the massive Verma module repeats in this case the structure of the ‘auxiliary’ topological Verma module [ST3].

Further degenerations are given by (various combinations of) the following effects. First, the auxiliary topological Verma module may become an actual submodule in the massive Verma module, in which case the entire *topological Verma*-module embedding diagram joins the diagram (3.7) via embeddings performed by charged singular vectors. Second, the embedding diagram growing from the auxiliary topological Verma module may acquire a special form, which would also affect the ‘massive’ embedding diagram.

III $_{\pm}$ (1): either $h = \frac{1+2n+(r-st)}{t}$ or $h = \frac{1+2n-(r-st)}{t}$, $n \in \mathbb{Z}$. Here, the auxiliary topological Verma module becomes a submodule in the massive Verma module; we then have the usual subcases depending on the sign of n :

III $_{\pm}$ (1,-): $n \in -\mathbb{N}$, diagram (3.9).

$\text{III}_{\pm}(1,+)$: $n \in \mathbb{N}_0$, diagram (3.10).

These diagrams are finite or infinite depending on whether $t < 0$ (III_{-}) or $t > 0$ (III_{+}), respectively. In (3.9) and (3.10), the top topological Verma module is the submodule in the massive Verma module associated with a charged singular vector. Each of the subsequent topological Verma modules is embedded via a charged singular vector into the corresponding massive Verma module.

III_{\pm}^0 : Either $(\frac{r}{t} \in \mathbb{Z}, st \notin \mathbb{Z})$ or $(\frac{r}{t} \notin \mathbb{Z}, st \in \mathbb{Z})$. Thus, we have either, *but not both*, of the conditions $r = \alpha p$ and $s = \beta q$, $\alpha, \beta \in \mathbb{Z}$. The interplay of these cases is rather interesting. Recall that, for the Virasoro algebra, the condition that singles out the III^0 case is that (in the current notations) the line $y = tx - \mu_1 + \mu_2$ intersect one of the x, y axes at an integral point [FF]. For the usual $\widehat{s\ell}(2)$ Verma modules, on the other hand, this means two *different* cases: either $2j + 1 \in \mathbb{Z}$ or $(2j + 1)/t \in \mathbb{Z}$, where j is the spin of the highest-weight vector; it is only the Hamiltonian reduction that erases the difference between the two cases. However, since the Virasoro algebra is a subalgebra of the $N = 2$ algebra, one may expect these to become again a single $N = 2/\text{relaxed-}\widehat{s\ell}(2)$ pattern, which is indeed the case.

$\text{III}_{\pm}^0(0)$: $ht - 1 + st - r \notin 2\mathbb{Z}$ and $ht - 1 - (st - r) \notin 2\mathbb{Z}$. We then have a single-chain of massive Verma modules, diagram (3.11). The single chain takes the place of the double chain because each submodule in \mathcal{U} corresponds to a *pair* of submodules in the auxiliary topological Verma module \mathcal{V} [ST3].

$\text{III}_{\pm}^0(1)$: either $h = \frac{1+2n+(r-st)}{t}$ or $h = \frac{1+2n-(r-st)}{t}$, with $n \in \mathbb{Z}$ and $st \notin \mathbb{Z}$ (hence we should have $\frac{r}{t} \in \mathbb{Z}$; then, respectively, $h = \frac{q}{p}(1 + 2n) \pm (\alpha q - s)$ and $\ell = -\frac{n^2 q}{p} \mp n(\alpha q - s)$).

$\text{III}_{\pm}^0(1,-)$: $n \in -\mathbb{N}$, diagram (3.12);

$\text{III}_{\pm}^0(1,+)$: $n \in \mathbb{N}_0$, the vertical mirror of (3.12) (where, as we have discussed, the modules satisfying Eq. (4.27) are replaced by those satisfying (4.28)).

$\text{III}_{\pm}^0(2)$: $h = \frac{q}{p}(1 + 2n \pm (r - \beta p))$ with $\frac{r}{p} \notin \mathbb{Z}$. Then $\ell = -\frac{q}{p}n(n \pm (r - \beta p))$. This can also be expressed as $h = \frac{1+n+m}{t}$, $\ell = -\frac{nm}{t}$ for some $m, n \in \mathbb{Z}$ such that $\frac{m-n}{t} \notin \mathbb{Z}$. Accordingly, there are two charged singular vectors in the massive Verma module on one side of the highest-weight vector. The following subcases depend on the sign of these two integers:

$\text{III}_{\pm}^0(2,-)$: $n \in -\mathbb{N}$, $m \in -\mathbb{N}$, diagram (3.13).

$\text{III}_{\pm}^0(2,+)$: $n \in \mathbb{N}_0$, $m \in \mathbb{N}_0$, a mirror diagram of (3.13).

$\text{III}_{\pm}^0(2,-+)$: $n \in -\mathbb{N}$, $m \in \mathbb{N}_0$, diagram (3.32).

The diagrams are finite or infinite depending on whether $t < 0$ or $t > 0$ respectively. In the $\text{III}_{\pm}^0(2,-+)$ case, there are charged singular vectors on different sides of the highest-weight vector of the massive Verma module. One of the charged singular vectors comes with the embedding diagram of topological Verma modules, while the other contributes a similar (in fact, mirror-symmetric) diagram of twisted topological Verma modules

III_{\pm}^{00} : $\frac{r}{t} \in \mathbb{Z}, st \in \mathbb{Z}$. In the following, we use $\alpha, \beta \in \mathbb{Z}$ such that $r = \alpha p$ and $s = \beta q$ (thus, $\ell = \frac{1}{2}h - \frac{q}{4p} - \frac{h^2 p}{4q} + \frac{1}{4}(\alpha - \beta)^2 qp$).

$\text{III}_{\pm}^{00}(0)$: $ht - 1 + st - r \notin 2\mathbb{Z}$ and $ht - 1 - (st - r) \notin 2\mathbb{Z}$. The embedding diagram looks identical to (3.11), however it is half that long in the negative zone.

III $_{\pm}^{00}(2)$: $h = \frac{q}{p}(1 + 2n) \pm q(\alpha - \beta)$, then $\ell = \mp(\alpha - \beta)ng - \frac{n^2q}{p}$. This can also be written as $h = \frac{1+n+m}{t}$ and $\ell = -\frac{nm}{t}$ for some $n, m \in \mathbb{Z}$ such that $\frac{m-n}{p} \in \mathbb{Z}$. The following subcases depend on the signs of these two integers:

III $_{\pm}^{00}(2, --)$: $n \in -\mathbb{N}$, $m \in -\mathbb{N}$, diagram (3.35), which can be viewed as a degeneration of diagrams (3.12). It is finite or infinite depending on whether t is negative or positive respectively. *In the negative zone*, we can further distinguish the following two cases depending on how the modules arrange near the bottom of the embedding diagram:

- i) $\beta - \alpha$ is odd ($\frac{m-n}{p}$ is odd), the first diagram in (3.37).
- ii) $\beta - \alpha$ is even ($\frac{m-n}{p}$ is even), the second diagram in (3.37).

III $_{\pm}^{00}(2, ++)$: $n \in \mathbb{N}_0$, $m \in \mathbb{N}_0$, the diagram is the mirror of (3.35). *In the negative zone*, in complete similarity with III $_{\pm}^{00}(2, --)$, we can distinguish two cases,

- i) $\beta - \alpha$ odd ($\frac{m-n}{p}$ odd),
- ii) $\beta - \alpha$ even ($\frac{m-n}{p}$ even),

which, again, are the mirror of (3.37).

III $_{\pm}^{00}(2, -+)$: $n \in -\mathbb{N}$, $m \in \mathbb{N}_0$, diagram (3.40). *In the negative zone*, we have to distinguish two possibilities of its structure near the bottom:

- i) $\beta - \alpha$ is odd ($\frac{m-n}{p}$ is odd),
- ii) $\beta - \alpha$ is even ($\frac{m-n}{p}$ is even), shown in (3.41).

Setting $t = -\frac{\tilde{t}}{q}$, we have an exceptional case whenever $|\alpha - \beta| = 2$, therefore

$$h = -\frac{2m-2\tilde{p}+1}{\tilde{p}}q, \quad \ell = \frac{m(m-2\tilde{p})}{\tilde{p}}q \quad (4.42)$$

This is described by diagram (3.42) *with no massive Verma submodules*.

Note that the Virasoro embedding diagrams are obtained simply by contracting all of the horizontal arrows in the diagrams (in particular, by dropping all of the \bullet and \circ dots).

4.6 $c = 3$ singular vectors and embedding diagrams

The case of $c = 3$ (i.e., $t \rightarrow \infty$) has to be considered separately, since the correspondence with $\widehat{sl}(2)$ modules then breaks down and the $N = 2$ Verma modules have to be analysed directly. We, thus, do not prove that the set of singular vectors we consider is complete; we simply apply the approach outlined at the end of Sec. 4.4 in the $t \rightarrow \infty$ limit.

First, let us consider topological Verma modules $\mathcal{V}_{h,\infty}$. Observe first of all that any submodule $\mathcal{V}_{h,\infty}$ is isomorphic to a twist of $\mathcal{V}_{h,\infty}$, i.e., the value of the h parameter does not change. A singular vector exists in $\mathcal{V}_{h,\infty}$ whenever $h \in \mathbb{Z}$. For $h \in \mathbb{N}_0$, we denote $h = s - 1$ with $s \in \mathbb{N}$, then we have the singular vectors

$$\begin{aligned} |e(r, s)\rangle^+ &= \lim_{t \rightarrow \infty} \left(\frac{1}{t^{r(s-1)}} |E(r, s, t)\rangle^+ \right) \\ &\equiv e^+(r, s) |s - 1, \infty\rangle_{\text{top}} \end{aligned} \quad (4.43)$$

for all $r \in \mathbb{N}$. The vector $|e(r, s)\rangle^+$ satisfies the twisted topological highest-weight conditions with the twist parameter $\theta = -r$; its \mathcal{H}_0 -charge and level are given by

$$\begin{aligned}\mathcal{H}_0 |e(r, s)\rangle^+ &= (s - 1 + r)|e(r, s)\rangle^+, \\ \mathcal{L}_0 |e(r, s)\rangle^+ &= \frac{1}{2}r(r + 2s - 1) |e(r, s)\rangle^+.\end{aligned}\tag{4.44}$$

Moreover, the singular vector operators compose as follows:

$$e(1, s)^{+,-1} e^+(1, s) = e^+(2, s)\tag{4.45}$$

(where $e(r, s)^{+,\theta}$ is the spectral flow transform of the singular vector operator) and, thus, all of the singular vectors (4.43) belong to the submodule generated from $|e(1, s)\rangle^+$.

Similarly, for $h = -s \in -\mathbb{N}$, we have the singular vectors

$$\begin{aligned}|e(r, s)\rangle^- &= \lim_{t \rightarrow \infty} \left(\frac{1}{t^{r(s-1)}} |E(r, s, t)\rangle^- \right) \\ &\equiv e^-(r, s) | -s, \infty \rangle_{\text{top}}\end{aligned}\tag{4.46}$$

for all $r \in \mathbb{N}$. These satisfy the twisted topological highest-weight conditions with the twist parameter $\theta = r$, while

$$\begin{aligned}\mathcal{H}_0 |e(r, s)\rangle^- &= -(s + r)|e(r, s)\rangle^-, \\ \mathcal{L}_0 |e(r, s)\rangle^- &= \frac{1}{2}r(r + 2s - 1) |e(r, s)\rangle^-.\end{aligned}\tag{4.47}$$

The singular vector operators compose as follows:

$$e(1, s)^{-,1} e^-(1, s) = e^-(2, s)\tag{4.48}$$

hence all of the singular vectors (4.46) belong to the submodule generated from $|e(1, s)\rangle^-$.

Thus, the embedding diagram of $\mathcal{V}_{h,\infty}$ is a single-chain of modules $(\mathfrak{B}_{h,\infty;-r})_{r \in \mathbb{N}}$ if $h \in \mathbb{N}_0$ and $(\mathfrak{B}_{h,\infty;r})_{r \in \mathbb{N}}$ if $h \in -\mathbb{N}$.

As regards singular vectors in massive Verma modules $\mathcal{U}_{h,\ell,\infty}$, we begin with the simplest case of the charged singular vectors. These exist in $\mathcal{U}_{h,\ell,\infty}$ whenever $\ell = -nh$, $n \in \mathbb{Z}$, and read

$$|E(n, h, \infty)\rangle_{\text{ch}} = \begin{cases} \mathcal{Q}_{-n} \dots \mathcal{Q}_0 |h, -nh, \infty\rangle & n \geq 0, \\ \mathcal{G}_n \dots \mathcal{G}_{-1} |h, -nh, \infty\rangle, & n \leq -1. \end{cases}\tag{4.49}$$

If $h = 0$, the module $\mathcal{U}_{0,0,\infty}$ contains all singular vectors $|E(n, 0, \infty)\rangle_{\text{ch}}$, $n \in \mathbb{Z}$. The embedding diagram has the following, rather curious, form:



where we do *not* follow the convention that all of the embeddings via charged singular vectors are shown with horizontal arrows; that convention was particularly natural on the $\widehat{s\ell}(2)$ side, however in the present diagram—which has no $\widehat{s\ell}(2)$ analogues—we place the submodules on different levels, in accordance with the actual expression for the charged singular vectors. In fact, the *embedding* diagram looks in this case very much like the *extremal* diagram of the module, because a submodule is generated from every extremal state of the module (except the highest-weight one); thus, it may be even more natural to place the dots in (4.50) on the two half-parabolas, as in (4.10).

As to the massive singular vectors, further, we see that (one of) the states (4.30) and (4.31) admits a singular vector and at the same time (one of) the roots θ' and θ'' of Eq. (4.29) has a finite limit as $t \rightarrow \infty$ if and only if $h = \pm s$. Thus, massive singular vectors in the massive Verma module $\mathcal{U}_{h,\ell,\infty}$ exist whenever $h \in \mathbb{Z} \setminus \{0\}$. For $h \equiv -s \in -\mathbb{N}$, the massive singular vectors in $\mathcal{U}_{-s,\ell,\infty}$ are constructed as follows:

$$|\sigma(r, s, \ell)\rangle^- = g(-rs, \frac{\ell}{s} + r - 1) e(r, s)^{-, \ell/s} g(\frac{\ell}{s}, -1) |-s, \ell, \infty\rangle, \quad (4.51)$$

where, as before, $e(r, s)^{-, \theta}$ is the spectral flow transform of the singular vector operator $e(r, s)^-$.

Whenever the module $\mathcal{U}_{-s,\ell,\infty}$ contains, in addition, a charged singular vector, a somewhat special case occurs for $\frac{\ell}{s} \in -\mathbb{N}$. Then the vector $|\sigma(r, s, \ell)\rangle^-$ belongs to the submodule generated from the charged singular vector

$$\left| E(\frac{\ell}{s}, -s, \infty) \right\rangle_{\text{ch}} = \mathcal{G}_{\frac{\ell}{s}} \dots \mathcal{G}_{-1} |-s, \ell, \infty\rangle \quad (4.52)$$

since, obviously, $|\sigma(r, s, sn)\rangle^-$ with $n \in -\mathbb{N}$ is a descendant of the state

$$|\bar{\sigma}(r, s, sn)\rangle^- = e(r, s)^{-, n} \mathcal{G}_n \dots \mathcal{G}_{-1} |-s, ns, \infty\rangle \quad (4.53)$$

that satisfies twisted topological highest-weight conditions with the twist parameter $\theta = r + n$. In that case, there always exists the state

$$|x(r, s, sn)\rangle^- = g(r + n + 1, r + n - 1) |\bar{\sigma}(r, s, sn)\rangle^- \quad (4.54)$$

which satisfies twisted massive highest-weight conditions with the twist parameter $\theta = r + n + 1$ and generates a *massive* Verma submodule.

Next, for $h \equiv s \in \mathbb{N}$, singular vectors in $\mathcal{U}_{s,\ell,\infty}$ are of the form

$$|\sigma(r, s, \ell)\rangle^+ = q(-rs, r + \frac{\ell}{s} - 1) e(r, s)^{+, -\ell/s} q(\frac{\ell}{s}, 0) |s, \ell, \infty\rangle. \quad (4.55)$$

These satisfy the twisted massive highest-weight conditions with the twist parameter $rs + 1$.

Again, a simultaneous occurrence of a charged singular vector requires some attention when $\frac{\ell}{h} \in -\mathbb{N}_0$. Then vectors (4.55) are descendants of the charged singular vector

$$\mathcal{Q}_{\ell/s} \dots \mathcal{Q}_0 |s, \ell, \infty\rangle. \quad (4.56)$$

Moreover, $|\sigma(r, s, -sn)\rangle^+$ with $n \in \mathbb{N}_0$ is inside the submodule built on the vector

$$|\bar{\sigma}(r, s, -sn)\rangle^+ = e(r, s)^{+, n} \mathcal{Q}_{-n} \dots \mathcal{Q}_0 |s, -sn, \infty\rangle, \quad (4.57)$$

which satisfies the twisted topological highest-weight conditions with the twist parameter $n - r$. In that case, there exist the vector

$$|x(r, s, -sn)\rangle^+ = q(n - r + 1, n - r - 1)|\sigma(r, s, -sn)\rangle^+ \quad (4.58)$$

from which the respective massive Verma submodule is generated.

Therefore, when $h \in \mathbb{Z} \setminus \{0\}$ but $\frac{\ell}{h} \notin \mathbb{Z}$, the embedding diagrams are simply a single chain of massive Verma modules. When, in addition, $\frac{\ell}{h} \in \mathbb{Z}$, the embedding diagram takes the form (again in the convention that the embedding via charged singular vectors are shown with horizontal arrows)

$$(4.59)$$

or the vertical mirror of this with the \bullet modules replaced by \circ modules.

We, thus, arrive at the following cases, which can be labelled as I_∞ and III_∞ (no II cases exist at $c = 3$):

I_∞ : $h \notin \mathbb{Z}$ or $h = 0$.

$I_\infty(0)$: $h \neq 0$, $\ell/h \notin \mathbb{Z}$. There are no submodules in $\mathcal{U}_{h,\ell,\infty}$ whatsoever, the embedding diagram is the lonely massive Verma module.

$I_\infty(1)$: $h \neq 0$, $\ell/h \in \mathbb{Z}$. Then, we have the respective diagrams from (3.2) in the cases where

$I_\infty(1, -)$: $\ell/h \in \mathbb{N}$.

$I_\infty(1, +)$: $\ell/h \in -\mathbb{N}_0$.

$I_\infty(\infty)$: $\ell = 0$, $h = 0$. Here, the embedding diagram is of the form (4.59).

III_∞ : $h \in \mathbb{Z} \setminus \{0\}$.

$III_\infty(0)$: $\ell/h \notin \mathbb{Z}$, the embedding diagram being the same as in (3.11).

$III_\infty(1)$: $\ell/h \in \mathbb{Z}$,

$III_\infty(1, -)$: $\ell/h \in \mathbb{N}$, the embedding diagram (4.59), which is ‘topologically’ identical to the diagrams in (3.12).

$III_\infty(1, +)$: $\ell/h \in -\mathbb{N}_0$, with the embedding diagram being the vertical mirror of the previous one.

5 Conclusions

In this paper, we have constructed the $N = 2$ embedding diagrams, which at the same time are the embedding diagrams of the relaxed $\widehat{sl}(2)$ Verma modules. Let us point out once again that the $N=2$ /relaxed- $\widehat{sl}(2)$ embedding diagrams are made up of *embeddings*, i.e., of mappings with trivial kernels. On the $N=2$ side, this matter appears to have caused some confusion in the literature, because the existence of fermions was believed to lead to the vanishing of certain would-be embeddings. In the $\widehat{sl}(2)$ terms, however, this problem is obviously absent, hence it is but an artefact on the $N = 2$ side as well. The vanishing of some compositions of “embeddings” observed previously is nothing but the manifestation of two facts: (i) states (4.11) vanish for $N \gg 1$ or for $M \gg 1$ once $|X\rangle$ is inside a (twisted) topological Verma module, and (ii) every submodule generated from a charged singular vector is necessarily a twisted topological Verma module. This is even more transparent on the $\widehat{sl}(2)$ side, where the charged singular vectors generate the usual (i.e., *not* relaxed) Verma modules, which obviously ‘defermionizes’ the whole picture.

As we have already remarked in the Introduction, an immediate consequence of the embedding diagrams constructed here would be the derivation of the ‘relaxed’ BGG-like resolution and, thus, of the $N=2$ /relaxed- $\widehat{sl}(2)$ characters. It should only be noted that constructing the BGG-resolution for the $N = 2$ representations requires slightly more work than in the ‘classical’ (affine) cases because of the two types of submodules existing in the massive $N = 2$ Verma modules. Unlike the embedding diagrams, the resolutions are constructed in terms of modules of only one type, therefore, on the way from the $N = 2$ *embedding* diagrams to the BGG *resolutions*, one has to additionally resolve all the topological Verma modules in terms of the massive ones.

In view of the results of [S2, S3] on the construction of $\widehat{sl}(2|1)$ representations out of the $N=2$ Verma modules and on the evaluation of $\widehat{sl}(2|1)$ singular vectors in the $N=2$ terms, certain elements of the above embedding diagrams must also be present in the $\widehat{sl}(2|1)$ embedding diagrams (cf. [BT]), where—as in the $N=2$ case—different types of Verma-like modules have been observed [S3].

Acknowledgements. We thank I. Tipunin for collaboration at an early stage of this work and many useful discussions, and also B. Feigin, F. Malikov, and I. Shchepochkina for useful remarks. The work of AMS was supported in part by the RFBR Grant 96-02-16117 and that of VAS, by the ISSEP grant a97-442.

References

- [A] M. Ademollo, L. Brink, A. D’Adda, R. D’Aura, E. Napolitano, S. Sciuto, E. Del Giudice, P. Di Vecchia, S. Ferrara, F. Gliozzi, R. Musto, R. Pettorino and J. Schwarz, *Dual String With U(1) Color Symmetry*, Nucl. Phys. B111 (1976) 77.
- M. Ademollo, L. Brink, A. D’Adda, R. D’Aura, E. Napolitano, S. Sciuto, E. Del Giudice, P. Di Vecchia, S. Ferrara, F. Gliozzi, R. Musto and R. Pettorino, *Dual String Models With Nonabelian Color and Flavor Symmetries*, Nucl. Phys. B114 (1976) 297.
- [BH] K. Bardakçi and M.B. Halpern, Phys. Rev. D3 (1971) 2493.
- [BGG] I. Bernshtein, I. Gelfand, and S. Gelfand, Funk. An. Prilozh. 10 (1976) 1.
- [BLNW] M. Bershadsky, W. Lerche, D. Nemeschansky, and N.P. Warner, Nucl. Phys. B401 (1993) 304.
- [BO] M. Bershadsky and H. Ooguri, *Hidden Osp(N, 2) Symmetries in Superconformal Field Theories*, Phys. Lett. B229 (1989) 374.

- [BLLS] A. Boreesch, K. Landsteiner, W. Lerche, and A. Sevrin, *Superstrings from Hamiltonian Reduction*, Nucl. Phys. B436 (1995) 609–637;
- [BFK] W. Boucher, D. Friedan, and A. Kent, *Determinant Formulae and Unitarity For the $N = 2$ Superconformal Algebras in Two-Dimensions or Exact Results on String Compactification*, Phys. Lett. B172 (1986) 316.
- [BT] P. Bowcock and A. Taormina, *Representation theory of the affine Lie superalgebra $sl(2|1)$ at fractional level*, Commun. Math. Phys. 185 (1997) 467–493.
- [CGP] S. Cecotti, L. Girardello, and A. Pasquinucci, Int. J. Mod. Phys. A6 (1991) 2427; S. Cecotti, Int. J. Mod. Phys. A6 (1991) 1749; Nucl. Phys. B355 (1991) 755.
- [CV] S. Cecotti and C. Vafa, Nucl. Phys. B367 (1991) 359;
- [Di] J. Dixmier, *Algèbres Enveloppantes*, Gauthier-Villars, 1974.
- [Do] V.K. Dobrev, *Characters of Unitarizable Highest Weight Modules over the $N = 2$ Superconformal Algebra*, Phys. Lett. B186 (1987) 43.
- [D] M. Dörrzapf, *Analytic Expressions for Singular Vectors of the $N = 2$ Superconformal Algebra*, Commun. Math. Phys. 180, 195 (1996).
- [EY] T. Eguchi and S.-K. Yang, *$N = 2$ superconformal models as topological field theories*, Mod. Phys. Lett. A5 (1990) 1653.
- [EG] W. Eholzer and M.R. Gaberdiel, *Unitarity of rational $N = 2$ superconformal theories*, Commun. Math. Phys. 186 (1997) 61–85.
- [FST] B.L. Feigin, A.M. Semikhatov, and I.Yu. Tipunin, *Equivalence between Chain Categories of Representations of Affine $sl(2)$ and $N = 2$ Superconformal Algebras*, hep-th/9701043.
- [FF] B.L. Feigin and D.B. Fuchs, *Representations of the Virasoro Algebra*, in: *Representations of Lie Groups and Related Topics*, eds. A.M. Vershik and A.D. Zhelobenko, Gordon & Breach, 1990.
- [FFr] B.L. Feigin and E.V. Frenkel, *Representations of Affine Kac–Moody Algebras and Bosonization*, in: *Physics and Mathematics of Strings*, eds. L. Brink, D. Friedan, and A.M. Polyakov, World Sci.
- [FoF] J.M. Figueroa-O’Farrill, *Untwisting Topological Field Theories (1996); Affine algebras, $N=2$ superconformal algebras, and gauged WZNW models*, Phys. Lett. B316 (1993) 496; *$N=2$ Structures in String Theories*, hep-th/9507145.
- [FMS] D.H. Friedan, E.J. Martinec, and S.H. Shenker, *Conformal Invariance, Supersymmetry and String Theory*, Nucl. Phys. B271 (1986) 93.
- [GRS] B. Gato-Rivera and A.M. Semikhatov, *$d \leq 1 \cup d \geq 25$ and W Constraints From BRST-Invariance in the $c \neq 3$ Topological Algebra*, Phys. Lett. B293 (1992) 72.
- [G] D. Gepner, Phys. Lett. B199 (1987) 380; Nucl. Phys. B 296 (1988) 757.
- [Get] E. Getzler, *Manin Triples and Topological Field Theory*, hep-th/9509057; *Manin Triples and $N = 2$ Superconformal Field Theory*, hep-th/9307041.
- [Get2] E. Getzler, *Batalin-Vilkovisky algebras and two-dimensional topological field theories*, Commun. Math. Phys. 159 (1994), 265–285.
- [IK] K. Ito and H. Kanno, *Hamiltonian Reduction and Topological Conformal Algebra in $c \leq 1$ Non-Critical Strings*, Mod. Phys. Lett. A9 (1994) 1377.
- [K] V.G. Kač *Infinite Dimensional Lie Algebras*, Cambridge University Press, 1990.
- [KS] Y. Kazama and H. Suzuki, *New $N = 2$ Superconformal Field Theories and Superstring compactification*, Nucl. Phys. B321 (1989) 232.
- [KL] S.V. Ketov and O. Lechtenfeld, *The String Measure and Spectral Flow of Critical $N = 2$ Strings*, Phys. Lett. B353 (1995) 463.
- [Kir] E.B. Kiritsis, *Character Formulae and Structure of the Representations of the $N = 1, N = 2$ Superconformal Algebras*, Int. J. Mod. Phys. A(1988) 1871.
- [KM] D. Kutasov and E. Martinec, *New Principles for String/Membrane Unification*, Nucl. Phys. B477 (1996) 652; D. Kutasov, E. Martinec, and M. O’Loughlin, *Vacua of M -theory and $N = 2$ strings*, Nucl. Phys. B477 (1996) 675.
- [LVW] W. Lerche, C. Vafa, and N.P. Warner, *Chiral Rings In $N = 2$ Superconformal Theories*, Nucl. Phys. B324 (1989) 427.

- [LZ] B.H. Lian and G.J. Zuckerman, *New Selection Rules and Physical States in 2-D Gravity: Conformal Gauge*, Phys. Lett. B254 (1991) 417–423;
Semiinfinite Homology and 2-D Gravity. 1. Commun. Math. Phys. 145 (1992) 561–593;
- [Mal] F. Malikov, *Verma Modules over Rank-2 Kač–Moody Algebras*, Algebra i Analiz 2 No. 2 (1990) 65.
- [MFF] F.G. Malikov, B.L. Feigin, and D.B. Fuchs, *Singular Vectors in Verma Modules over Kač–Moody Algebras*, Funk. An. Prilozh. 20 N2 (1986) 25.
- [M] N. Marcus, *A Tour through $N = 2$ strings*, talk at the Rome String Theory Workshop, 1992, hep-th/9211059.
- [Mar] E. Martinec, Phys. Lett. B217 (1989) 431; *Criticality, Catastrophes, and Compactifications*, in: *Physics and Mathematics of Strings*, ed. L. Brink, D. Friedan, and A. M. Polyakov (World Scientific, 1990)
- [Mat] Y. Matsuo, *Character Formula of $C < 1$ Unitary Representation of $N = 2$ Superconformal Algebra*, Prog. Theor. Phys. 77 (1987) 793.
- [OS] N. Ohta and H. Suzuki, *$N = 2$ Superconformal Models and their Free Field Realization*, Nucl. Phys. B332 91990) 146–168.
- [OV] H. Ooguri and C. Vafa *Geometry of $N = 2$ Strings*, Nucl. Phys. B361 (1991) 469–518;
 $N = 2$ Heterotic Strings, Nucl. Phys. B367 (1991) 83–104.
- [RSS] E. Ragoucy, A. Sevrin and P. Sorba, *Strings from $N = 2$ Gauged Wess–Zumino–Witten Models*, Commun. Math. Phys. 181 (1996) 91–129.
- [RCW] A. Rocha-Caridi and N.R. Wallach, *Highest Weight Modules over Graded Lie Algebras: Resolutions, Filtrations, and Character Formulas*, Trans. Amer. Math. Soc. 277 (1983) 133–162.
- [SS] A. Schwimmer and N. Seiberg, *Comments on the $N = 2$, $N = 3$, $N = 4$ Superconformal Algebras In Two-Dimensions*, Phys. Lett. B184 (1987) 191.
- [S] A.M. Semikhatov, *The MFF singular vectors in topological conformal theories*, Mod. Phys. Lett. A9 (1994) 1867.
- [S2] A.M. Semikhatov, *The Non-Critical $N = 2$ String is an $sl(2|1)$ Theory*, Nucl. Phys. B478 (1996) 209–234.
- [S3] A.M. Semikhatov, *Verma Modules, Extremal Vectors, and Singular Vectors on the Non-Critical $N = 2$ String Worldsheet*, hep-th/9610084.
- [ST] A.M. Semikhatov and I.Yu. Tipunin, *Singular Vectors of the Topological Conformal Algebra*, Int. J. Mod. Phys. A11 (1996) 4597.
- [ST2] A.M. Semikhatov and I.Yu. Tipunin, *All Singular Vectors of the $N = 2$ Superconformal Algebra via the Algebraic Continuation Approach*, hep-th/9604176.
- [ST3] A.M. Semikhatov and I.Yu. Tipunin, *The Structure of Verma Modules over the $N = 2$ Superconformal Algebra*, hep-th/9704111, Commun. Math. Phys., to appear.
- [VW] C. Vafa and N.P. Warner, Phys. Lett. B218 (1989) 51.
- [W] E. Witten, *Topological Sigma Models*, Commun. Math. Phys. 118 (1988) 411.